

AN E.S.R. STUDY OF SOME  
NITROGEN SUBSTITUTED  
FREE RADICALS

by

P. M. HOYLE

A thesis submitted for the degree of  
Doctor of Philosophy  
in the University of London

Bedford College,  
Regent's Park.

December 1978

ProQuest Number: 10098365

All rights reserved

INFORMATION TO ALL USERS

The quality of this reproduction is dependent upon the quality of the copy submitted.

In the unlikely event that the author did not send a complete manuscript and there are missing pages, these will be noted. Also, if material had to be removed, a note will indicate the deletion.



ProQuest 10098365

Published by ProQuest LLC(2016). Copyright of the Dissertation is held by the Author.

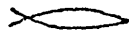
All rights reserved.

This work is protected against unauthorized copying under Title 17, United States Code.  
Microform Edition © ProQuest LLC.

ProQuest LLC  
789 East Eisenhower Parkway  
P.O. Box 1346  
Ann Arbor, MI 48106-1346

## ACKNOWLEDGEMENTS

I would like to express my appreciation of the help and advice of the late Dr. W. T. Dixon and my gratitude to Dr. D. Murphy and Dr. D. M. Hall for their help and encouragement since summer 1977. I would also like to thank Professor G. H. Williams for providing research facilities and the University of London for a university research studentship.



Lauda, Sion, Salvatorem,

Lauda ducem et pastorem,

In hymnis et canticis.

Quantum potes, tantum aude:

Quia major omni laude

Nec laudare sufficis.

## ABSTRACT

An e.s.r. study of the reaction between 1,4-benzoquinone and sodium azide was made and spectra obtained of some novel triazolo-1,4-semiquinones and also some hitherto unobserved amino-1,4-semiquinones.

These results are interpreted in terms of two competing types of addition of  $\text{HN}_3$  to quinone, one being dipolar addition, leading to triazolohydroquinones and the other leading to azidohydroquinones. The decomposition of azidohydroquinones provides a new route to amino-substituted radicals.

Using the McLachlan method for calculating Hückel molecular orbital energies in the anilino radical cation, suitable Hückel parameters for nitrogen were derived. These parameters were tested by calculating spin distributions in the aminophenoxyl series and were then used to confirm the assignments of experimental splitting constants in the amino- and heterocyclic semiquinones.

The occurrence of negative McLachlan spin densities in some of the radicals has been discussed and an attempt has been made to interpret the high-field line broadening in the triazolo-1,4-semiquinone spectrum.

## CONTENTS

	Page
CHAPTER 1 INTRODUCTION	1
1. Starting Point	2
Part A. Theory	
2. Electron Spin Resonance	3
3. Nuclear Hyperfine Interaction	5
4. Mechanism of Hyperfine Interaction in $\pi$ Radicals	9
5. Simple Molecular Orbital Theory	11
The Hückel Method	11
The McLachlan Method	13
6. Heteroatoms and Parameterisation	18
Part B. Nitrogen Substituted Compounds	
7. Addition of Hydrogen Azide to Quinones	21
8. Nucleophilic Substitution by Azide Ion	23
9. 1,3-Dipolar Addition of Azides	23
10. 1,2,3-Triazoles	25
11. Aminoquinones	26
12. E.s.r. of Aminoquinones	26
 CHAPTER 2 E.S.R. SPECTRA	 30
1. Experimental	31
Instrumental	31
Generation of Radicals	31
Materials	31

2. Amino-1,4-semiquinones	36
2,5-Diamino-1,4-semiquinone	36
2-Amino-5-methyl-1,4-semiquinone	42
2-Amino-1,4-naphthosemiquinone	46
Secondary Aminosemiquinone Radicals	46
3. Triazolo-1,4-semiquinones	52
2,3-Triazolo-1,4-semiquinone	52
2,3;5,6-Bis-triazolo-1,4-semiquinone	56
2-Methyl-triazolo-1,4-semiquinone	61
2-t-Butyl-triazolo-1,4-semiquinone	64
2,3-Triazolo-1,4-naphthosemiquinone	68
4. Azido-1,4-semiquinones	71
2,3,5,6-Tetraazido-1,4-semiquinone	71
2-Azido-3,6-di-t-butyl-1,4-semiquinone	73
CHAPTER 3 NITROGEN MOLECULAR ORBITAL PARAMETERS	75
1. Amino Group Spin Density Distribution	76
2. "Experimental" Spin Densities in Anilino Radical Cation	77
3. Sigma-pi Interaction in the Amino-fragment	79
4. The Aminophenoxy Series	81
CHAPTER 4 MOLECULAR ORBITAL CALCULATIONS	85
1. Heterocyclic Semiquinones	86
2. Aminosemiquinones	88
3. Hydroxyl Protons	92

CHAPTER 5 DISCUSSION	93
1. Interaction of 1,4-Benzoquinone with Sodium Azide	94
2. Symmetry Considerations	100
3. Amino Group Spin Densities	103
4. Line-broadening in the Spectrum of Triazolosemiquinone	107
REFERENCES	114
LIST OF TABLES	123
LIST OF FIGURES	125
PUBLICATION	



CHAPTER 1

INTRODUCTION

## 1. Starting Point

The e.s.r. spectra of semiquinones are well known<sup>1,2,3,4</sup> and the effects upon their spin density distribution, of many types of substituent, have been examined.<sup>5,6,7</sup> The work reported here started from an attempt to produce a 1,4-semiquinone bearing an azido-group ( $-N_3$ ).

Our interest in the azido-group was two-fold. In spite of the number and variety of organic azides,<sup>8,9,10</sup> no e.s.r. spectrum has ever been reported for an organic azide radical. Besides the prospect of seeing a signal from an azido-semiquinone, the azido-group itself can be regarded as a conveniently blocked amino-group, from which  $-NH_2$  may be released on mild reduction. The conditions required to generate a free radical from a quinone (or hydroquinone<sup>2</sup>) parent, might also be expected to lead to some hitherto elusive amino-semiquinones.

The second point of interest was in the observation of any semiquinones with substituents containing nitrogen, since evidence of such species is scant and poorly characterised.<sup>11,12,13,14</sup> This would provide additional material for testing simple molecular orbital theory, by correlating calculated spin densities with appropriate hyperfine coupling constants.

## Part A. Theory

### 2. Electron Spin Resonance

For a molecule to give an e.s.r. spectrum, it must possess an unpaired electron. Because of its spin motion, the unpaired electron possesses a net angular momentum and associated with this, a magnetic dipole which can interact with an external magnetic field. The quantum mechanical solution to this interaction allows only two orientations (characterised by the quantum number,  $M_s = +\frac{1}{2}, -\frac{1}{2}$ ) of the electron's magnetic dipole with respect to the field. Each orientation represents an energy level, the separation of which depends upon the strength of the applied field (see Fig. 1, page 4).

The basis of the resonance technique is to cause transitions between these orientations, or energy levels, by supplying the appropriate energy radiation, ( $h\nu$ ). The resulting transition is then detected as an absorption of energy, which is described by a resonance condition, relating the radiation frequency to the strength of the external magnetic field,  $H_r$ , at resonance

$$h\nu = \Delta E = g\beta H_r \quad \dots \text{Eq. 1}$$

For transitions between electron spin energy levels,  $g$  is a constant particular to the system, near to 2.00 for most

organic free radicals,<sup>15</sup> and determines the required strength of the magnetic field. In Eq. 1,  $\beta$  is the Bohr Magneton,<sup>16</sup> the constant converting electron angular momentum to magnetic moment;  $h$  is Planck's constant. Shown in Fig. 1 is an e.s.r. transition (dotted line) for two possible spin states,  $M_s = +\frac{1}{2}, -\frac{1}{2}$ , where  $E_1$  and  $E_2$  represent the lower and higher energy states, respectively. In this diagram, the frequency is constant and the energy level separation is shown as a function of field strength,  $H$ .

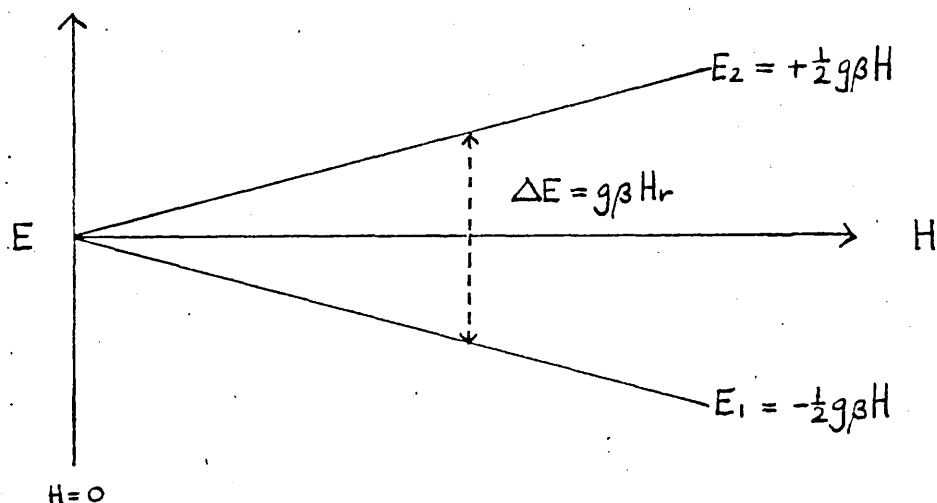


Fig. 1 An e.s.r. transition for  $M_s = +\frac{1}{2}$

In order to generate the spectrum, either the separation of energy levels is fixed, by keeping  $H$  constant, and the incident radiation varied until the resonant frequency is found or, the frequency is held constant and the field strength varied. Conventionally, e.s.r. is the variation of energy

level separation by varying the external magnetic field. The population of two different energy states is, in conditions of thermal equilibrium, a Boltzman distribution,

$$\frac{n_2}{n_1} = \exp \left\{ \frac{-g\beta H}{kT} \right\} \quad \dots \text{Eq. 2}$$

where  $n_1$  and  $n_2$  are the number of spins in the lower and upper states respectively. The equation shows that as the field strength increases,  $n_2/n_1$  decreases and the probability of a net absorption increases.

### 3. Nuclear Hyperfine Interaction

The magnetic dipole of an electron may also interact with a nucleus in its vicinity, if the nucleus possesses intrinsic spin with a resultant nuclear magnetic moment. Nuclear spin is also quantised and in a magnetic field, for a nucleus of spin  $I$ , there are  $(2I+1)$  possible spin or energy states, where  $I$  may be any integral multiple of  $\frac{1}{2}$ . These can be aligned parallel or antiparallel to the electron spin states, so that the electron experiences not only the applied field,  $H$ , but also local fields due to the magnetic nucleus,

$$\Delta E = g\beta(H + H_{local}) \quad \dots \text{Eq 3}$$

where the values in brackets are represented in the resonance condition (Eq. 1) by  $H_r$ . For the simplest nucleus,  $I = \frac{1}{2}$ , the electron will experience two possible local fields corresponding to  $M_I = +\frac{1}{2}$ ,  $-\frac{1}{2}$ , and resonance will occur at two values of the applied field,  $H$ . When the nuclear spin is parallel to the applied field, the value required for resonance will be lower and when it opposes the field, the value required will be higher. Fig. 2(a) shows the four possible spin states in the system  $M_S = \pm\frac{1}{2}$ ,  $M_I = \pm\frac{1}{2}$ , where  $H_{eff}$  is the effective field felt by the electron in the vicinity of nucleus I. A selection rule,  $\Delta M_I = 0$ ,  $\Delta M_S = \pm 1$ , governs the observable transitions so that only those in which  $M_I$  does not change are permitted. Fig. 2(b) shows the two allowed transitions for this system in which the single absorption line in Fig. 1 has become a doublet corresponding to those transitions. The dotted lines show the energy levels and single transition for the system shown in Fig. 1 where  $M_S = \pm\frac{1}{2}$ .

For a particular  $M_S$  value, the energy gap between  $M_I$  levels is comparatively so small that the nuclear spin states are approximately equally populated. Transitions from both  $M_I$  states are approximately equally probable so that the absorptions are of about equal intensities and a 1:1 doublet is observed (Fig. 2(b)). The spacing between the absorption

$M_s$	$M_I$	$H_{\text{eff}}$	
$\uparrow \alpha$	$\uparrow \alpha$	$H + H_{\text{local}}$	
$\uparrow \alpha$	$\downarrow \beta$	$H - H_{\text{local}}$	
$\downarrow \beta$	$\downarrow \beta$	$H - H_{\text{local}}$	
$\downarrow \beta$	$\uparrow \alpha$	$H + H_{\text{local}}$	

Fig. 2(a) Four possible spin states for a system with  $M_s = \pm \frac{1}{2}$ ,  $M_I = \pm \frac{1}{2}$  showing effective field,  $H_{\text{eff}}$ , felt by the electron in the vicinity of the nucleus.

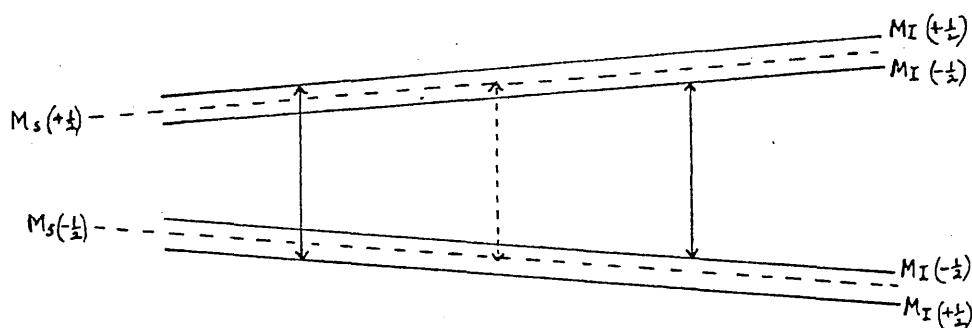


Fig. 2(b) The energy levels and allowed transitions between them shown as arrows, for the above system as a function of the applied field,  $H$ .

lines, called the hyperfine coupling, is a function of the separation of the nuclear energy levels and is characteristic of each individual nucleus causing the splitting of the single absorption line. The number of splittings from a single magnetic nucleus depends upon the nuclear spin value  $I$  and is the same as the multiplicity of spin states  $(2I+1)$ . The relative intensities of the lines depend upon the degeneracies of the energy levels. Where there is a coincidence of two levels, transitions involved with them will be reflected in one line, twice as intense. The degeneracy of each line of a set of  $n$  equivalent nuclei is given by the coefficients of expansion of  $(a+b+c\dots)^n$  where the number of terms in brackets is equal to the multiplicity value,  $(2I+1)$ . For a nuclear spin of  $\frac{1}{2}$ , there are two terms and the degeneracies, for  $n$  of these nuclei, are those of the binomial expansion  $(a+b)^n$  and are given by Pascal's Triangle. For a  $^{14}\text{N}$  atom ( $I=1$ ) the degeneracies are shown in Fig. 3.

$n$	relative amplitude of spectral lines									
1				1	1	1				
2			1	2	3	2	1			
3		1	3	6	7	6	3	1		
4	1	4	10	16	19	16	10	4	1	

Fig. 3 Degeneracy ratios of a set of  $n$  equivalent nitrogens.



In general, for  $n$  equivalent nuclei of spin  $I$ , the resultant hyperfine splitting involves  $(2nI+1)$  lines. Where there are non-equivalent nuclei, each nucleus interacts with the unpaired electron differently, though sometimes there is a fortuitous equivalence of coupling constants. For a set of  $n$  equivalent and  $m$  equivalent nuclei, there will be a maximum number of possible lines given by  $(2nI+1)(2mI+1)$ .

The overall spread of a spectrum is given by,

$$\text{width} = 2 \sum I_i a_i \quad \dots \text{Eq. 4}$$

where  $a_i$  is the coupling constant of the nucleus,  $i$  (of spin  $I_i$ ) and where the summation is over all nuclei contributing to the splitting pattern.

#### 4. Mechanism of Hyperfine Interaction in $\pi$ radicals<sup>17</sup>

There are two types of nuclear hyperfine interaction, anisotropic and isotropic. Interaction between electron and nuclear dipoles gives rise to the anisotropic component of hyperfine coupling, which is dependent upon the orientation of the nuclear spin with respect to electron spin. In a

liquid of low viscosity, anisotropic interactions are, through rapid tumbling, averaged to zero.<sup>17</sup>

Isotropic (or so-called Fermi) interaction depends upon there being finite unpaired electron density at the nucleus concerned. This implies that there should be no isotropic interaction between the unpaired electron in a carbon  $2p_z$  orbital and a nucleus situated in its nodal plane. However,  $\pi$  radicals do show hyperfine interaction with protons situated in this plane although this is only some five-percent of the maximum possible interaction for a hydrogen atom. McConnell<sup>18</sup> found that the observed coupling with protons bonded to a carbon in an aromatic system,  $a_{CH}^H$ , is related to the unpaired  $\pi$  electron density,  $\rho_C^\pi$ , on the carbon atom by a simple linear proportionality,

$$a_{CH}^H = Q_{CH}^H \rho_C^\pi \quad \dots \text{Eq. 5}$$

where  $Q_{CH}^H$  is the proportionality constant, sometimes called the sigma-pi parameter.<sup>18</sup> This interaction arises from the presence of net spin density (as distinct from unpaired electron density) at the proton. This is accounted for<sup>18,19</sup> by the unpairing, or polarising, effect which the unpaired electron in the carbon  $2p_z$  orbital exerts upon the paired electrons in the adjacent C-H sigma bond. The spin density engendered at the proton is opposite in sign to that of the unpaired electron, so that the sigma-pi parameter  $Q_{CH}^H$  should be negative;<sup>18</sup>

this has been confirmed experimentally by the negative sign of some aromatic proton coupling constants.<sup>19,20</sup> Negative spin densities may sometimes occur at the carbon atoms however, as demonstrated by proton couplings which are positive in sign.<sup>5</sup>

## 5. Simple Molecular Orbital Theory

The magnetic nuclei in a free radical act as sensitive indicators of the distribution of the unpaired electron throughout the molecule. Using molecular orbital theory, experimental coupling constants can be correlated with the theoretical spin density distribution, which may make possible predictions and assignments in related species.

The business of simple molecular orbital methods<sup>21</sup> is to find approximate solutions to the Schrödinger wave equation, corresponding to the energy states or orbitals, which lead to values for the spin densities in the unpaired electron orbital. One basis for this operation is the Hückel method for planar conjugated systems.<sup>22</sup>

### The Hückel M.O. Method

The Hückel method obtains the energies of the  $\pi$  electrons from sets of linearly combined atomic orbitals (molecular

orbitals).<sup>22</sup> The molecular orbitals are assumed to be doubly filled and the unpaired electron assigned to the next highest unfilled orbital, according to the Aufbau principle.

The wave function coefficients, adjusted to minimise the total energy of the system (Variation method<sup>21</sup>), dictate the signs and magnitudes of each separate atomic orbital's contribution to the molecular orbital, giving both a qualitative view of the orbital (bonding or antibonding, how many nodal planes it has) and also an indication of the relative distribution of the unpaired electron. The unpaired electron density,  $\rho_i$ , for atom  $i$ , is given by

$$c_{ij}^2 = \rho_i \quad \dots \text{Eq. 6}$$

where  $C_{ij}$  is the atomic orbital coefficient of atom  $i$  in the  $j^{\text{th}}$  molecular orbital, (no. of electrons =  $2j-1$ ).

Out of the Variation method arise certain integrals which expand into secular equations.<sup>21</sup> Two which are important in the Hückel method, are the coulomb and resonance integrals. The coulomb integral, written as  $\alpha$  (not to be confused with spin state  $\alpha$ ), represents the energy of the carbon 2p orbital in a non-bonding state. The resonance integral, written as  $\beta$ , represents the effect of bonding upon the energy of the orbital. In the Hückel method, these two integrals are not evaluated in themselves but yield a set of roots (or solutions)

to the secular equations, which represent a series of energy levels,

$$E_i = \alpha + m_i \beta \quad (i = 1, \dots, n) \quad \dots \text{Eq. 7}$$

relative to an energy zero ( $m_i = 0$ ). Since both  $\alpha$  and  $\beta$  are negative quantities,<sup>22</sup> positive  $m_i$  values ( $\alpha + m_i \beta$ ) represent more stable (bonding) energy levels. Fig. 4 shows the Hückel energies of benzene and benzoquinone, in terms of  $\alpha$  and  $\beta$ .

#### The McLachlan Method<sup>23</sup>

The Hückel method does not take into account the difference between electron spins (up or  $\alpha$ -spin and down or  $\beta$ -spin, conventionally) and neglect of repulsions between paired and unpaired spins is a serious limitation of this method, failing to account for the appreciable negative spin densities which many aromatic radicals containing heteroatoms show.<sup>24,25</sup> The McLachlan method accounts for negative spin densities by introducing a simple perturbation of the  $\pi$  electrons into the Hückel calculation.

The unpaired electron will, if say, of  $\alpha$ -spin, affect a paired  $\alpha$ -spin electron differently from the way it affects

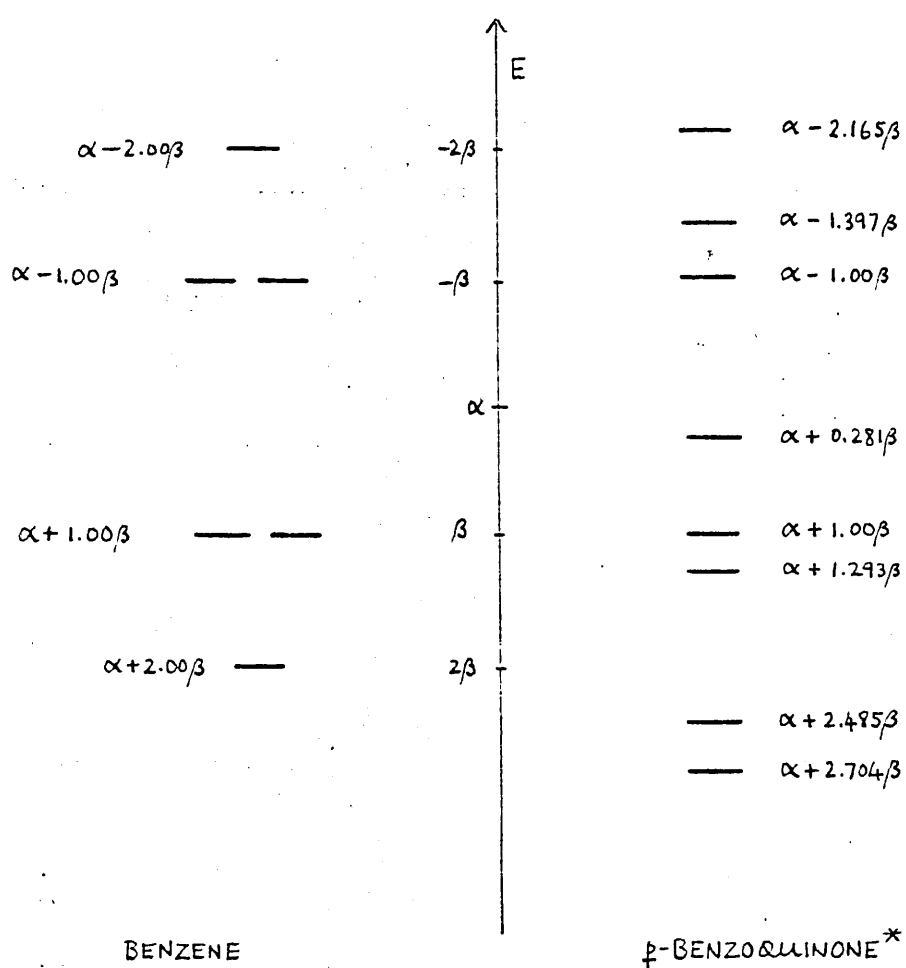


Fig. 4. Hückel orbital energies for benzene and *p*-benzoquinone with the reference energy taken as  $\alpha$  (\* calculated with Hückel parameters  $\alpha_0 = \alpha + 1.6\beta$ ,  $\beta_{CO} = 1.3\beta$ , see 1-6).

a paired  $\beta$  electron because there is an exchange interaction<sup>26</sup> between it and paired electrons of like spin. The unpaired electron is treated as occupying a perturbed molecular orbital<sup>27</sup> (and by convention, designated as  $\alpha$ -spin) so that for a system with  $(2n+1)$  electrons,  $(n+1)$  occupy perturbed (or modified Hückel) orbitals and  $(n)$  occupy unperturbed (or ordinary Hückel) orbitals. Fig. 5 shows the unperturbed orbitals,  $B_i$ , obtained by normal Hückel calculation. The perturbed orbitals,  $A_j$ , are obtained by modifying the Hückel coulomb integral,  $\alpha_r$ , for each atom by the appropriate calculated Hückel unpaired electron density  $(b_o^r)^2$ ,

$$\alpha_r \text{ (modified)} = \alpha_r + 2\lambda (b_o^r)^2 \quad \dots \text{Eq. 8}$$

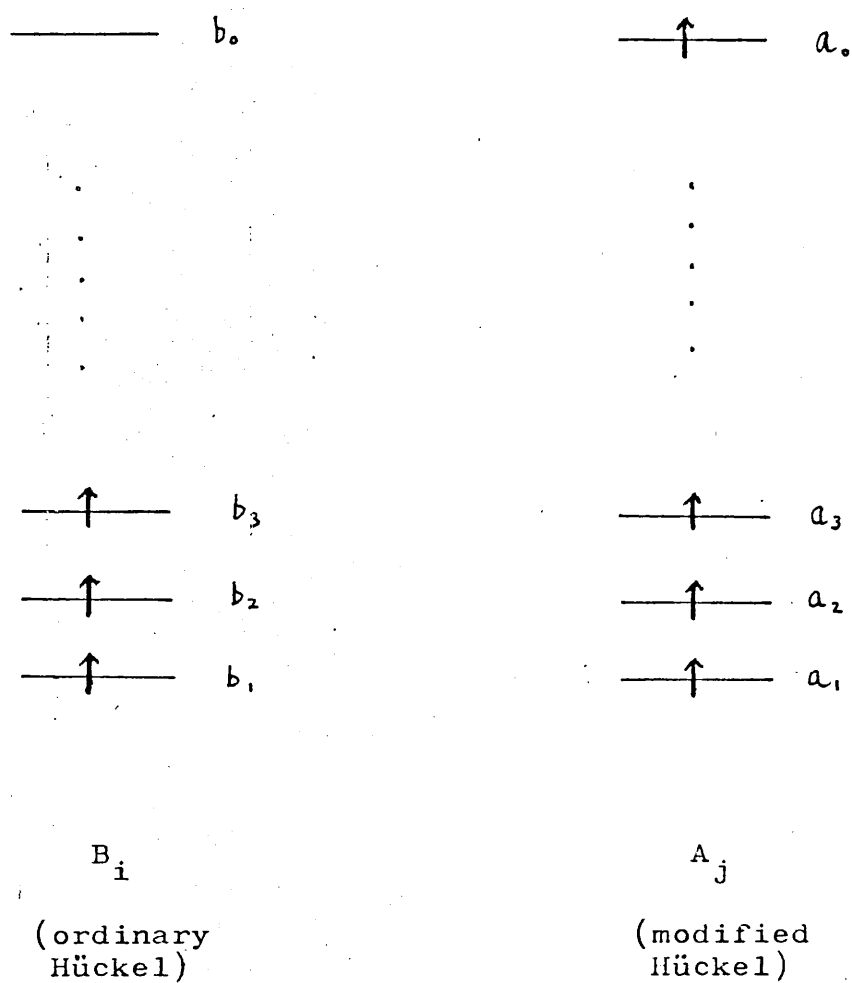
where  $\lambda$  is a constant set to 1.2.<sup>23</sup>

The total  $\alpha$ -spin density on atom  $r$ , is given by a summation of the atomic orbital coefficients,  $a_j^r$ , as

$$\sum_j (a_j^r)^2 = (a_1^r)^2 + (a_2^r)^2 + (a_3^r)^2 + \dots + (a_o^r)^2 \quad \dots \text{Eq. 9}$$

$(j = n+1)$

where  $a_o^r$  is the coefficient of the  $(n+1)^{\text{th}}$  orbital containing

ORBITALS

(o represents unpaired electron orbital)

Fig. 5 Showing the occupancy of the unperturbed (Hückel) and perturbed (modified) molecular orbitals (Aufbau).



the unpaired electron.<sup>27</sup> Total  $\beta$ -spin density is likewise given by,

$$\sum_i (b_i^r)^2 = (b_1^r)^2 + (b_2^r)^2 + (b_3^r)^2 + \dots + (b_n^r)^2 \quad \dots \text{Eq. 10}$$

(i=n)

The net spin density at atom r, is then given by the difference between the perturbed ( $\alpha$ ) and unperturbed ( $\beta$ ) spin density functions for that point. This is where the possibility of negative spin density arises, since the total  $\beta$ -spin density may sometimes amount to more than the total  $\alpha$ -spin density at a particular point. Resultant net spin density,  $\rho_r$ , is computed from

$$\rho_r = (a_0^r)^2 + \sum_{\text{occupied}} [(a_j^r)^2 - (b_i^r)^2] \quad \dots \text{Eq. 11}$$

(i, j  $\neq$  0)

## 6. Heteroatoms and Parameterisation<sup>25</sup>

In applying Hückel molecular orbital theory to aromatic radicals, heteroatoms are treated as pseudo-carbon atoms, with appropriate changes made to the coulomb and resonance integrals by introducing two parameters,  $h$  and  $k$ , associated with the heteroatom and bond respectively,

$$\alpha_x = \alpha + h_x \beta \quad \dots \text{Eq. 12}$$

$$\beta_{cx} = k_{cx} \beta \quad \dots \text{Eq. 13}$$

where  $\alpha$  and  $\beta$ , without subscripts, refer to aromatic carbon  $p^\pi$  orbitals.

The relation between  $^{14}\text{N}$  hyperfine coupling and spin density at the nitrogen atom, has already been examined for a number of free radicals, where nitrogen forms part of a heteroaromatic ring,<sup>28,29,30,31,32,33</sup> or is part of a substituent group attached to an aromatic system.<sup>34</sup> Adjacent atom spin densities<sup>35</sup> were thought to contribute to the nitrogen coupling constant,<sup>28,29,31</sup>  $a_N$ , but there is some evidence that these are insignificant<sup>36,37,38</sup> and a linear dependence of  $a_N$  on nitrogen spin density,  $\rho_N$ ,

$$a_N = Q_N \rho_N \quad \dots \text{Eq. 14}$$

has been established for some heteroaromatic radicals.<sup>28,33,39</sup>

In amino-substituted radicals, the near equivalence of nitrogen and aminoproton hyperfine coupling,

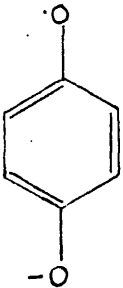
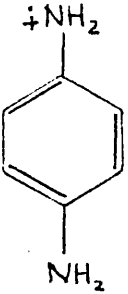
$$a_{\text{NH}}^{\text{H}} \approx a_{\text{N}} \quad \dots\text{Eq. 15}$$

has been observed<sup>13,33</sup> and rationalised in terms of a spin polarisation mechanism.<sup>34,39</sup>

Ideally, the parameters used in spin density calculations should be derived from first principles, but in practice are found empirically on the basis of the best fit to experimental coupling. By suitably varying  $h_x$  and  $k_{\text{cx}}$  (Eqs. 12,13), excellent agreement with a small number of couplings may be reached, but in isolation such parameters are virtually meaningless. Furthermore, there are no unique values for  $h_x$ ,  $k_{\text{cx}}$  or for Q-values. For highly symmetric structures like *p*-benzosemiquinone (I) or *p*-phenylenediamine (II), more than one set of values can be found to reproduce the experimental values, (see Table 1) and the usefulness of molecular orbital correlation must depend on how many successful predictions can be made using comparatively few parameters. By deriving better oxygen atom parameters and using the McLachlan procedure for calculation, a marked improvement over previous work<sup>5,6</sup> was obtained with substituted phenoxy radicals<sup>25,41</sup> and we have used these parameters unchanged (see Chapter 3).

Table 1

## Molecular Orbital Parameters

Experimental couplings a/Gauss <sup>2,34</sup>		Parameters used for calculation					
 <p>I</p>	$a_{\text{CH}}^{\text{H}} = 2.14$	$h_{\text{O}}$	$k_{\text{CO}}$	$Q_{\text{CH}}^{\text{H}}$	Ref.		
		1.2	1.56	22	5		
		1.6	1.3	30	25		
 <p>II</p>	$a^{\text{N}} = 5.29$	$h_{\text{N}}$	$k_{\text{CN}}$	$Q_{\text{N}}$	$Q_{\text{NH}}^{\text{H}}$	$Q_{\text{CH}}^{\text{H}}$	Ref.
	$a_{\text{NH}}^{\text{H}} = 5.88$	0.85	1.0	25	25	28	34
	$a_{\text{CH}}^{\text{H}} = 2.13$	1.3	1.0	25	30	30	40

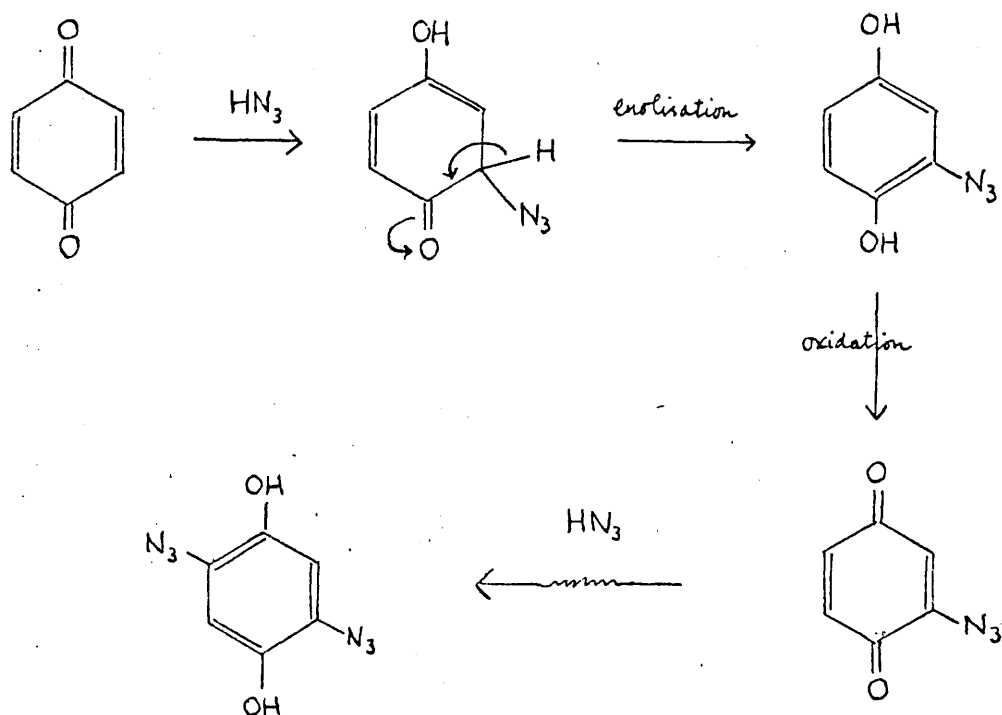
Part B. Nitrogen Substituted Compounds

7. Additions of Hydrogen Azide to Quinones

Reactions of benzoquinones with hydrogen azide ( $\text{HN}_3$ ) in organic solvents, leading to azidohydroquinones, were established in 1915;<sup>42</sup> more recently it was shown that similar additions of  $\text{HN}_3$  are effected with acidified aqueous solutions of sodium azide.<sup>43,44,45</sup>

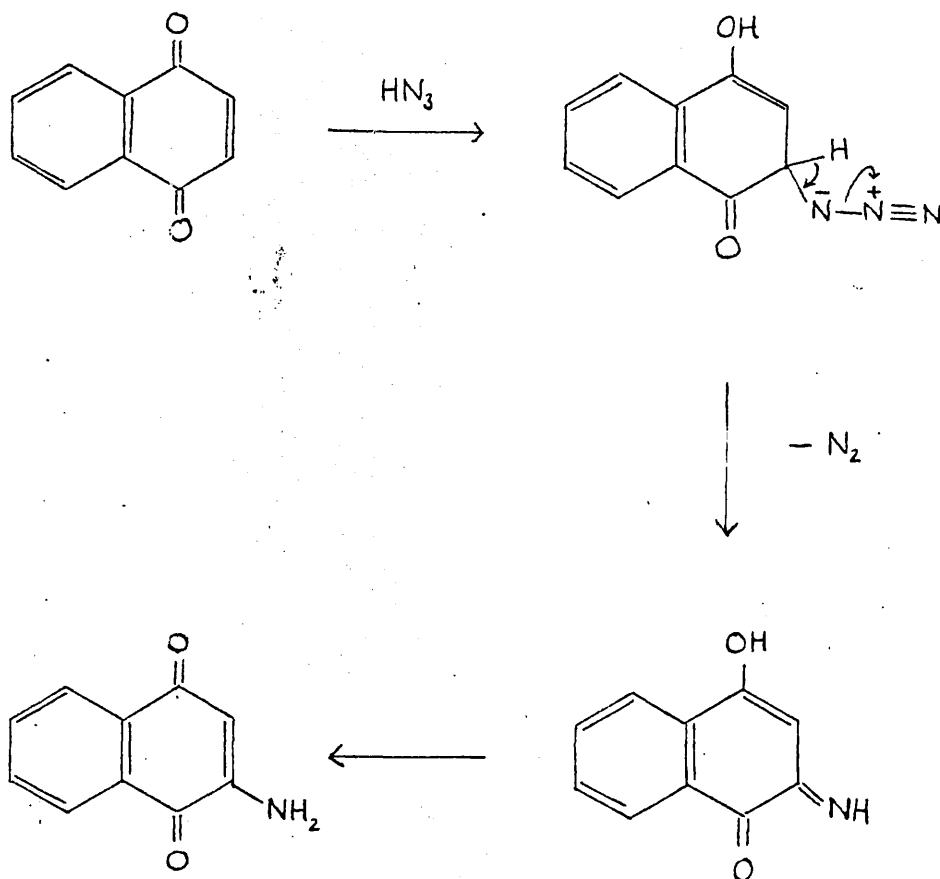
These reactions follow a pattern of easy additions to  $\alpha,\beta$ -unsaturated carbonyl compounds,<sup>46</sup> in which the initial addition<sup>42,47</sup> is followed by enolisation, oxidation and further addition.<sup>44</sup>

Scheme 1



In some cases, aminoquinones are formed directly as a result of reaction between sodium azide and a quinone.<sup>43</sup>

Scheme 2

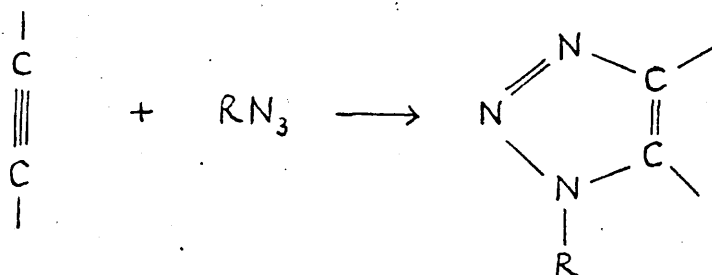


8. Nucleophilic Substitution by Azide Ion

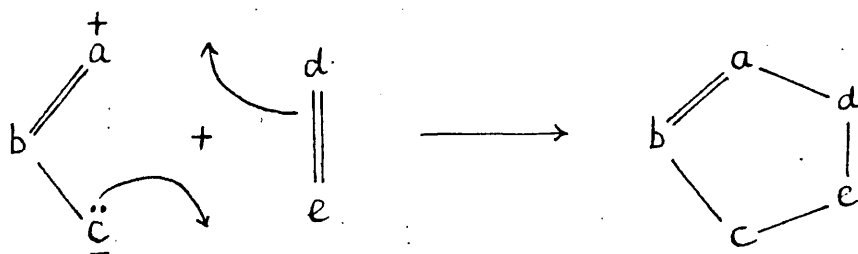
Synthesis of azidoquinones by reaction between halogenoquinones and sodium azide is well established,<sup>48</sup> in which nucleophilic substitution by azide ion ( $\text{N}_3^-$ ) of a suitable leaving group, takes place.

9. 1,3-Dipolar Addition of Azides

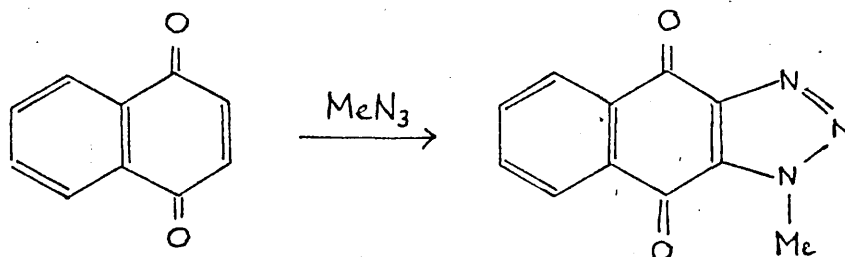
Reaction between organic azides ( $\text{RN}_3$ ) and acetylenes to produce 1,2,3-triazoles,<sup>49</sup>



were the first examples of what was later classified as 1,3-dipolar cycloaddition<sup>50,51,52</sup> (see over)



Methyl<sup>53</sup> and phenyl<sup>54</sup> azides are known to undergo such additions to 1,4-quinones to form N-substituted triazole compounds.

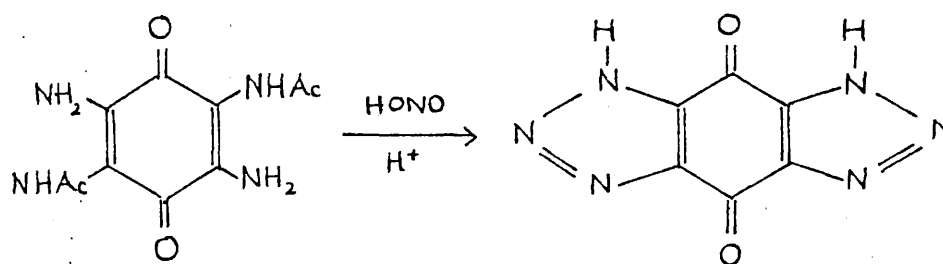


However, although a mechanism via a triazole intermediate was proposed for the addition of  $\text{HN}_3$  to 1,4-naphthoquinone, leading to 2-amino-1,4-naphthoquinone,<sup>56</sup> there is no report of a triazole resulting from the addition of  $\text{HN}_3$  to carbon-carbon double bonds.



10. 1,2,3-Triazoles

1,2,3-Triazoles have been synthesised by ring closure between suitable groups<sup>57,58</sup> as exemplified by bis-triazolo-1,4-quinone.<sup>55</sup>



Considering the variety of chemical reactions which triazole compounds undergo,<sup>58</sup> the triazole ring is remarkable in its resistance to reduction, oxidation and stability to high temperature, although benzotriazole<sup>57</sup> was reported to decompose explosively during distillation.<sup>59</sup>

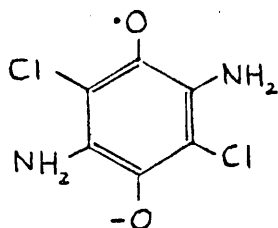
## 11. Aminoquinones

Azidoquinones have been shown by experiment to disproportionate readily to aminoquinones.<sup>43,44,45</sup> However, pure aminoquinones are not available commercially and cannot be synthesised easily. Synthesis results in products of low purity which are difficult to separate from other products of reaction.<sup>14,44</sup> Aminoquinones have a poor solubility,<sup>14</sup> except in concentrated acids where dissolution is accompanied by chemical reaction<sup>60</sup> and in concentrated bases, where marked solvolysis also occurs.<sup>61</sup>

## 12. E.s.r. of Aminoquinones

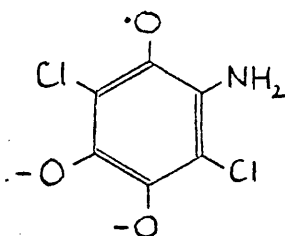
The first amino-substituted benzosemiquinone reported<sup>11</sup> was 2,5-diamino-3,6-dichloro-1,4-semiquinone (III),

III



whose couplings were rationalised by comparison with a spectrum of 2-amino-5-hydroxy-3,6-dichloro-1,4-semiquinone (IV),

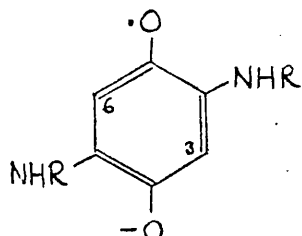
IV



Although the latter was poorly resolved,<sup>11</sup> the expected triplet of triplets ( $^1\text{H}(2)$ ,  $^{14}\text{N}(1) \equiv 1:2:1 \times 1:1:1$ ) could be analysed.

More recently, the semiquinone radical anions of some N-substituted aminoquinones,  $\text{C}_6\text{H}_2\text{O}_2(\text{NHR})_2^-$

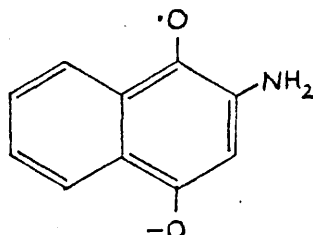
V-IX



(where R = methyl, ethyl, isopropyl, n-propyl and t-butyl, V-IX) were reported<sup>14</sup> showing a general pattern of couplings from the amino groups and ring protons, 3 and 6. Another report<sup>12</sup> of 2,5-bis(t-butylamino)-1,4-semiquinone (IX) shows slightly different coupling constants, probably due to solvent effects.<sup>62</sup>

Two separate reports<sup>13,14</sup> of the species 2-amino-1,4-naphthosemiquinone, (X),

X



show differing couplings from the amino groups (see Table 2) in different solvents.

The radicals, in all cases but one,<sup>12</sup> were generated from the quinone precursors and the reports suggest hampering of any definitive analysis by poor resolution and low signals. No mention has been made so far in the literature of the species, 2,5-diamino-1,4-semiquinone.

Table 2

E.s.r. Coupling Constants of Aminosemiquinones  
from the Literature.

Radical Species	E.s.r. Coupling Constants (a/Gauss)				Ref.
	$a_N$	$a_{NH}^H$	$a_{alkyl}^H$	$a_{ring}^H$	
III <sup>a</sup>	2.3	1.5			11
IV <sup>a</sup>	2.5	0.6			11
V-VIII <sup>b,c</sup>	3.0	2.3	3.0	0.8	14
IX <sup>c</sup>	2.98	2.44		0.76	14
IX <sup>d</sup>	2.06	1.54		0.52	12
X <sup>e</sup>	1.07	1.07			13
X <sup>f</sup>	1.37	0.78			14

a Radicals by sodium dithionite reduction in pyridine, ethylene glycol and KOH solvent mixture (see 11).

b Coupling constants averaged for series V-VIII (maximum deviation/Gauss,  $a_N \pm 0.17$ ,  $a_{NH}^H \pm 0.2$ ,  $a_{ring}^H \pm 0.03$ ,  $a_{alkyl}^H \pm 0.47$ ).

c Radicals by electrolytic reduction in aqueous media at pH 11-13.

d Radical from both quinone and hydroquinone in DMSO/tertiarybutyl alcohol solvent mixture (see Ref. 12).

e Radical by electrolytic reduction in acetonitrile.

f Radical by electrolytic reduction in aqueous ethanol.

## CHAPTER 2

E.S.R. SPECTRA

## 1. Experimental

### Instrumental

E.s.r. spectra were obtained on a Varian E4 spectrometer operating at a microwave frequency of ca. 9.5 GHz with a linearly varied static magnetic field strength of ca. 3400 Gauss ( $1 \text{ G} \equiv 10^{-4} \text{ T}$ ) for the radicals under investigation (g-factors ca. 2.00).

### Generation of radicals

Most radicals were generated in static autoxidation conditions<sup>1</sup> at room temperature. In a typical experiment, 1,4-benzoquinone (0.001 mole), dissolved in N,N-dimethylformamide (DMF) ( $10 \text{ cm}^3$ ), was treated with excess concentrated aqueous sodium azide (0.01 mole) and following a characteristic colour change and exothermia, the solution was investigated by adding aqueous, alkaline (1% NaOH) sodium dithionite ( $\text{Na}_2\text{S}_2\text{O}_4$ ).<sup>1</sup> Alternatively, a precursor such as 2,5-diazido-hydroquinone (0.1 g) was dissolved in water and with colour change, mild exothermia and evolution of nitrogen, the radical was generated as described. Previous studies<sup>63</sup> have shown that some radicals have induction periods of an hour or more. When no spectra were obtained within a few minutes, investigations were made repeatedly over a period of some hours.

### Materials

Materials which were available commercially were used with,

or without, further purification, as described below (Table 3). Other materials were prepared according to literature methods (Table 4); where ever it was possible to ascertain, their physical constants were compatible with those stated in the literature.

The obvious difficulties in identifying certain starting materials and, in some cases, analysis of reaction products, were due to the hazardous nature of organic azides<sup>64,65,45,10,(and refs. within)</sup> and possibly, in spite of their reported stability,<sup>58</sup> triazoles also.<sup>59</sup> We have shown in the subsequent pages that reaction solutions of quinones and azide may contain triazolo-, azido- and amino- compounds. Attempts were made to separate the complex and tarry mixtures by the usual extraction procedures,<sup>66</sup> but these were fruitless; one separation of a purple crystalline material resulted in total loss by explosion and no further investigation of this kind was pursued. Instead we attempted to prove the identity of the radical species by synthesising its immediate precursor. Details of the preparation of starting materials and their identification are shown below in Table 4.



Table 3. Commercial Materials

The following materials were available commercially and were used without further purification:

---

sodium azide
dimethylformamide
hexamethylphosphoramide
2,5-disulphonato-1,4-hydroquinone dipotassium salt
2-sulphonato-1,4-hydroquinone potassium salt
2-methyl-1,4-hydroquinone
2,5-di-t-butyl-1,4-hydroquinone
2-t-butylhydroquinone

---

The following materials were purified by recrystallisation:

---

Compound	Solvent	Physical Data
1,4-benzoquinone	light petroleum (80-100°)	golden yellow leaflets m.p. 113° (lit. <sup>67</sup> 115°)
1,4-naphthoquinone	ethanol	yellow needles m.p. 123° (lit. <sup>68</sup> 125°)
2,3,5,6-tetra- -chloro-1,4-quinone	toluene and benzene	golden yellow leaflets m.p. 283° (lit. <sup>69</sup> 290° sealed tube).

---

Table 4. Syntheses of Starting Materials

1. 2,5-diazido-1,4-hydroquinone from quinone,<sup>45</sup> white needles<sup>45</sup> rapidly discolouring after recovery, becoming red on long exposure to light or air. Deep red brown solution with alkaline sodium dithionite solution with evolution of nitrogen. 1,4-diacetoxy derivative m.p. 161°.<sup>45</sup>
2. 1,4-diacetoxy-2,5-diazidobenzene from 1.<sup>45</sup> m.p. 160-161° (lit.<sup>45</sup> 160-161°) white amorphous precipitate, yellowing on exposure. As for 1. when treated with alkaline dithionite solution.
3. 2,3;5,6-bis-triazolo-1,4-quinone\* from quinone,<sup>55</sup> yellow crystalline solid. Yellow solution with alkaline dithionite solution.
4. 2,3-triazolo-1,4-naphthoquinone\* from 1,4-naphthoquinone,<sup>55</sup> colourless crystals. Red solution with alkaline dithionite solution.
5. 2,5-dichloro-1,4-quinone<sup>67</sup> from quinone.<sup>71,72</sup>
6. 2,5-diamino-1,4-quinone from 1.<sup>45</sup> black crystalline solid m.p. > 360°;<sup>45</sup> also from 5. by passing gaseous NH<sub>3</sub> through an ethanolic suspension. Identity supported by elementary analysis.
7. 2-methyl-1,4-quinone from toluhydroquinone,<sup>67</sup> extracted with benzene, m.p. 63° (lit.<sup>70</sup> 69°).
8. 2-chloro-5-methyl-1,4-quinone from 7.<sup>71</sup>
9. 2,5-di-t-butyl-1,4-quinone from the hydroquinone;<sup>67</sup>

compound rapidly discolours and furs on exposure to air; bright yellow needles if suspended under glacial acetic acid until required. m.p.  $151^{\circ}$  (lit.  $153^{\circ}$ ).

10. 3-chloro-2,5-di-t-butyl-1,4-quinone from 9,<sup>74</sup> yellow oil.
11. 2,3,5,6-tetra-azido-1,4-quinone,<sup>65</sup> lustrous blue-black crystals; gives bright red solution with hexamethylphosphoramide (HMPA); undergoes various colour changes (deep cherry  $\rightarrow$  brown  $\rightarrow$  clear orange) with increasingly alkaline sodium dithionite solution, with evolution of nitrogen.

---

\* numbering throughout refers to quinone ring positions.

## 2. Amino-1,4-semiquinones

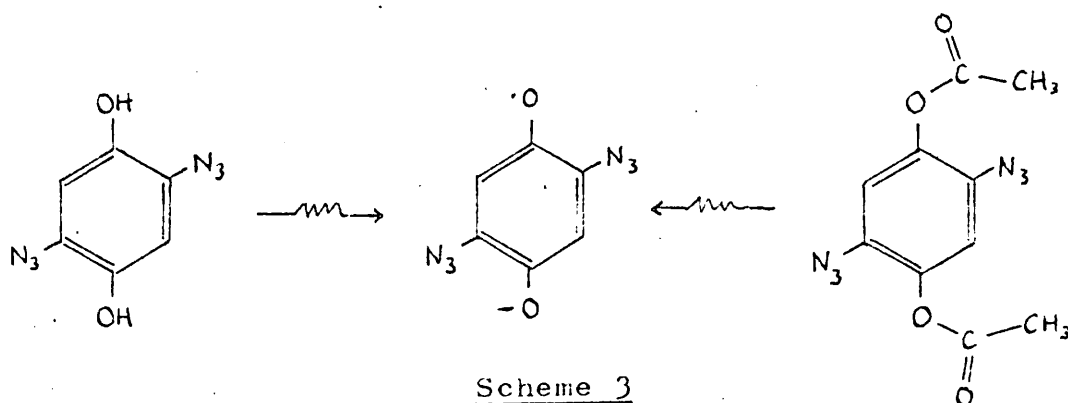
### 2,5-Diamino-1,4-semiquinone

Our initial experiment sought to generate a diazido-semiquinone which ought to give a simple hyperfine splitting pattern due to its symmetry.

When an aqueous solution of 2,5-diazido-1,4-hydroquinone<sup>45</sup> was treated with a trace of alkaline dithionite solution (see Generation of Radicals, page 31), a radical was generated whose spectrum is shown in Fig. 6. The signal persisted for sometime and later experiments showed that the radical remained stable in solution for several hours.

The spectrum was analysed as having three coupling constants: a large nitrogen quintet of 2.6 Gauss and two other couplings of 0.9 and 0.7 Gauss due to protons, a quintet and a triplet, respectively.

Because it is not possible to confirm the identity of the starting material,<sup>45</sup> its diacetoxy derivative, 1,4-diacetoxy-2,5-diazidobenzene was also investigated. Both starting materials would be expected to give rise to the same semiquinone anion in basic medium<sup>1</sup> (Scheme 3).



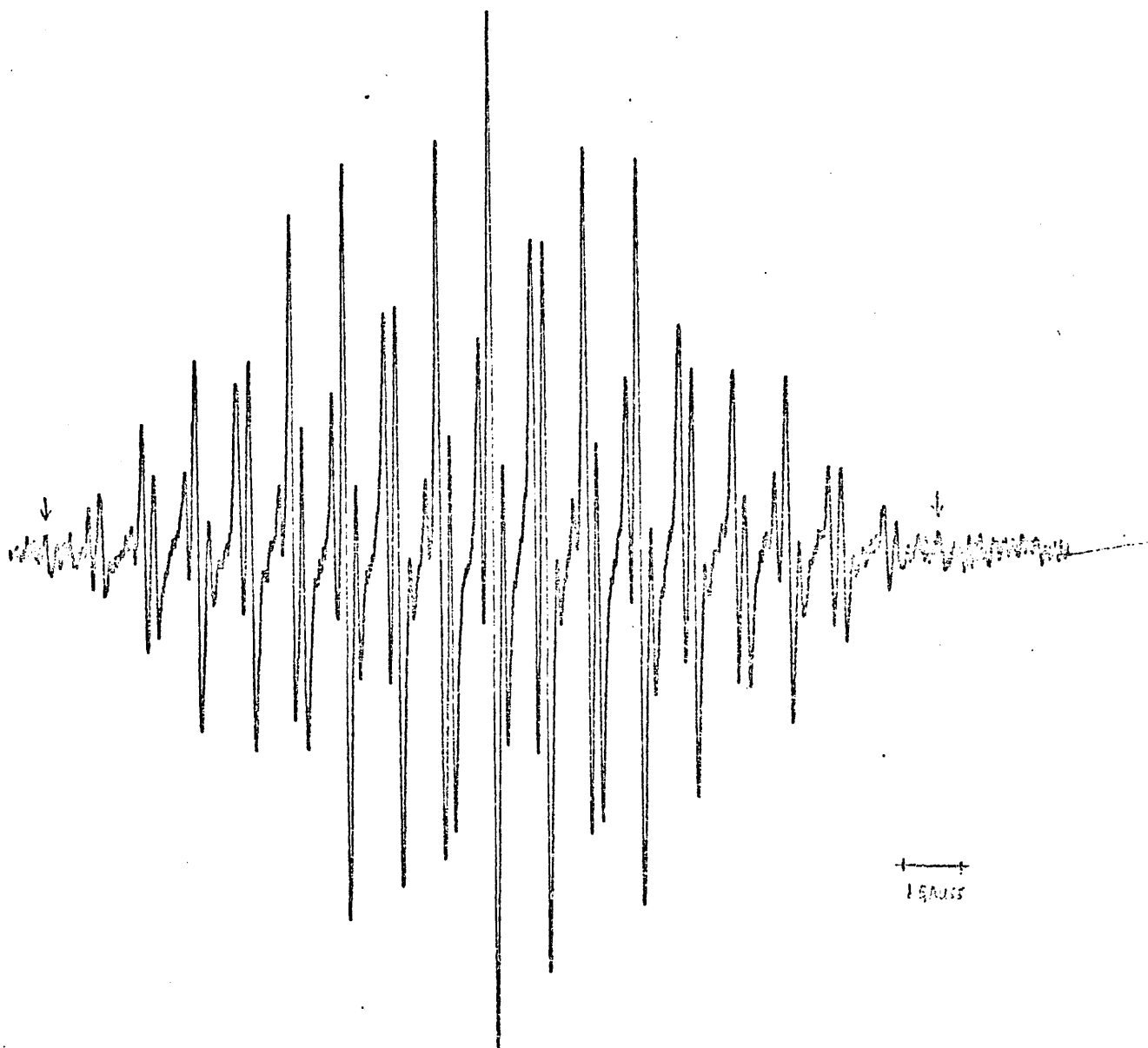
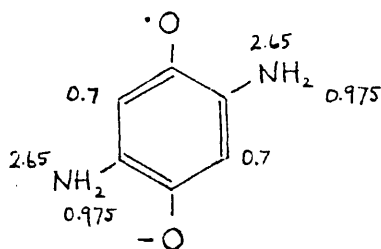


Fig. 6

However, no signal was observed after treatment of an aqueous solution of the diacetoxy compound with sodium hydroxide, but as with the hydroquinone starting material, treatment with alkaline dithionite gave a spectrum identical to that shown in Fig. 6.

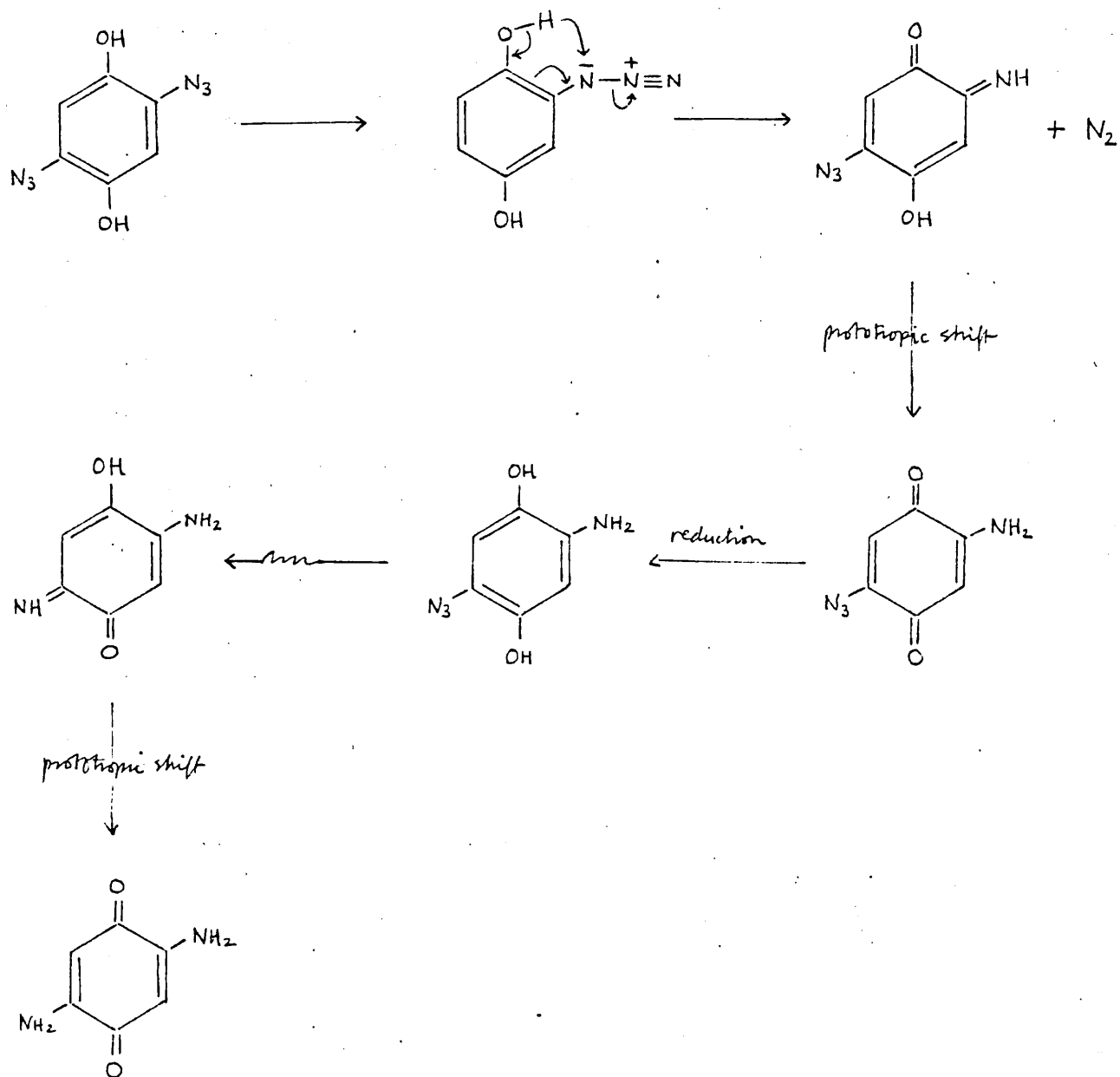
The three coupling constants were assigned to the structure 2,5-diamino-1,4-semiquinone, XI.

XI



Experimental  
Couplings/Gauss

The assumption that the amino-substituents bore a 2,5- relationship with each other followed naturally from a consideration of the starting material, but this was confirmed later by the theoretical spin density distribution for this species (see Chapter 4). The radical XI must derive from the rearrangement, with loss of nitrogen, of 2,5-diazido-1,4-hydroquinone (see Scheme 4). Figure 7 shows a wing of the same spectrum (Fig. 6) at the expanded field scan of 20 Gauss and Figure 8 shows two reconstructions of this wing from which the better fit of assigning the 0.7 Gauss splitting to the proton triplet can be seen. A simulation of this spectrum with a linewidth of 0.45 Gauss and a mainly Lorentzian line-shape

Scheme 4

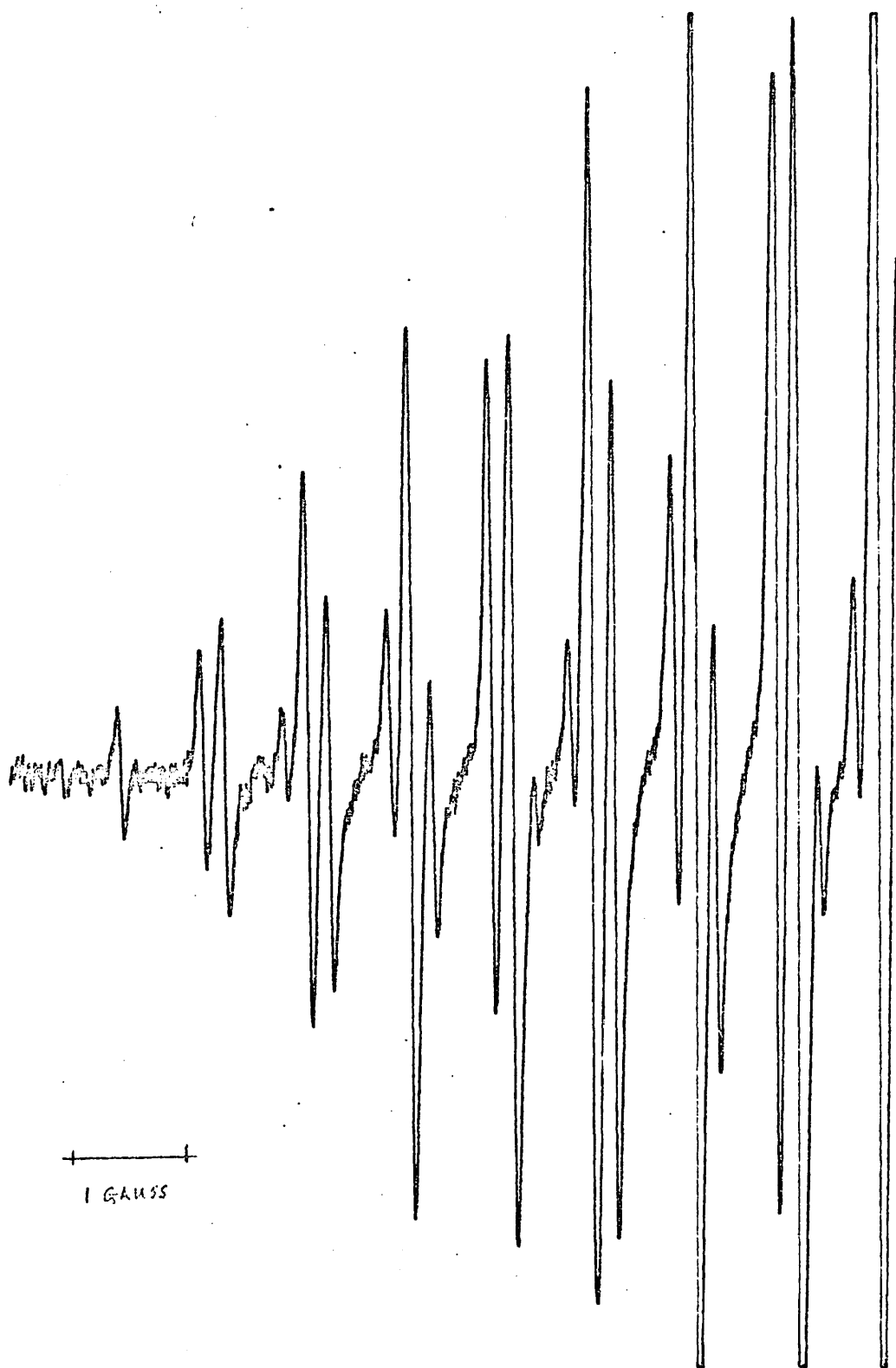
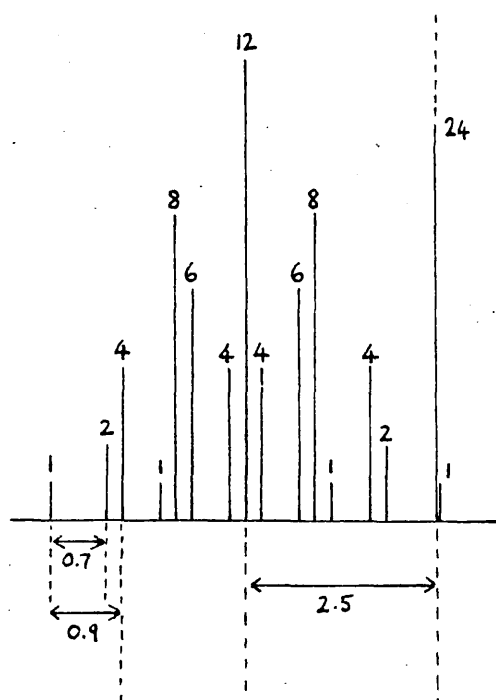


Fig. 7



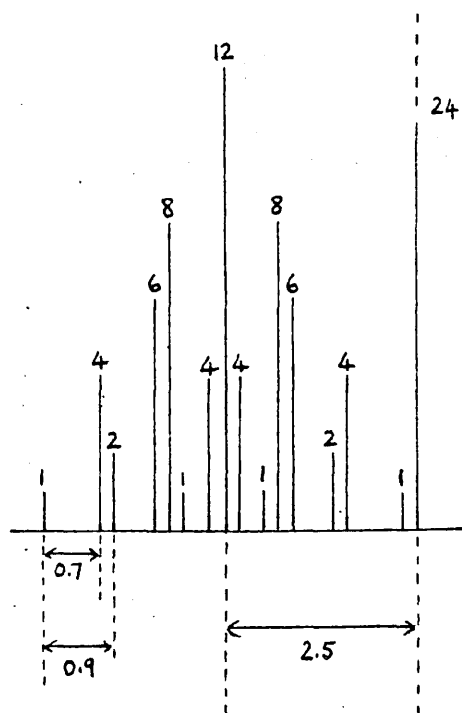


$$a(2H) = 0.7 \text{ Gauss}$$

$$a(4H) = 0.9 \text{ Gauss}$$

$$a(2N) = 2.5 \text{ Gauss}$$

1 GAUSS



$$a(2H) = 0.9 \text{ Gauss}$$

$$a(4H) = 0.7 \text{ Gauss}$$

$$a(2N) = 2.5 \text{ Gauss}$$

Fig. 8 Reconstruction of spectrum shown in Fig. 6, showing the effect upon theoretical line-heights of two different assignments.

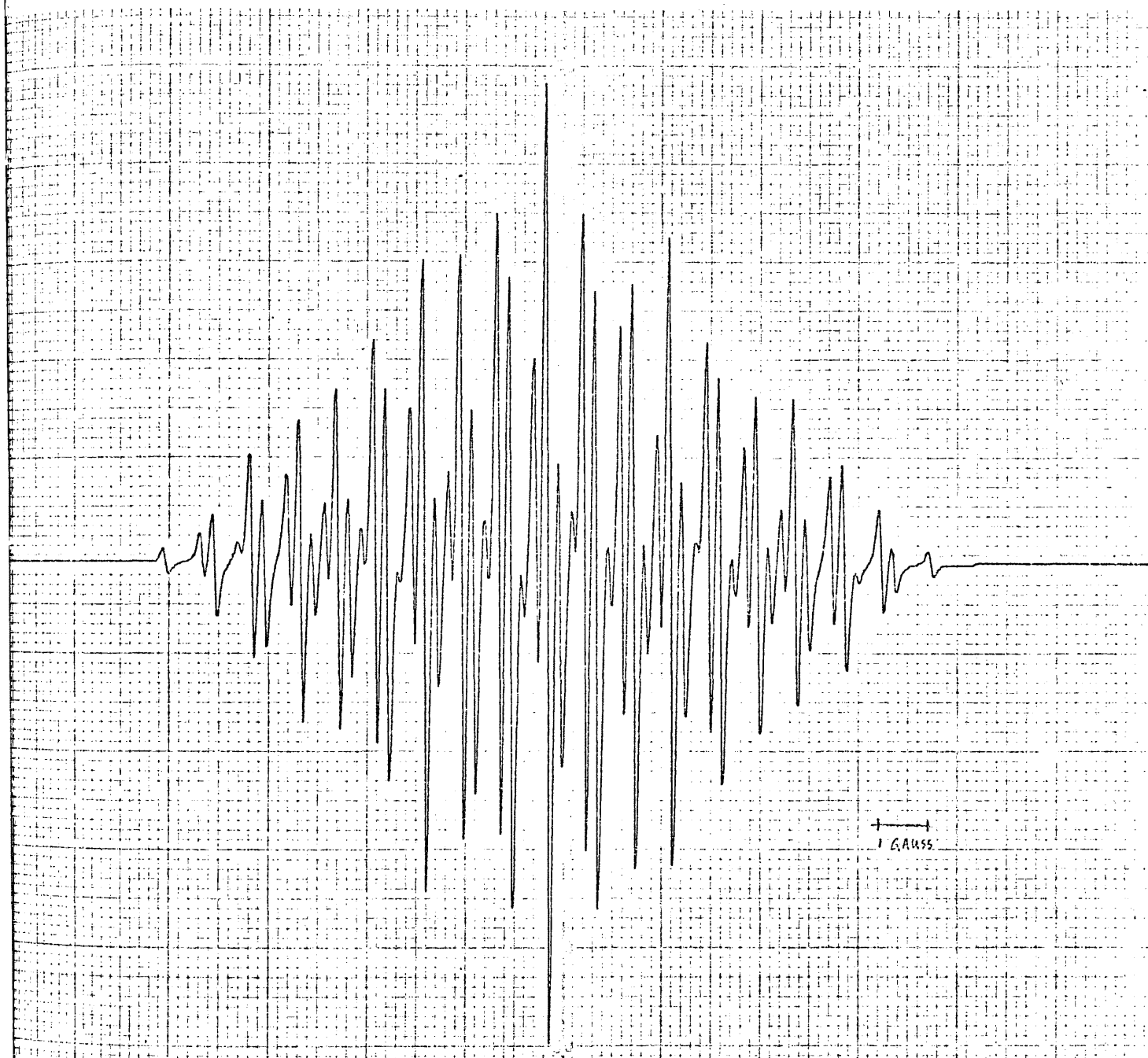


Fig. 9

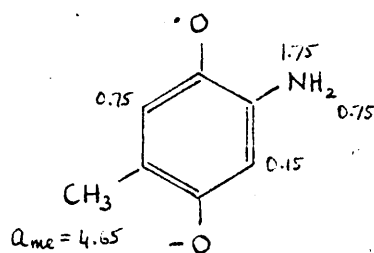
is shown in Figure 9.

It is interesting that we did not observe this species when 2,5-diamino-1,4-quinone was examined.

2-Amino-5-methyl-1,4-semiquinone

Azidoquinones are readily formed by displacement of suitable leaving groups<sup>48</sup> by azide ion ( $N_3^-$ ) and when 2-chloro-5-methyl-1,4-benzoquinone, dissolved in aqueous DMF,<sup>45</sup> was treated with a concentrated aqueous solution of sodium azide, there was immediate reaction, with colour change, exothermia and evolution of nitrogen. Treatment with alkaline dithionite solution gave various mixtures of radicals, but when a drop of methanol was added to a sample of the original reaction solution, a trace of alkaline dithionite gave the spectrum shown in Figure 10. The spectrum consisted of a large methyl splitting of 4.65 Gauss, a nitrogen triplet of 1.75 Gauss, a proton quartet of 0.75 Gauss and a small proton doublet of 0.15 Gauss. The couplings were assigned to 2-amino-5-methyl-1,4-semiquinone, XII

XII



Experimental  
Couplings/Gauss

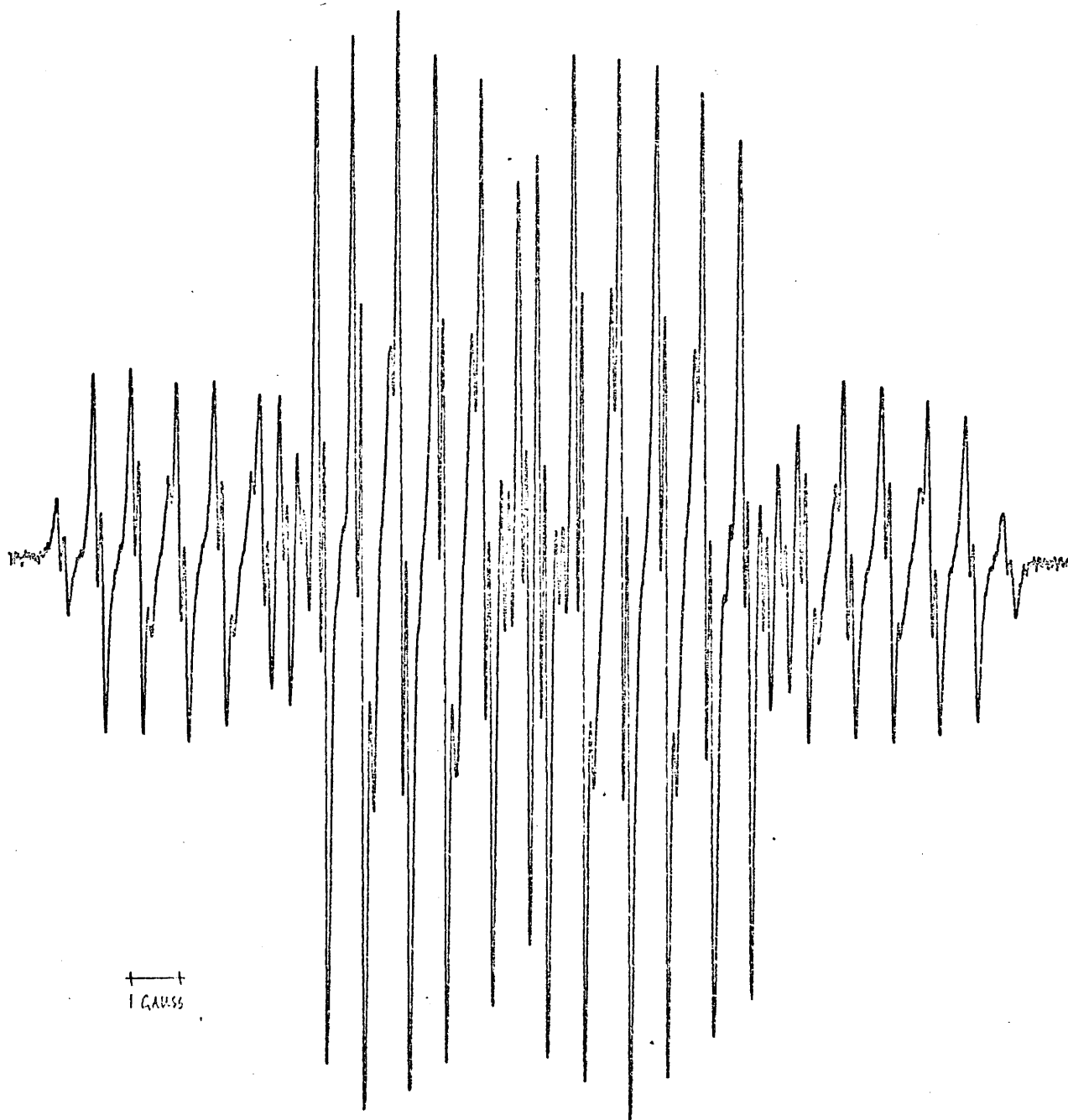
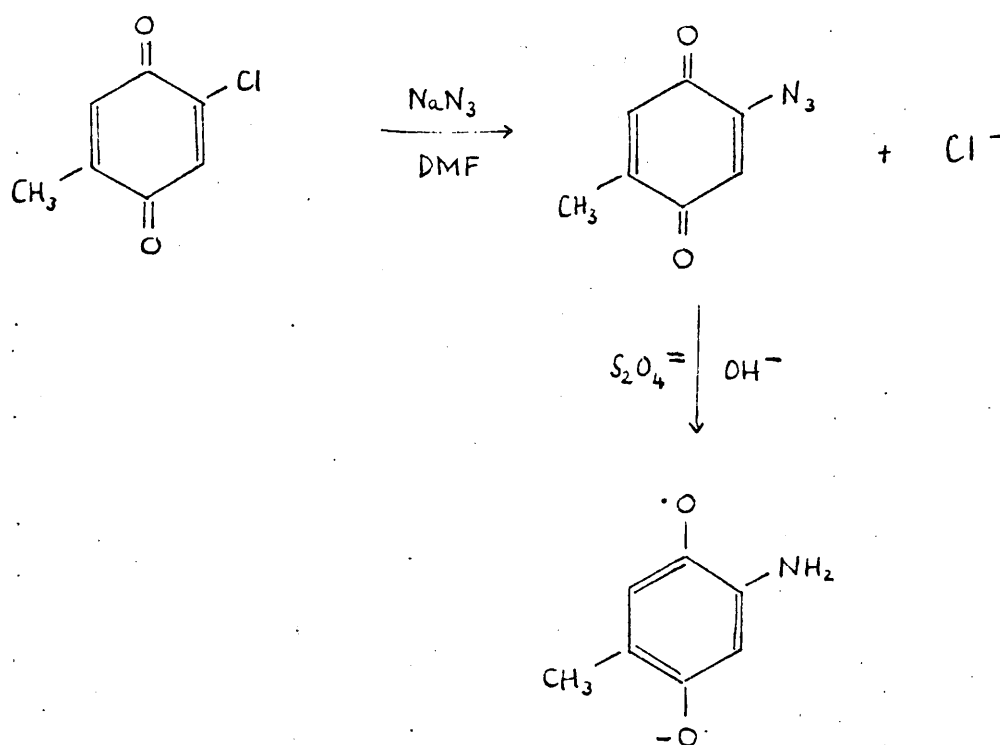


Fig. 10

which must result from rearrangement, with loss of nitrogen, of the intermediate azido compound, (see Scheme 5).

Scheme 5

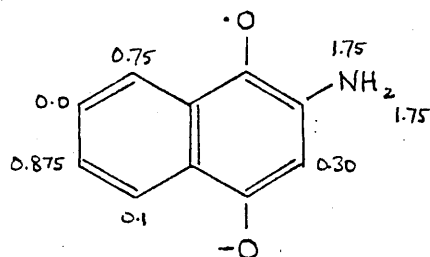


The smaller proton quartet is presumably due to fortuitous equivalence of the two amino protons and one ring proton. The smaller ring proton coupling has been assigned ortho to the amino group by analogy with hydroxysemiquinones.<sup>1</sup>

2-Amino-1,4-naphthoquinone

When an aqueous DMF solution of 2-chloro-1,4-naphthoquinone was treated with sodium azide, as described before, immediate reaction followed with a colour change, exothermia and evolution of nitrogen. Treatment of the reaction solution with alkaline dithionite gave a radical whose spectrum is shown in Figure 11 attributed to 2-amino-1,4-naphthosemiquinone XIII, with couplings assigned by analogy with the corresponding 2-hydroxy compound.<sup>6</sup>

XIII



Experimental  
Couplings/Gauss

Secondary aminosemiquinone radicals<sup>1</sup>

In some instances, we observed varying spectra due to mixtures of secondary radicals from the starting material 2,5-diazido-1,4-hydroquinone.

The spectrum shown in Fig. 12 consists of a single

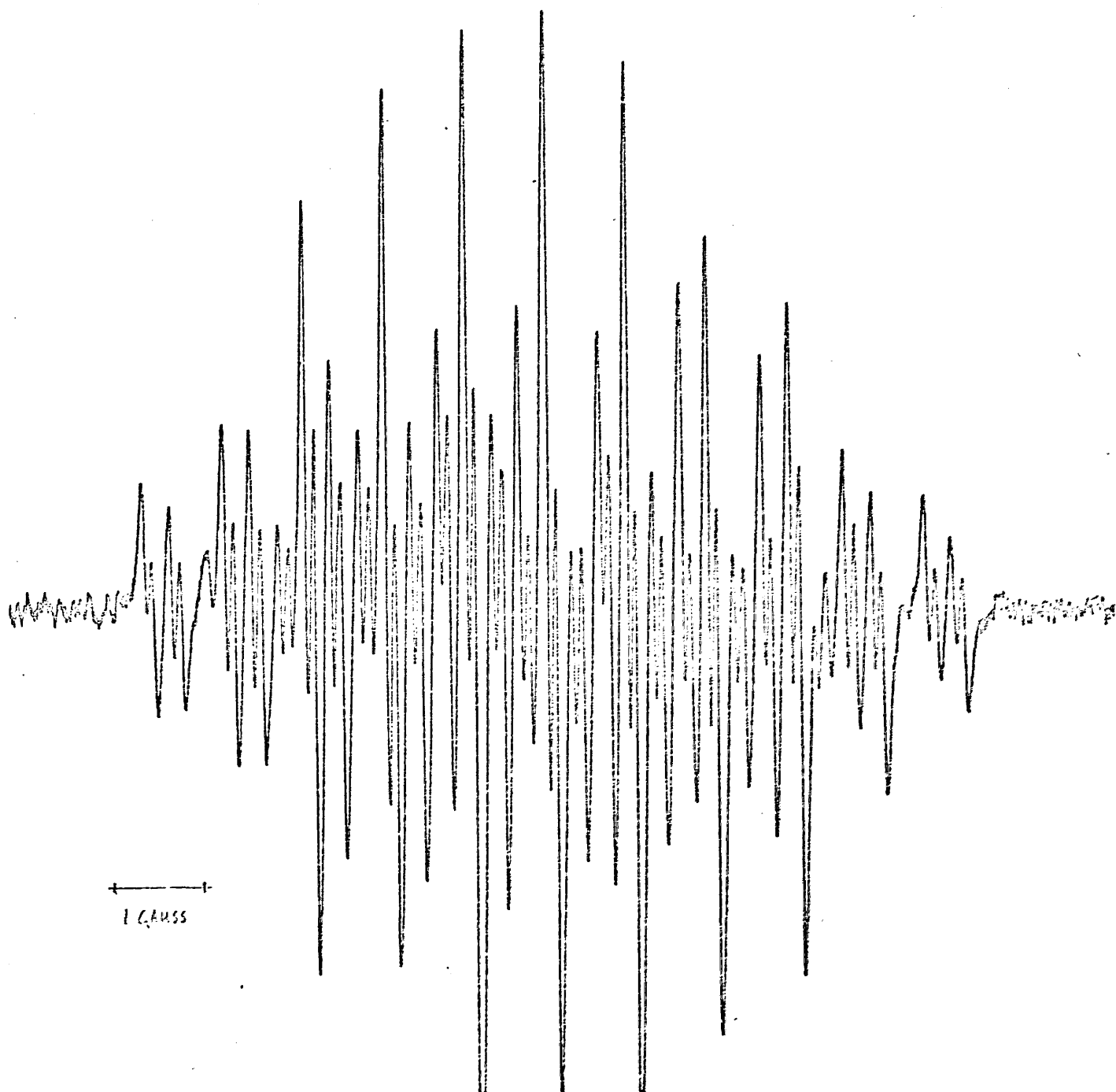


Fig. 11

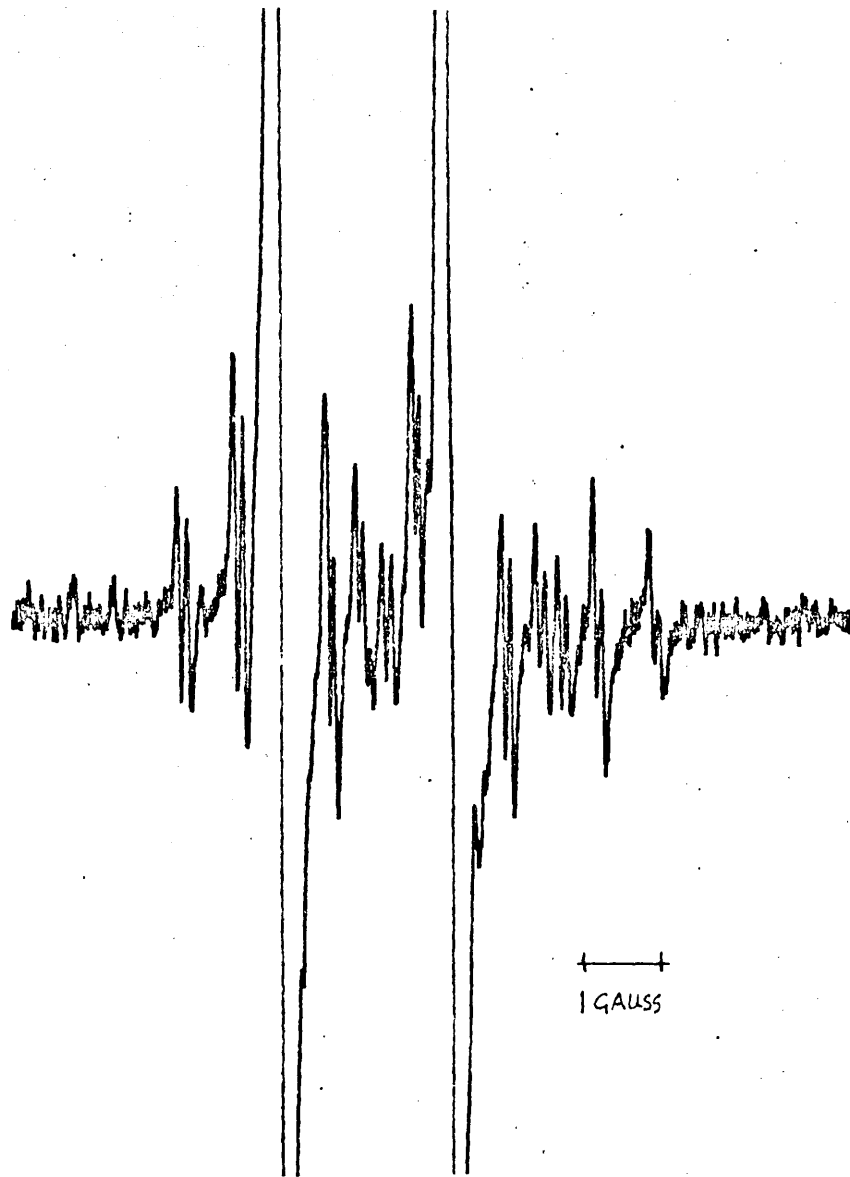
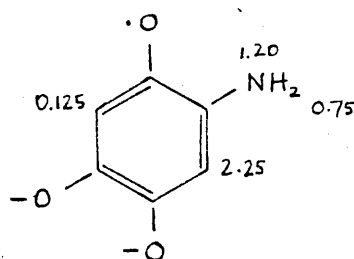


Fig. 12



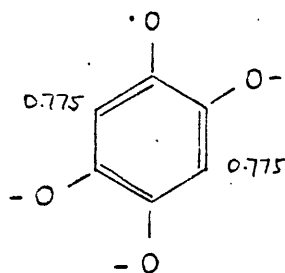
nitrogen triplet, a proton triplet and two further proton doublets, with a large superimposed doublet due to a separate species. We have tentatively assigned the spectrum to the secondary species, 2-amino-5-hydroxy-1,4-semiquinone, XIV, with the ring proton couplings assigned by analogy with other semiquinone secondary radicals.<sup>1</sup>

XIV

Experimental  
Couplings/Gauss

Electrolytic oxidation in water of the same starting material generated the spectrum of a proton triplet, assigned to XV.

XV

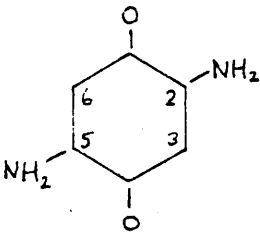
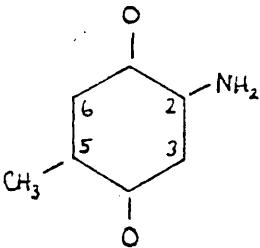
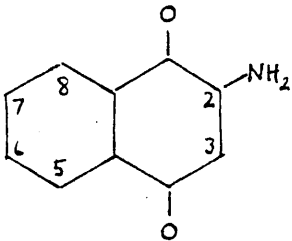
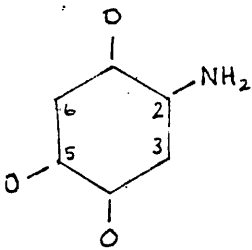
Experimental  
Coupling/Gauss

A similar triplet has been observed from the starting material 2-n-butyl-5-amino-1,4-quinone.<sup>12</sup>

These radical species, XIV and XV must derive from a 2,5-diamino-substituted intermediate resulting from rearrangement, with loss of  $N_2$ , of 2,5-diazido-1,4-hydroquinone, with subsequent substitution of amino-groups by oxygen ( $O^-$ ).<sup>61</sup>

Couplings of the amino-semiquinones are summarised in Table 5.

Table 5. E.s.r. Coupling Constants (a/Gauss) for  
Amino-1,4-semiquinones

radical skeleton	$a_2$	$a_3$	$a_5$	$a_6$
XI 	$a_N = 2.50$	0.70	$a_N = 2.50$	0.70
	$a_{NH}^H = 0.90$		$a_{NH}^H = 0.90$	
XII 	$a_N = 1.75$	0.15	$a_{CH_3} = 4.65$	0.75
	$a_{NH}^H = 0.75$			
XIII 	$a_N = 1.75$	$a_3 = 0.30$	$a_5 = 0.10$	$a_6 = 0.875$
	$a_{NH}^H = 1.75$		$a_7 = 0.0$	$a_8 = 0.75$
XIV 	$a_N = 1.2$	2.25		0.125
	$a_{NH}^H = 0.75$			

### 3. Triazolo-1,4-semiquinones

#### 2,3-Triazolo-1,4-semiquinone

Since an azidosemiquinone species could not be detected from azido starting materials in normal autoxidation<sup>1</sup> or reduction conditions,<sup>1</sup> various reaction solutions, in which the starting quinones and sodium azide were present, were investigated.

Reaction between 1,4-benzoquinone and sodium azide, in aqueous DMF, gave a deep purple-brown reaction solution (see Generation of Radicals, page 31) from which was generated a radical whose spectrum is shown in Figure 13. The radical was present in good concentration and the spectrum is sharply resolved (linewidth ~ 0.1 Gauss) although the lines are broadened towards the high field end of the spectrum.

From inspection, the three coupling constants can easily be picked out: a 0.65 Gauss triplet and a 0.9 Gauss quintet from a single and a pair of equivalent nitrogens and a large proton triplet of 3.5 Gauss. The couplings ruled out other possible products of reaction,<sup>45</sup> 2,5-diazido-1,4-semiquinone, 2-azido-5-amino-1,4-semiquinone and 2,5-diamino-1,4-semiquinone (Scheme 6),

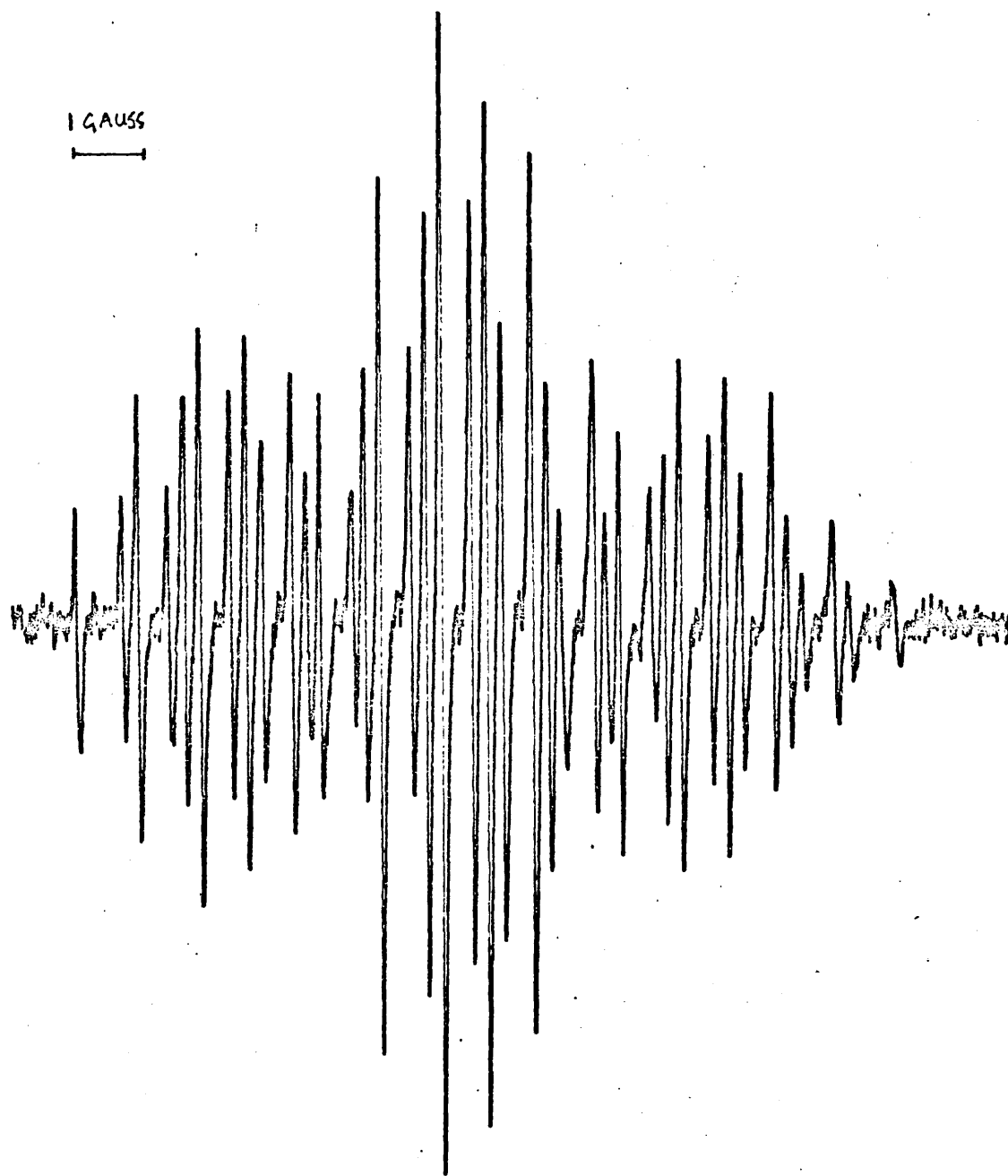
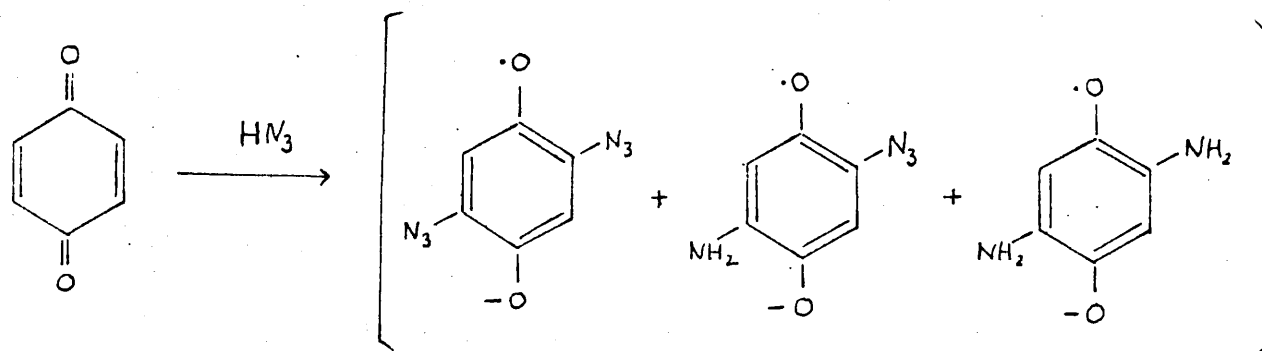


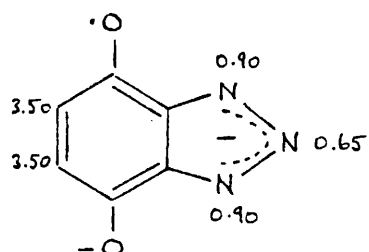
Fig. 13



Scheme 6

and the spectrum was assigned to the heterocyclic semiquinone, 2,3-triazolo-1,4-semiquinone, XVI,

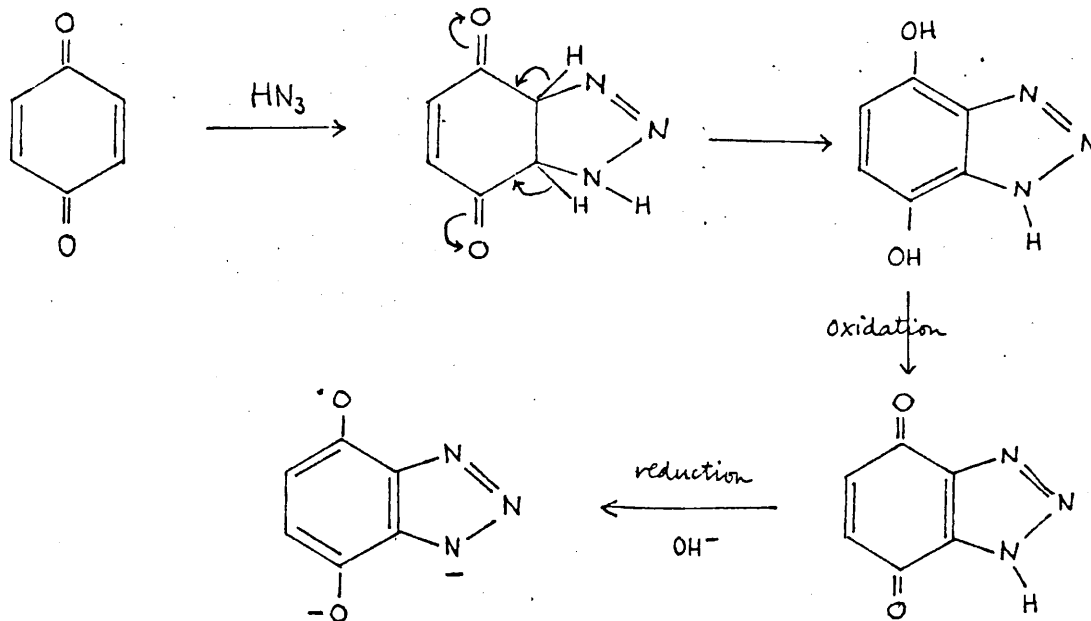
XVI



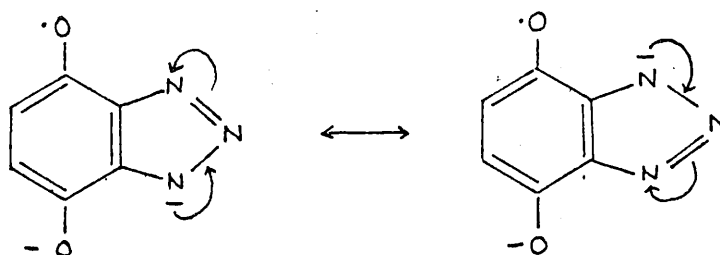
Experimental Couplings/Gauss

presumably resulting from a dipolar addition of  $\text{HN}_3$  to one of the quinone carbon-carbon double bonds, (cf. Chapter 1, page 23) with ionisation of the labile iminic proton,<sup>77,55</sup> (see Scheme 7).

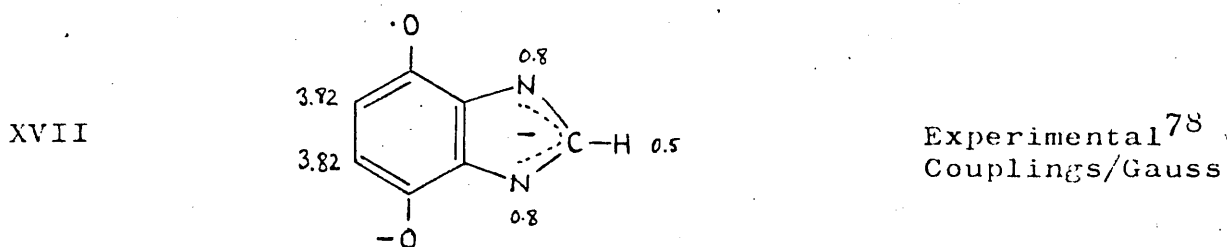
Scheme 7



The symmetrical radical species would result from delocalisation in the triazole ring:



There is no report in the literature of a mono-triazole quinone or hydroquinone which would be the parent of XVI but support for this assignment came from a semiquinone radical anion, imidazo-1,4-semiquinone, XVII, generated from the parent quinone,<sup>32,78</sup> whose couplings are remarkably similar:-



A reconstruction of the spectrum of XVI (Fig. 13) is shown in Figure 14.

The triazolo-semiquinone, XVI, was also generated by flowing an aqueous DMF reaction solution of 1,4-benzoquinone (0.03 M) and sodium azide (0.15 M) against aqueous sodium dithionite solution ( $\sim 0.1$  M) which had been adjusted to pH  $\sim 9.0$  with sodium hydroxide.

#### 2,3;5,6-Bistriazolo-1,4-semiquinone

Sodium azide reacted with an acidified mixture of 2,5-disulphonato-1,4-hydroquinone dipotassium salt and sodium dichromate<sup>67</sup> to give a deep purple reaction solution. The



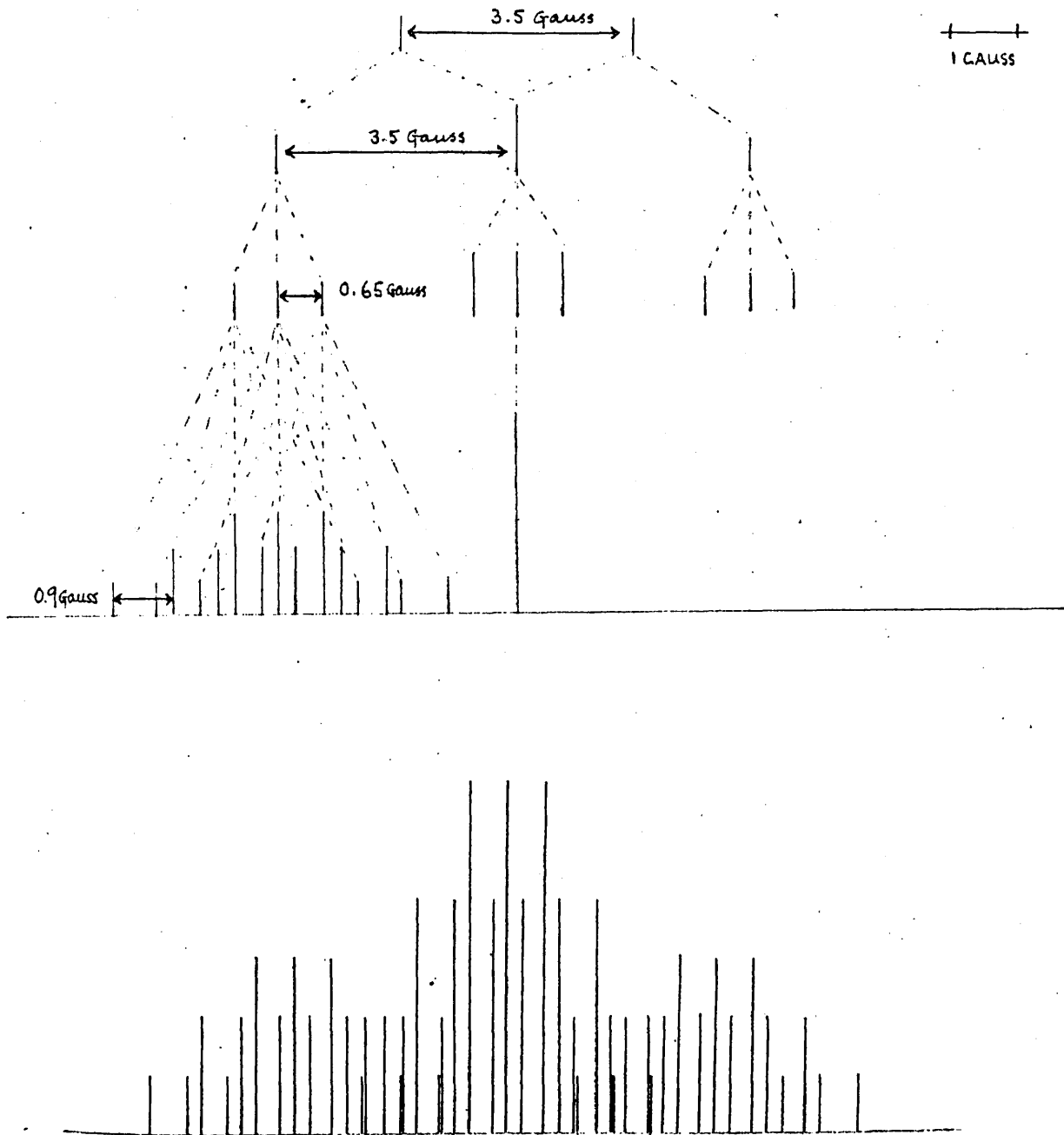
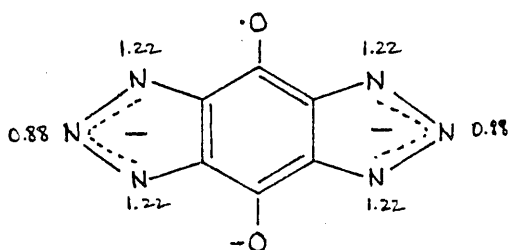


Fig. 14 Reconstruction of spectrum shown in Fig. 13.

reaction solution, extracted with ether and concentrated, gave a radical on treatment with alkaline dithionite whose spectrum is shown in Figure 15. The same spectrum was also generated in the same way from the mono-substituted starting material. In some instances, this spectrum was also observed after 1,4-benzoquinone, dissolved in aqueous DMF, had reacted with sodium azide, in conditions identical to those in which the mono-triazolo-semiquinone was observed, although the two radical species were never observed simultaneously.

The spectrum consists of 31 lines and the ends of the spectrum had to be ascertained at high modulation amplitude (see Figure 16) since broadening of high field lines obscured the exact extent. The pattern was consistent with two sets of (four and two) equivalent nitrogens, with no proton splitting. Four equivalent nitrogen atoms would give nine peaks of intensity ratios 1:4:10:16:19:16:etc. Figure 16 shows how many of the lines are coincident. The lack of contribution from protons appeared to rule out other possible products of reaction (see Scheme 6, page 54). The spectrum was interpreted, in the light of the spectrum of XVI, as being due to the 2,3;5,6-bis-triazolo-1,4-semiquinone, XVIII,

XVIII



Experimental  
Coupling/Gauss

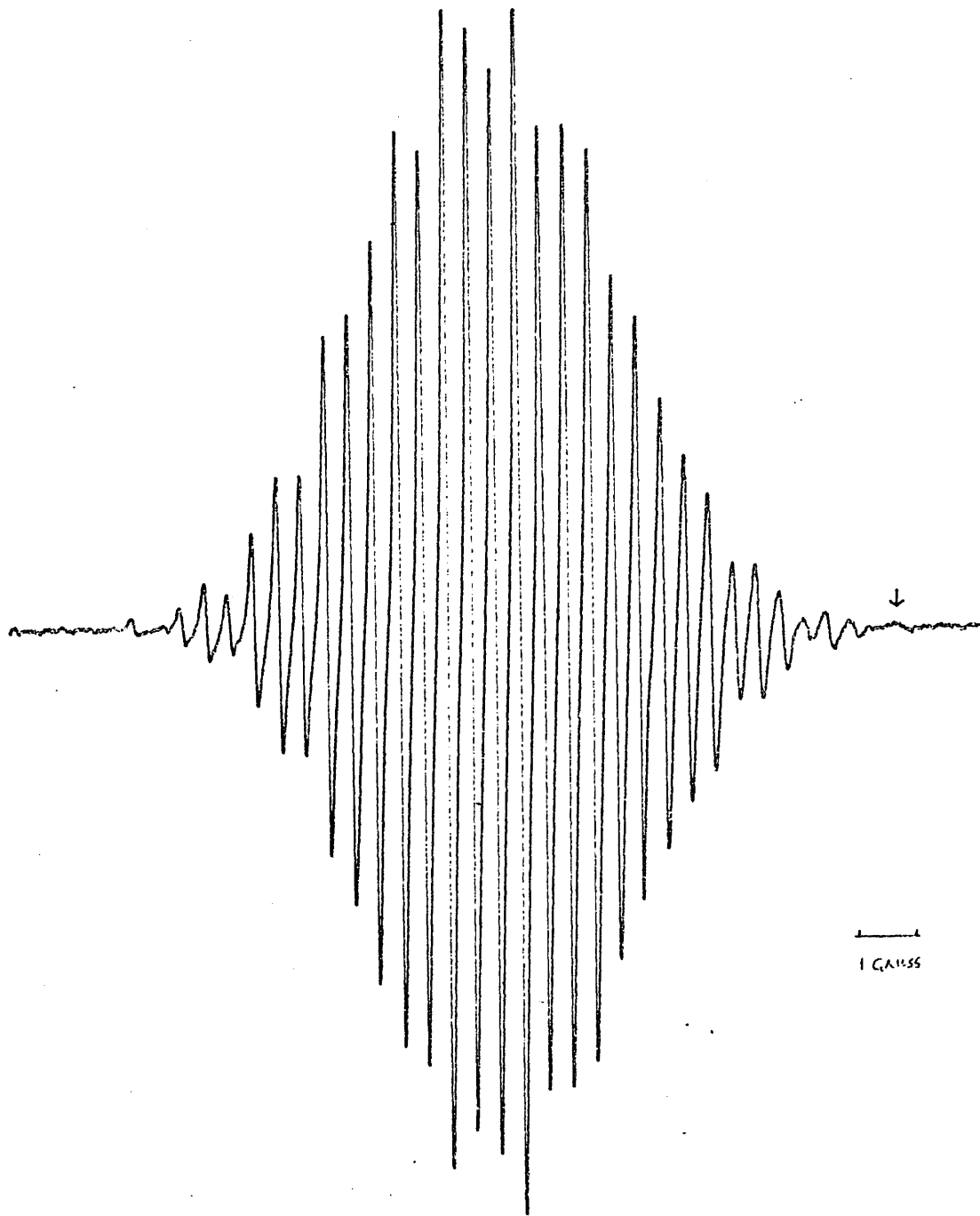


Fig. 15

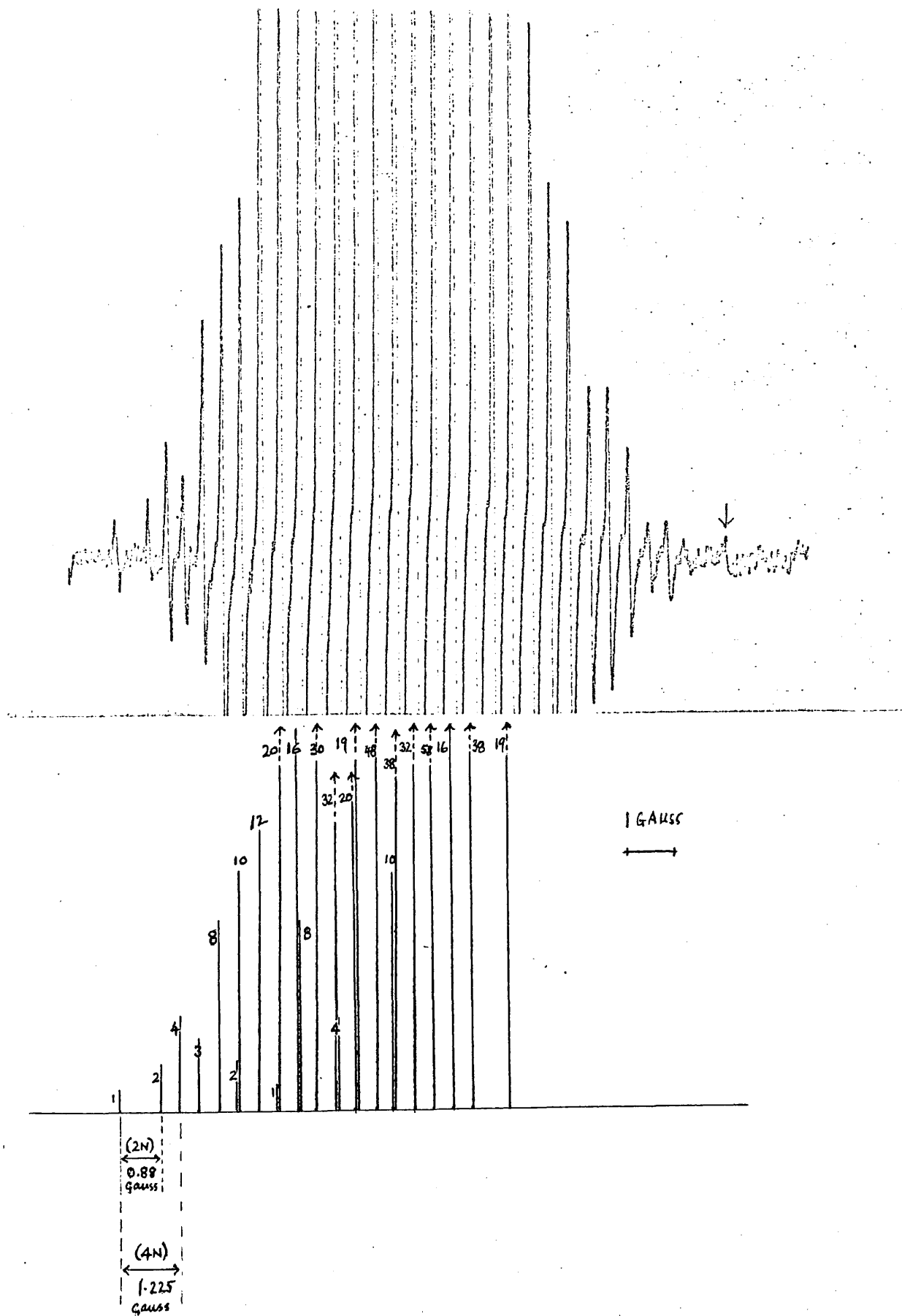


Fig. 16 Reconstruction of spectrum shown in Fig. 15.

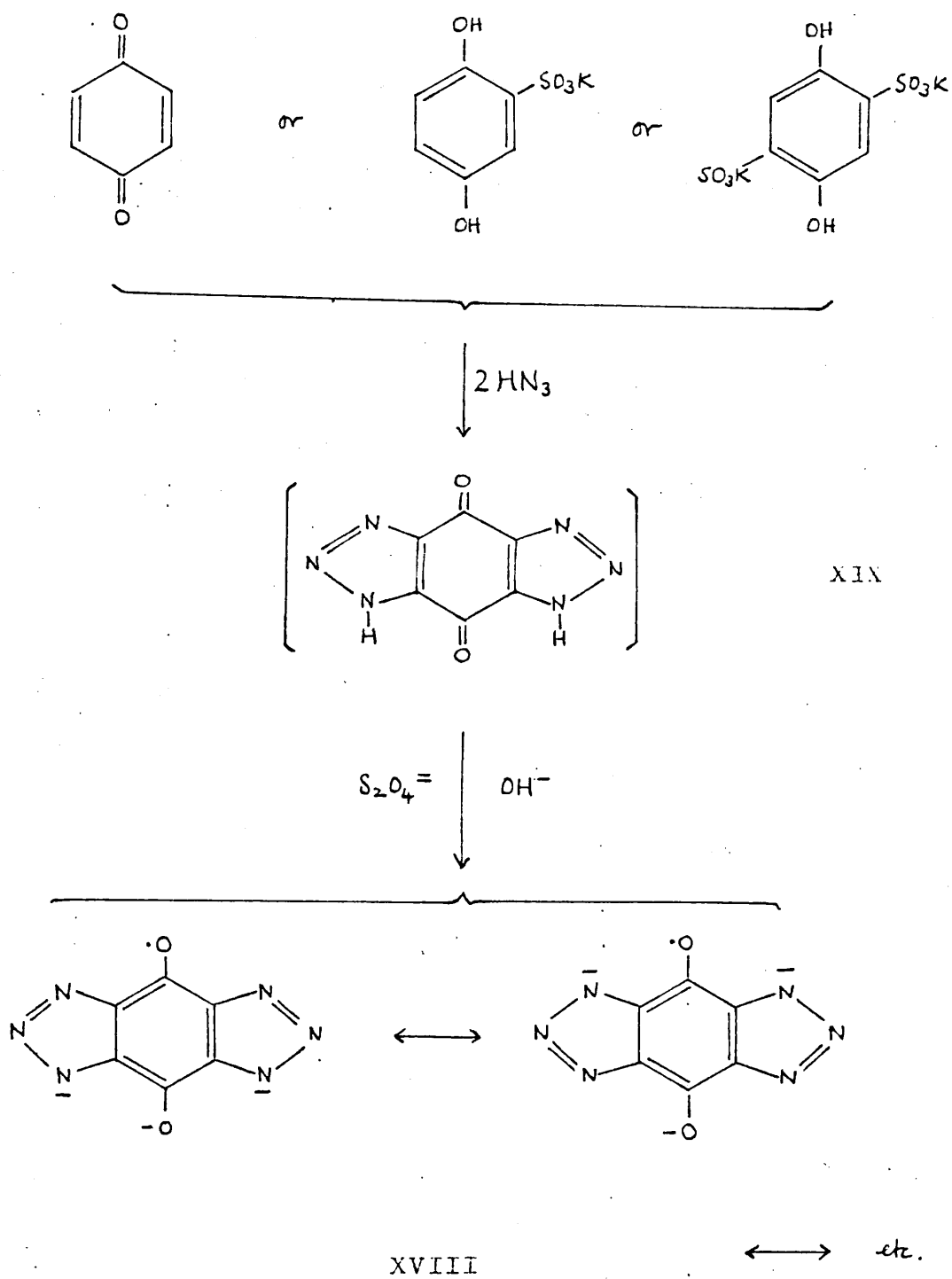
which must result from dipolar addition of  $\text{HN}_3$  to both sides of the quinone nucleus, followed by ionisation and delocalisation (Scheme 8). Confirmation of this analysis came when the same spectrum (Fig. 15) was generated from an authentic sample<sup>55</sup> of 2,3;5,6-bis-triazolo-1,4-benzoquinone, XIX.

It was interesting that the signal generated from pure crystalline starting material, (XIX), was considerably longer-lived than the same signal generated from a reaction solution, in which the likely mixture of reaction products would contribute to the decomposition of the observed species. When the signal was generated from one of the three previously mentioned starting materials (see Scheme 8), it persisted for 20-30 minutes, after which time it decayed in favour of a new signal, eventually strong, of the species 2,5-diamino-1,4-semiquinone, XI. (Spectrum shown in Fig. 6). The diamino species was not observed with the bis-triazolo-quinone starting material (XIX).

#### 2-Methyl-triazolo-1,4-semiquinone

An aqueous DMF solution of toluquinone reacted with sodium azide to give, with alkaline dithionite treatment, spectra due to a mixture of radical species. Figure 17 shows a spectrum in which, a proton doublet, a single and two equivalent nitrogen couplings and a large methyl quartet are discernible. Lines from another species of similar  $g$ -value are also visible, but these are not identified. The methyl

## Scheme 8



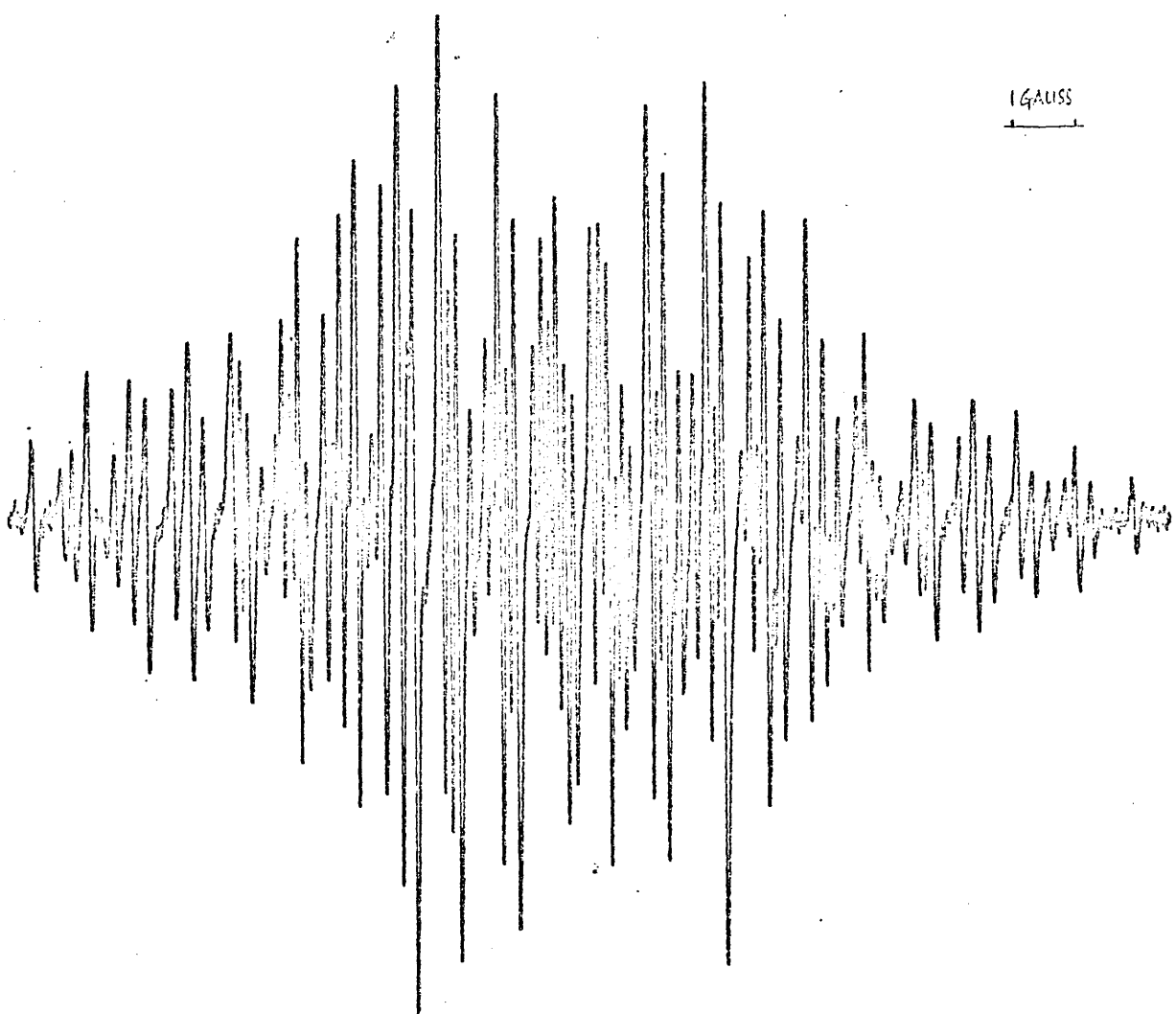
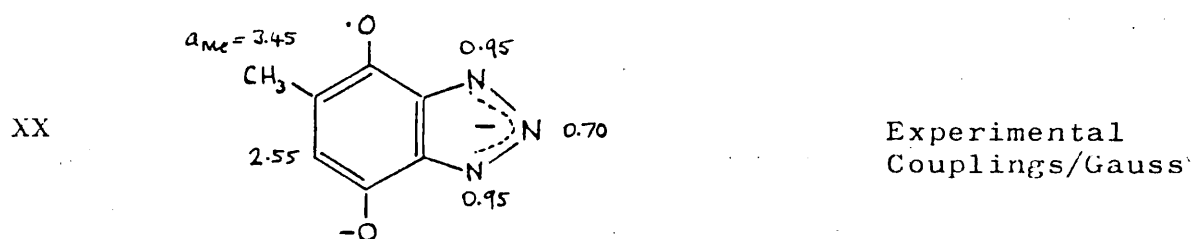


Fig. 17

quartet has a separation of 3.45 Gauss, reminiscent of the ring proton triplet in the triazolo-1,4-semiquinone XVI, and the nitrogen couplings of 0.70 Gauss and 0.95 Gauss are also close to the triazole ring in XVI. The spectrum is attributed to 2-methyl-triazolo-1,4-semiquinone, XX.



resulting from dipolar addition of  $\text{HN}_3$  to toluquinone (cf. Scheme 7, page 55).

#### 2-t-Butyl-triazolo-1,4-semiquinone

Reaction between 3-chloro-2,5-di-t-butyl-1,4-quinone and sodium azide produced spectra due to complex mixtures, which were not analysed. Proceeding in the usual way with 2,5-di-t-butyl-1,4-quinone, in DMF, no spectrum was obtained which could be attributed either to a triazolo- or to an amino-semiquinone; but when the reaction solution was boiled, treatment with alkaline dithionite gave rise to a species whose spectrum is shown in Figure 18 in which there are ten



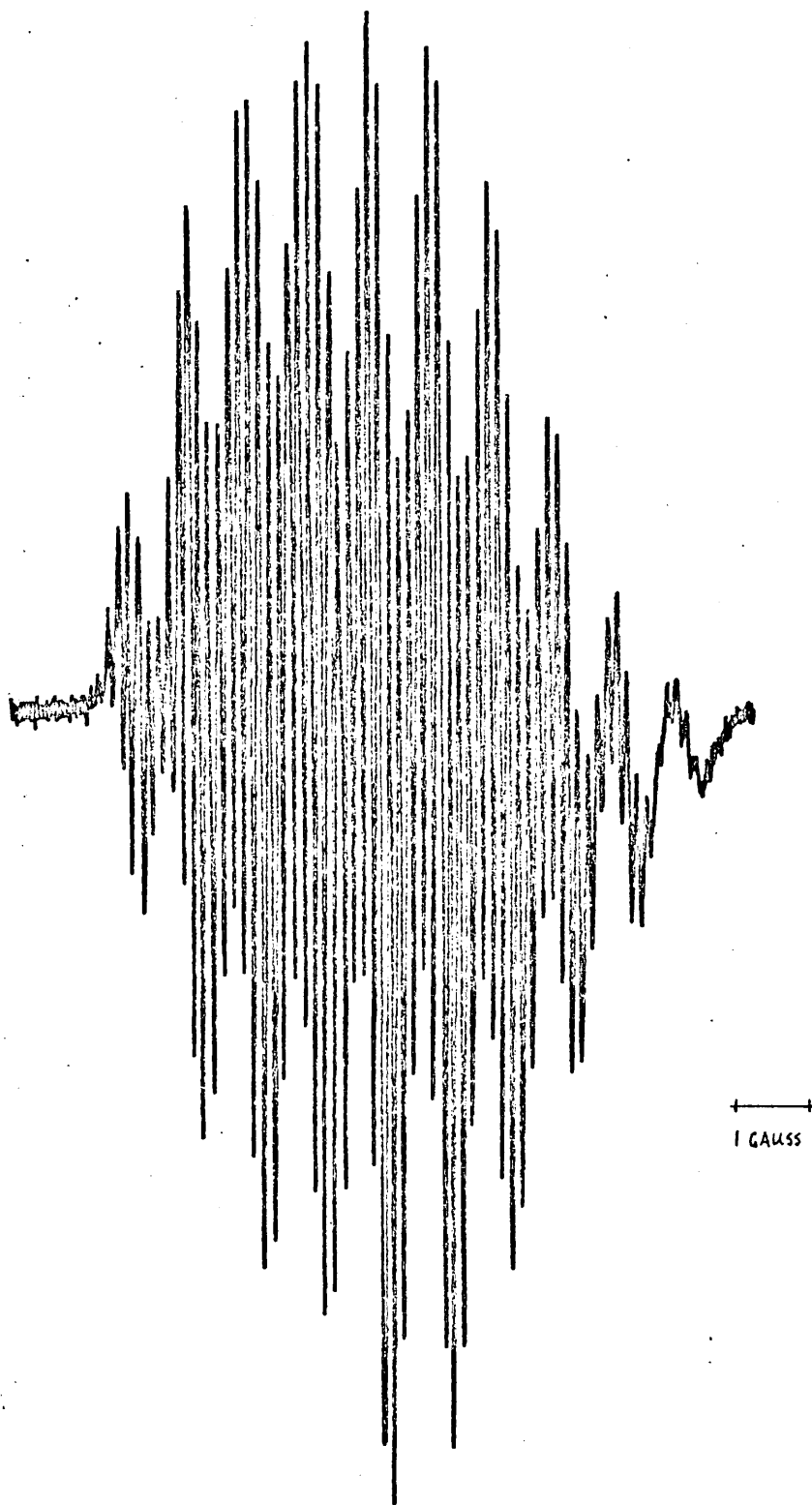
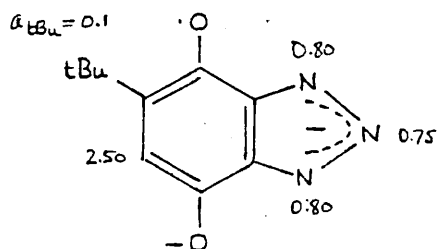


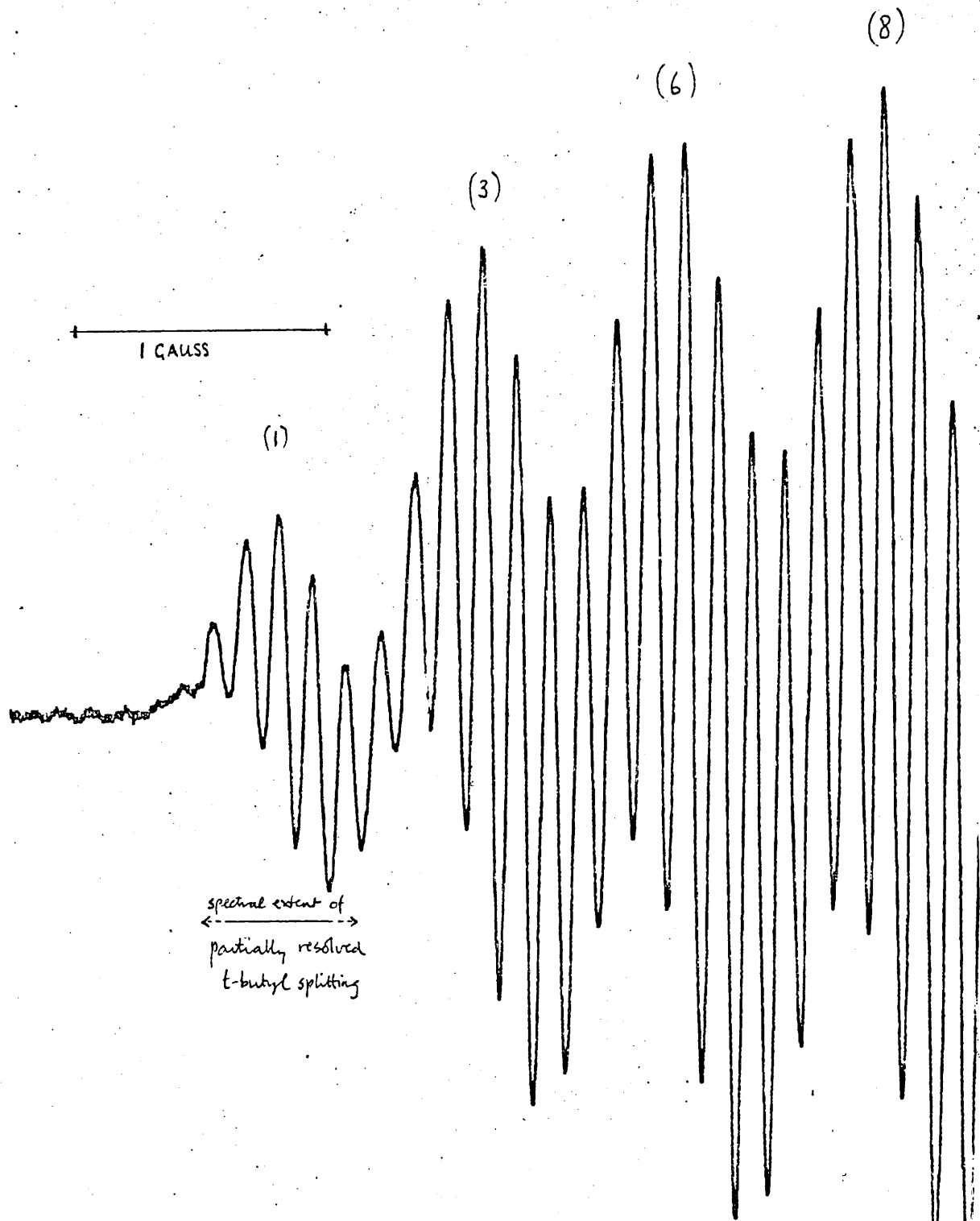
Fig. 18

multiplets, due to coupling from three nitrogens and a proton. Fig. 19 shows a part of this spectrum at expanded scan (10 Gauss). The fine structure in each multiplet is attributed to partially resolved tertiary-butyl splitting. Not all the tertiary-butyl lines can be seen but they are of the same order as the line-widths and this can lead to a reduction of intensity or annihilation of some lines.<sup>79</sup> Broadening of high field lines is well displayed in this spectrum. The spectrum is assigned to 2-t-butyl-triazolo-1,4-semiquinone, XXI.

XXI

Experimental  
Couplings/Gauss

No spectrum was generated when the starting material was 2-t-butyl-1,4-benzoquinone and no trace of the mono-t-butyl compound could be detected in the di-t-butyl starting material. This result suggests that, in the course of dipolar addition of  $\text{HN}_3$ , a novel dealkylation reaction has occurred. Other examples of dealkylation have been reported.<sup>80</sup>



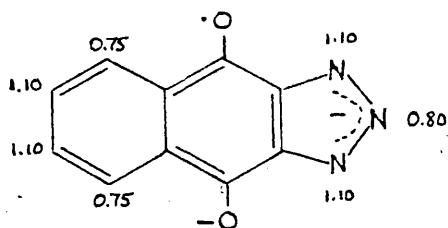
(2N)	1	2	3	2	1														
(H)	← 0.8 Gauss →					1	2	3	2	1									
	← 2.45 Gauss →																		
	1	2	3	3	3	3	3	2	1										
(N)	← 0.7 Gauss →	2	1/3	2/3	3/3	3/3	3/3	3/3	3/3	3/2	3/2	2/1	2/1	1					
(Resultant Multiplet)	1	3	6	8	9	9	8	6	3	1									

Fig. 19

2,3-Triazolo-1,4-naphthosemiquinone

Treatment of the DMF reaction solution containing 1,4-naphthoquinone and sodium azide, with alkaline dithionite gave rise to the species, shown in Figure 20, attributed to 2,3-triazolo-1,4-naphthosemiquinone, XXII,

XXII



Experimental  
Couplings/Gauss

resulting from dipolar addition of  $\text{HN}_3$  to naphthoquinone. (The assignments of  $a_5$ ,  $a_8$  and of  $a_6$ ,  $a_7$  are of course ambiguous). The identity of the species was confirmed when an identical spectrum was obtained from a crystalline sample of 2,3-triazolo-1,4-naphthoquinone.<sup>55</sup>

Coupling constants in all the triazole species are summarised in Table 6.

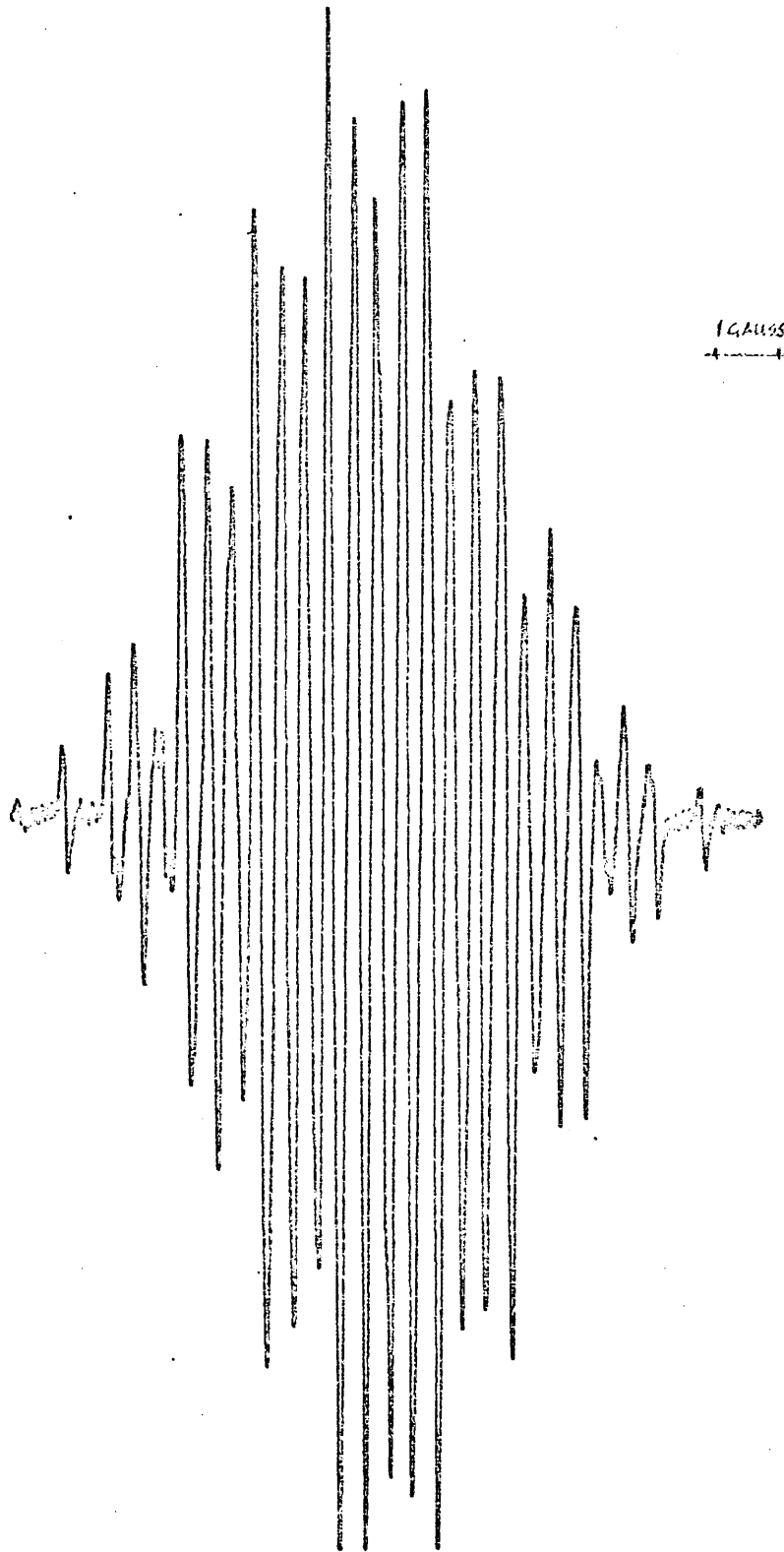
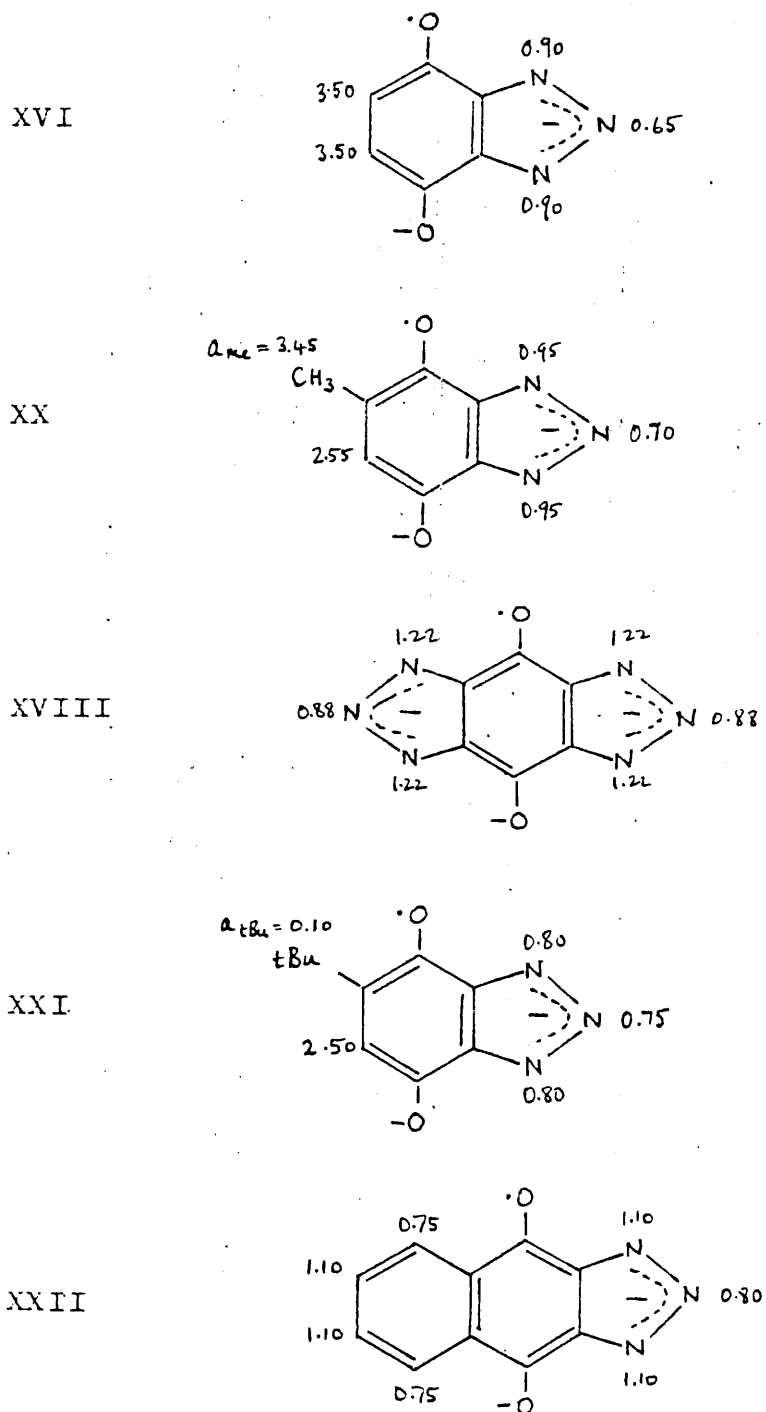


Fig. 20

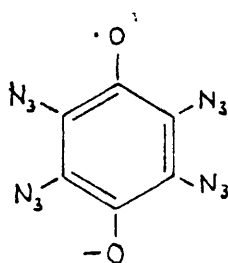
Table 6

E.s.r. Coupling Constants (a/Gauss) in Triazolosemiquinones

4. Azido-1,4-semiquinones2,3,5,6-Tetraazido-1,4-semiquinone

Tetraazido-1,4-benzoquinone<sup>65</sup> dissolved in hexamethylphosphoramide (HMPA) and treated with alkaline dithionite solution gave rise to the spectrum shown in Figure 21. The pattern consists of a 9 line multiplet, the pattern expected of four equivalent nitrogens, and is tentatively assigned to the tetraazido-1,4-semiquinone, XXIII.

XXIII

Experimental  
Couplings/Gauss

$$a_{4N} = 1.6$$

with other lines due to an unidentified species.

If this assignment is correct, then only one nitrogen in each azido group contributes to the hyperfine pattern.

Support for this assignment came from a spectrum of *m*-azidophenoxy,<sup>81</sup> in which there is coupling from only one nitrogen atom ( $a_N = 0.4$  Gauss).

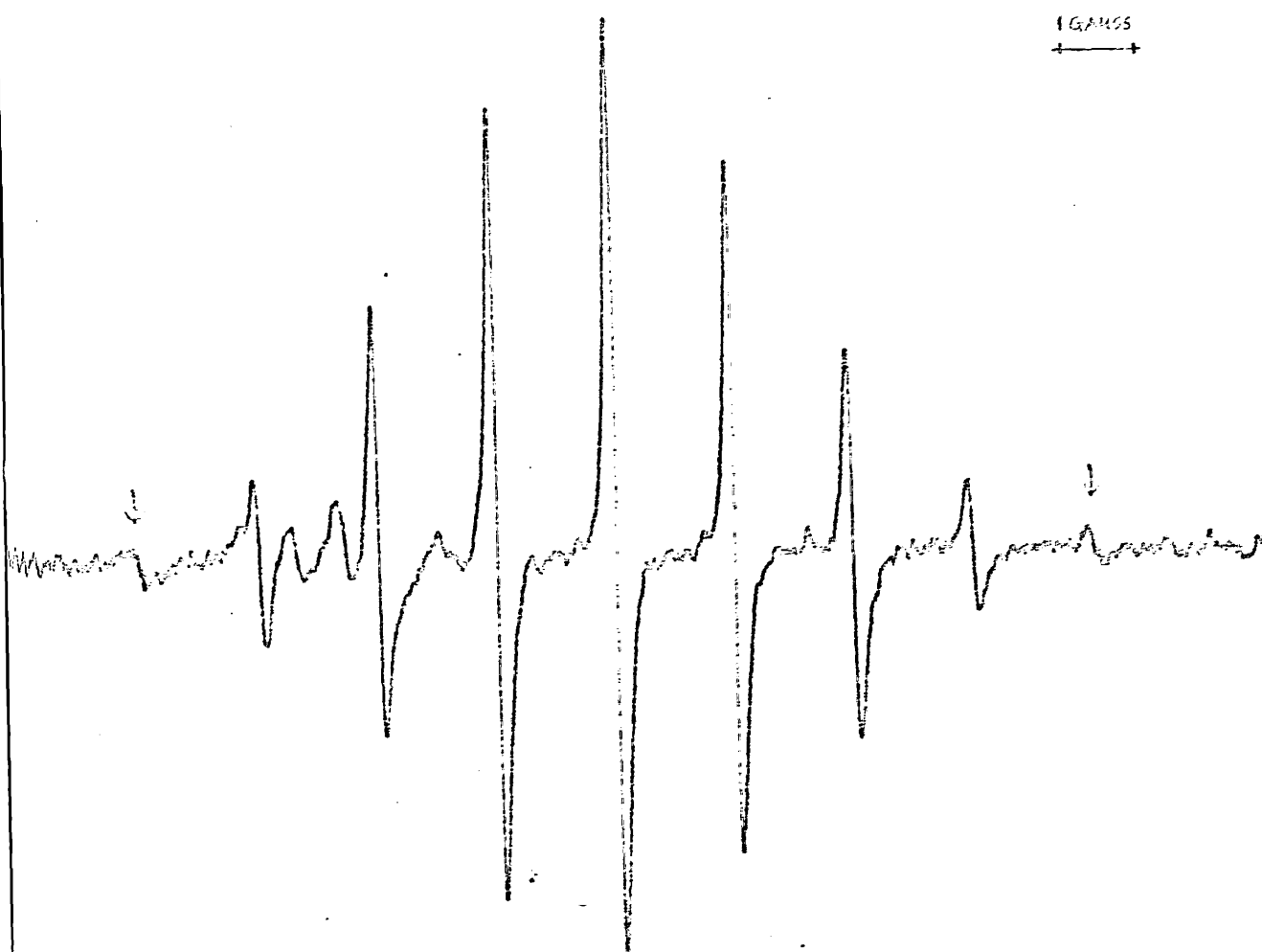


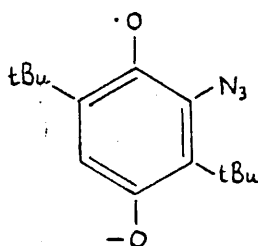
Fig. 21



2-Azido-3,6-di-t-butyl-1,4-semiquinone

The spectrum shown in Fig. 22 was obtained from the DMF reaction solution containing 2,5-di-t-butyl-1,4-quinone and sodium azide and is tentatively attributed to 2-azido-3,6-di-t-butyl-1,4-semiquinone, XXIV.

XXIV



Experimental  
Couplings/Gauss

$$a_{\text{H}} = 0.1$$

$$a_{\text{N}} \approx a_{\text{H}} \approx 1.0$$

The spectrum shows four multiplets, partially resolved into t-butyl fine structure, probably due to coupling from one nitrogen and one proton of about 1 Gauss. The coupling cannot be measured exactly since partial resolution of the t-butyl splitting makes it difficult to determine the exact extent of each multiplet.

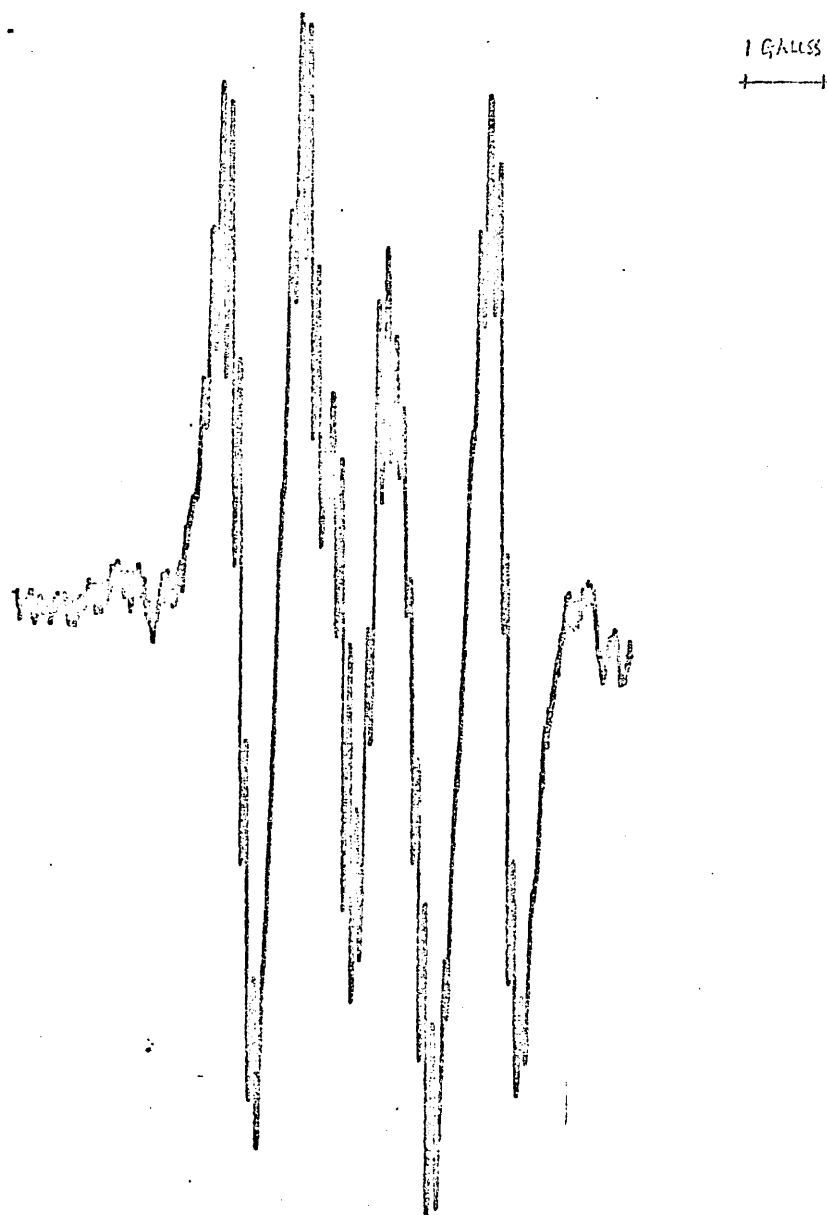


Fig. 22

## CHAPTER 3

NITROGEN MOLECULAR ORBITAL PARAMETERS

## 1. Amino-group Spin Density Distribution

Well-defined trends have been observed in the spin density distribution of substituted phenoxyl radicals,<sup>6,25,41</sup> but these studies have not so far been extended to include the amino substituent ( $-\text{NH}_2$ ). Since we have observed e.s.r. spectra of a number of amino-semiquinones, we were interested in seeing if the spin distribution within the amino-group itself could be accounted for. In the heteroatom model (see Chapter 1-6), the radical is regarded as a benzene positive ion perturbed by substituent X.<sup>83</sup> Where the substituent is nitrogen, two molecular orbital parameters are introduced, (see Equations 12 and 13, page 18) respectively  $h_N$  and  $k_{CN}$ .

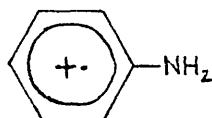
Three aminophenoxyl cations have been observed in acidic medium<sup>25</sup> and two neutral radicals in neutral solutions.<sup>61</sup> In both cases, exchange between amine protons and the medium is slow with respect to e.s.r. transitions and hyperfine splitting is observed from the amino-group. In order to derive the parameters,  $h_N$  and  $k_{CN}$ , we have used a simple radical structure in which there is a diprotonated nitrogen attached to a benzene ring, the aniline radical cation,  $(\text{C}_6\text{H}_5\text{NH}_2)^{\ddagger}$ . The values of  $h_N$  and  $k_{CN}$ , chosen to give the best fit to the experimental values, were then applied to the aminophenoxyl series, without altering the previously derived oxygen parameters.<sup>25,41</sup>

## 2. "Experimental" Spin Densities

The "experimental" spin densities of the three ring protons in the aniline radical cation were obtained (Table 7) via McConnell's relation for ring protons (Eq. 5, page 10), ( $Q_{CH}^H = -30 \text{ Gauss}^{25}$ ).

Table 7

Experimental Values of Coupling and Spin Densities in



Experimental couplings, "Experimental" spin densities  
a/Gauss

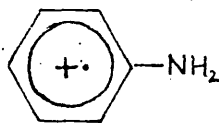
$a_o$	5.82	$\rho_o$	0.194
$a_m$	1.52	$\rho_m$	0.051
$a_p$	9.58	$\rho_p$	0.319
$a_H = Q_{CH}^H / \rho_c$		$Q_{CH}^H = -30 \text{ G}$	

Using the McLachlan molecular orbital method,<sup>23</sup> theoretical estimates of spin densities were correlated with these. Calculations were performed in which the parameters  $h_N$  and  $k_{CN}$  were varied over the range  $0.5 \leq h_N \leq 2.5$  and  $1.0 \leq k_{CN} \leq 2.5$ , with an initial interval of 1 unit and later

with finer intervals of 0.1 - 0.5 for both parameters, before  $k_{CN}$  was set at 1.0. The effect of varying  $h_N$  with  $k_{CN} = 1.0$  is shown in Table 8.

Table 8

Variation of Ring Proton Spin Densities\* in



with  $h_N$  value ( $k_{CN} = 1.0$ )

$h_N$	$\rho_{ortho}$	$\rho_{meta}$	$\rho_{para}$
1.0	.1926	-.0620	.2651
1.2	.1890	-.0572	.2890
1.3	.1861	-.0550	.3011
1.4	.1821	-.0516	.3114
1.6	.1738	-.0452	.3305

\* cf. Table 7.


More than one pair of values gives reasonable predictions, but the chosen values,  $h_N = 1.3$  and  $k_{CN} = 1.0$ , gave spin densities closest to the "experimental" spin densities. These values are reasonable: we should expect the overall electron density in the nitrogen  $\pi$  orbital to be somewhat less than that of oxygen in phenoxyl, where  $h_O$  is 1.0.

### 3. Sigma-pi Interaction in the Amino-fragment

Using this pair of values for  $h_N$  and  $k_{CN}$ , the spin density at the nitrogen was calculated to be 0.310. Correlation between this spin density value and the experimental coupling for nitrogen ( $a_N = 7.68$  Gauss<sup>84</sup>) gives a  $Q_N$  value of +25 Gauss (see Table 9), assuming Eq. 14 (page 18). The positive sign

Table 9

Correlation of Experimental Couplings and Theoretical Spin Densities for each Interacting Nucleus.

	$a^*$ (experimental) /Gauss	$\rho$ calculated <sup>**</sup>	$Q(a/\rho)$
H <sub>ortho</sub>	5.82	$\rho_3 = 0.185$	-31.46
H <sub>meta</sub>	1.52	$\rho_4 = -0.055$	-27.64
H <sub>para</sub>	9.58	$\rho_5 = 0.301$	-30.90
N	7.68	$\rho_N = 0.310$	24.77
H <sub>amino</sub>	9.58	$\rho_{NH}^H = -0.310^{\ddagger}$	-30.90 <sup>‡</sup>

\* Ref. 84

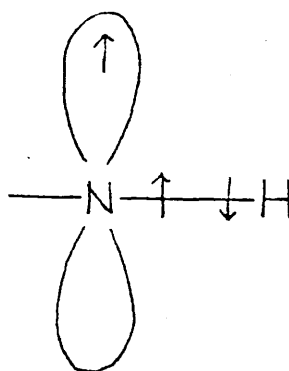
\*\*  $\rho_H = -(\rho_C)$ ;  $\rho_N$  using  $\alpha_N = \alpha + 1.3\beta$ ,  $\beta_{CN} = 1.0\beta$

<sup>‡</sup>  $\rho_{NH}^H = -(\rho_N)$

indicates the direct mechanism<sup>35</sup> by which positive spin density is induced at the nucleus.<sup>28,33,39</sup>

If we envisage a planar amino-fragment in which there is conjugation between the nitrogen  $2p_z$  orbital electrons and the aromatic ring, there is a net spin density at the proton because of spin polarisation<sup>33,34,39</sup> (see Fig. 23)

Fig. 23  
Spin Polarisation  
in the Amino-fragment



which is opposite in sign to the nitrogen  $\pi$  electron density, so that the sign of the ratio between  $\rho_N$  and  $a_{NH}^H$  should be negative.<sup>34,39</sup>

Since  $\rho_N$  is calculated to be 0.310 and the aminoproton coupling constant ( $a_{NH}^H$ ) is 9.58 Gauss,<sup>84</sup> the value of this ratio is approximately -30 Gauss (see Table 9) i.e.

$$a_{NH}^H = \rho_N \times -30 \text{ Gauss} \quad \text{Eq. 16}$$

Other values for  $\rho_N$  and  $a_{NH}^H$  are reported in the literature<sup>85,34</sup>



(see pp.18-20 ), but we would expect to require new  $Q$  values, where the parameters  $h_N$  and  $k_{CN}$  are different.

#### 4. The Aminophenoxyl Series

The exercise of reproducing the experimental values in a single structure is a trivial one, when five parameters are used to reproduce five coupling constants. A severe test lay in applying the parameters to the aminophenoxyl series in which there are some thirty experimental values to be accounted for without recourse to further parameterisation. The linear relations (Eq. 14, with  $Q_N = 25$  Gauss, and Eq. 16) are found to hold (see Table 10). As we would expect, the unsymmetrical structures present the severer test, but surprisingly good agreement is reached for all couplings (see Table 11).

Table 10

Correlation of Experimental\* Aminoproton Coupling with  
Calculated Nitrogen Spin Density.

Substituents in




	$a_{\text{NH}}^{\text{H}}$ (experimental) /Gauss	$\rho_{\text{N}}$ (calculated) <sup>‡</sup>	$Q(a_{\text{NH}}^{\text{H}}/\rho_{\text{N}})$ /Gauss
1-NH <sub>2</sub>	9.58	0.310	30.90
1,4-(NH <sub>2</sub> ) <sub>2</sub>	5.88	0.19	30.95
1-O <sup>-</sup> , 2-NH <sub>2</sub>	5.30	0.20	26.50
1-OH, 2-NH <sub>2</sub>	8.10	0.25	32.40
1-OH, 3-NH <sub>2</sub>	8.25	0.24	34.38
1-O <sup>-</sup> , 4-NH <sub>2</sub>	5.56	0.195	29.26
1-OH, 4-NH <sub>2</sub>	8.00	0.22	29.63

\* Experimental couplings from Refs. 84, 34, 61, 86.

‡ Parameters - see Table 11.

Table 11

\* Calculated Coupling Constants for Aminobenzene Radical Cations and Aminophenoxylys  
(Experimental values (a/Gauss) from Refs. 84, 34, 61, 86 in parentheses)

Substituents in		a <sub>1</sub>	a <sub>2</sub>	a <sub>3</sub>	a <sub>4</sub>	a <sub>5</sub>	a <sub>6</sub>
1-NH <sub>2</sub>		a <sub>N</sub> = 7.70 (7.68) H = 9.24 (9.58) a <sub>NH</sub>	5.60 (5.82)	-1.65 (1.52)	9.03 (9.58)	-1.65 (1.52)	5.60 (5.82)
1,4-(NH <sub>2</sub> ) <sub>2</sub>		a <sub>N</sub> = 4.71 (5.3) H = 5.65 (5.88) a <sub>NH</sub>	2.02 (2.10)	2.02 (2.10)	a <sub>N</sub> = 4.71 (5.3) H = 5.65 (5.88) a <sub>NH</sub>	2.02 (2.10)	2.02 (2.10)
1-O <sup>-</sup> , 2-NH <sub>2</sub>		a <sub>N</sub> = 5.03 (4.76) H = 6.06 (5.30) a <sub>NH</sub>		-0.5 (0.1)	4.24 (4.25)	2.52 (2.95)	1.04 (1.01)
1-OH, 2-NH <sub>2</sub>		a <sub>N</sub> = 6.21 (6.75) H = 7.94 (8.10) a <sub>NH</sub>		0.87 (2.6)	2.32 (1.6)	5.02 (6.6)	1.33 (0.9)
1-O <sup>-</sup> , 3-NH <sub>2</sub>			-0.53	a <sub>N</sub> = 2.51 H = 3.01 a <sub>NH</sub>	13.4	-3.25	11.74
1-OH, 3-NH <sub>2</sub>			0.515 (3.05)	a <sub>N</sub> = 5.91 (7.0) H = 7.09 (8.25) a <sub>NH</sub>	9.66 (8.6)	-2.78 (2.05)	11.39 (10.45)
1-O <sup>-</sup> , 4-NH <sub>2</sub>			2.99 (2.75)	1.57 (1.75)	a <sub>N</sub> = 4.63 (5.25) H = 5.56 (5.56) a <sub>NH</sub>	1.57 (1.75)	2.99 (2.75)
1-OH, 4-NH <sub>2</sub>			1.16 (0.5)	2.99 (4.0)	a <sub>N</sub> = 5.61 (6.60) H = 6.73 (8.00) a <sub>NH</sub>	2.99 (4.0)	1.16 (0.5)

(Table 11, cont.)

- \*  $a_{\text{NH}}^{\text{H}}$  from  $a_{\text{NH}}^{\text{H}} = \rho_{\text{N}} \times -30$  Gauss,  $a_{\text{N}}$  from  $a_{\text{N}} = \rho_{\text{N}} \times 25$  Gauss,  
 $a_{\text{ring}}^{\text{H}}$  from  $a_{\text{H}} = \rho_{\text{C}} \times -30$  Gauss.

Hückel parameters used

$$\alpha_{\text{N}} = \alpha + 1.3\beta, \quad \beta_{\text{CN}} = 1.0\beta, \quad \alpha_{\text{O}} = \alpha + 1.6\beta, \quad \beta_{\text{CO}} = 1.3\beta,$$

$$\alpha_{\text{OH}} = \alpha + 2.0\beta, \quad \beta_{\text{COH}} = 1.1\beta \text{ where } \alpha \text{ and } \beta, \text{ without}$$

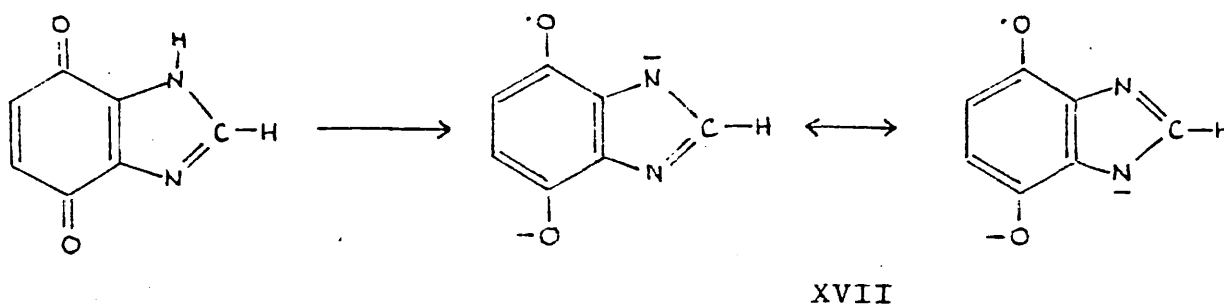
subscripts, refer to carbon  $p^{\pi}$  orbitals. (Oxygen parameters - see references 25,41).

## CHAPTER 4

MOLECULAR ORBITAL CALCULATIONS

## 1. Heterocyclic Semiquinones

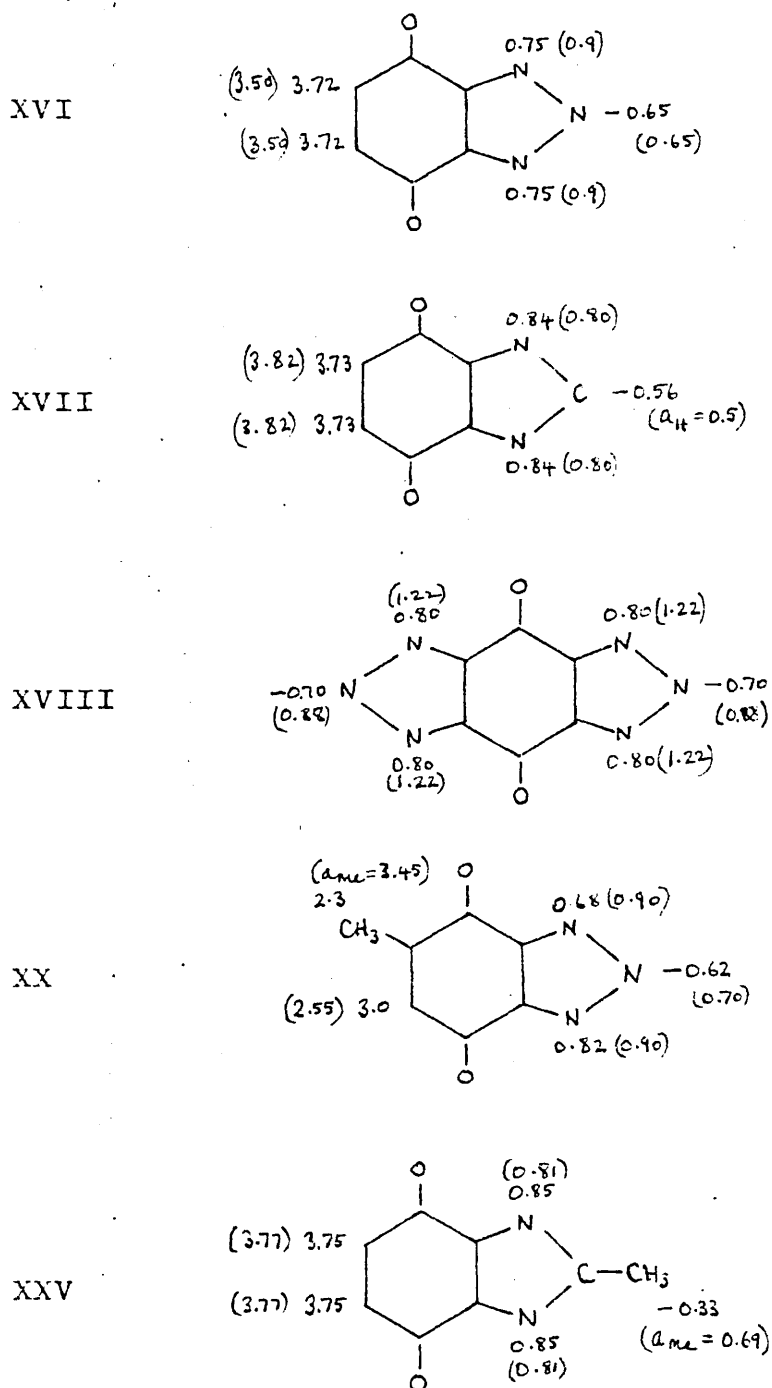
Using the parameters derived in Chapter 3, theoretical coupling constants are calculated for the heterocyclic semiquinones, triazolo-1,4-semiquinone (XVI), bis-triazolo-1,4-semiquinone (XVIII) and the analogous imidazo-1,4-semiquinone (XVII), (see Table 12). The assignment of the small proton coupling in imidazo-1,4-semiquinone is made by analogy with the triazolo-semiquinones, and from a consideration of the symmetry of the radical. Absence of an iminic proton would be expected considering the mobility of the iminic hydrogen.<sup>77</sup>



Also shown in Table 12 are the calculated couplings for 2-methyl-triazolo-1,4-semiquinone (XX) and 2-methylimidazo-1,4-semiquinone<sup>32,78</sup> (XXV), (numbering in XXV as in Ref. 78). A hyperconjugative model<sup>87</sup> for the methyl group has been employed. The spin density on the methyl hydrogen is obtained directly from the hydrogen group orbital, which is incorporated in the calculation with suitable parameterisation<sup>41</sup> (see Fig. 24).

Table 12

Calculated Coupling Constants for Heterocyclic Semiquinones  
(experimental, a/Gauss, in brackets)



$$\alpha_N = \alpha + 1.3\beta$$

$$\beta_{CN} = 1.0\beta$$

$$\alpha_O = \alpha + 1.6\beta$$

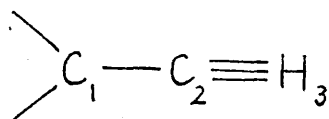
$$\beta_{CO} = 1.3\beta$$

$$Q_{CH}^H = -30 \text{ Gauss}$$

$$Q_N = +25 \text{ Gauss}$$

For methyl parameters, see Fig. 24.

Fig. 24



methyl group parameters

$$h_1=0.0 \quad h_2=-0.7 \quad h_3=-1.0$$

$$k_{12}=0.7 \quad k_{23}=2.5$$

$$a_{\text{H}_3} = 1/3 \rho_{\text{H}} \times 508 \text{ Gauss}^{41}$$

Calculations of methyl hydrogen coupling are on the low side, as found previously,<sup>41</sup> but the other coupling constants are all well predicted.

## 2. Aminosemiquinones


Calculations of theoretical coupling constants in the aminosemiquinones presented an interesting problem. Most of the experimental couplings are well predicted, but the relation proposed in Eq. 16 (page 80) for amino proton splitting in aminophenoxyis and aminobenzene radicals does not hold for the semiquinones. The experimental nitrogen couplings in the former are consistently near to, though slightly smaller than, their respective proton coupling and the ratio of nitrogen to



amino proton couplings always lies between 0.80 and 0.94,<sup>13,85,86</sup> (see Table 13). In the amino-semiquinones, the ratio is

Table 13

Ratio of Experimental Nitrogen and Amino Proton Couplings in Amino-Substituted Radicals.

Substituents in	$a_N/a_{NH}^H$
	
1-NH <sub>2</sub>	0.80
1,4-(NH <sub>2</sub> ) <sub>2</sub>	0.90
1-O <sup>-</sup> , 2-NH <sub>2</sub>	0.90
1-OH, 2-NH <sub>2</sub>	0.83
1-OH, 3-NH <sub>2</sub>	0.85
1-O <sup>-</sup> , 4-NH <sub>2</sub>	0.94
1-OH, 4-NH <sub>2</sub>	0.83
1,4-(O <sup>-</sup> ) <sub>2</sub> , 2,5-(NH <sub>2</sub> ) <sub>2</sub>	2.78
1,4-(O <sup>-</sup> ) <sub>2</sub> , 2-Me, 5-NH <sub>2</sub>	2.47
1,4,5-(O <sup>-</sup> ) <sub>3</sub> , 2-NH <sub>2</sub>	1.65

considerably higher and use of Equation 16 therefore predicts too high a calculated proton coupling. Correlation of the experimental proton coupling and the calculated spin density on the nitrogen (see Table 14) gives a lower  $Q_{NH}^H$  value, nearer

to -10 Gauss. If we use the relation,

$$a_{\text{NH}}^{\text{H}} \underset{\text{Semiquinone}}{=} \rho_{\text{N}} \times -10 \text{ Gauss} \quad \dots \text{Eq. 17}$$

prediction of the amino proton coupling is considerably improved (see Table 15).

Table 14

Correlation of Experimental Aminoproton Coupling ( $a_{\text{NH}}^{\text{H}}$ ) with Theoretical Nitrogen Spin Density ( $\rho_{\text{N}}$ ).

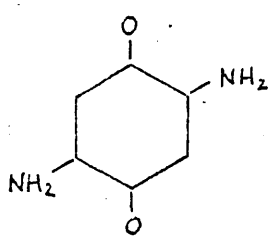
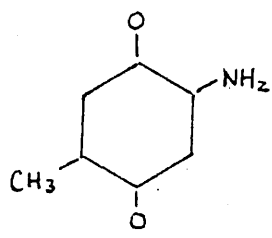
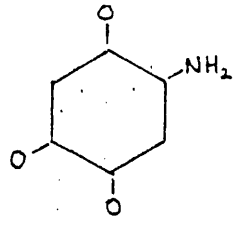
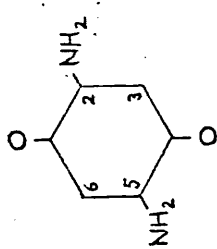
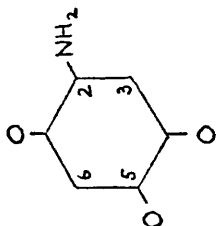
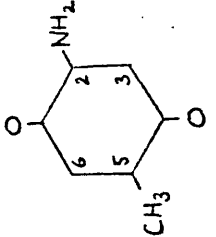
Radical skeleton	$a_{\text{NH}}^{\text{H}}$ /Gauss	$\rho_{\text{N}}$ (calc.)	$Q(a/\rho)$ /Gauss
	0.90	0.0964	9.34
	0.75	0.0870	8.62
	0.725	0.0998	7.26

Table 15

Calculated\* Coupling Constants in Aminosemiquinones  
(Experimental values (a/Gauss) in parentheses)

Radical skeleton	$a_2$	$a_3$	$a_5$	$a_6$
	$a_N = 2.40(2.50)$ $a_{NH}^I = 0.96(0.90)$	$-1.50(0.70)$	$a_N = 2.40(2.50)$ $a_{NH}^{II} = 0.96(0.90)$	$-1.50(0.70)$
	$a_N = 2.49(1.20)$ $a_{NH}^{II} = 1.20(0.725)$	$-1.60(2.25)$		$-1.5(0.125)$
	$a_N = 2.10(1.85)$ $a_{NH}^{II} = 0.84(0.75)$	$-1.20(0.18)$	$a_{CH_3} = 3.10(4.65)$	$0.66(0.75)$

\* Aminoproton couplings calculated from  $a_{NH}^{II} = \rho_N \times -10$  Gauss

Other parameters - see Tables 11 and 12

### 3. Hydroxyl Protons

The magnitude of  $a_{\text{NH}}^{\text{H}}$  in the aminosemiquinones is reminiscent of that of  $a_{\text{OH}}^{\text{H}}$  in some hydroxy radicals. Correlation, as above, between proton splitting and oxygen spin density indicates a similar relationship,

$$a_{\text{OH}}^{\text{H}} = \rho_{\text{O}} \times -10 \text{ Gauss} \quad \dots \text{Eq. 18}$$

Table 16 shows the calculated coupling constants, using Eq. 18 for the hydroxyl proton splitting.

Table 16

Comparison of Calculated ( $a_{\text{OH}}^{\text{H}} = \rho_{\text{O}} \times -10 \text{ Gauss}$ ) and Experimental Hydroxyl Proton Splitting.

(Experimental values in parentheses)

Radical	$a_{\text{OH}}^{\text{H}}/\text{Gauss}$
2-hydroxy-1,4-benzosemiquinone <sup>76</sup>	0.38(0.31)
3-hydroxy-1,2-benzosemiquinone <sup>76</sup>	0.34(0.36)
2,6-dihydroxyphenoxy <sup>76</sup>	0.62(0.72)
4-hydroxyphenoxy <sup>82</sup>	1.82(1.90)
3-hydroxy-2-acetylphenoxy <sup>25</sup>	0.98(1.00)

## CHAPTER 5

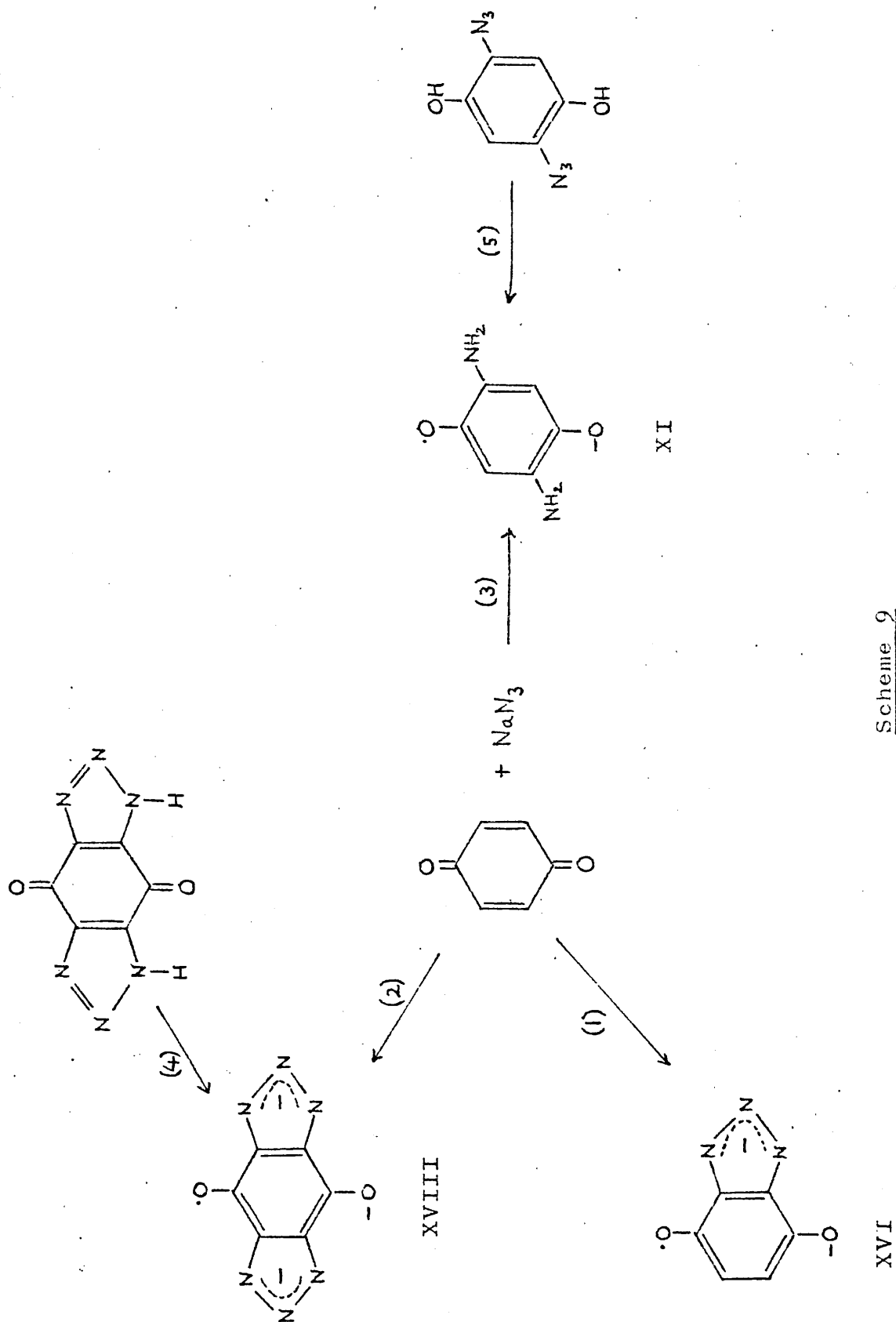
DISCUSSION

## 1. Interaction of 1,4-Benzoquinone with Sodium Azide

We have shown in Chapter 2 that reactions between quinones and sodium azide lead to two different types of radical species. Reaction between 1,4-benzoquinone and sodium azide (see Scheme 9) yields e.s.r. spectra of 2,3-triazolo- and 2,3;5,6-bis-triazolo-1,4-semiquinones (Paths 1 and 2) and a 2,5-disubstituted-1,4-semiquinone (Path 3) and it appears that two different types of addition take place.

It is reasonable to assume that one of them is a straightforward 1,4- addition of  $\text{HN}_3$ ,<sup>42,43,45,46</sup> since the same diamino-semiquinone is also generated from the related 2,5-diazido compound (Path 5), but we cannot know from the spectrum itself by what mechanism the heterocyclic semiquinones arise. Reaction of hydrogen azide with carbon-sulphur double bonds<sup>88</sup> and of azide ion with aromatic carbon-nitrogen double bonds<sup>89</sup> to give triazoles, may proceed via an anionic azido-intermediate, with cyclisation of the azido substituent occurring in preference to protonation,<sup>90</sup> but we reject the possibility of an intermediate carbanion in the case of quinone since this would imply localisation of a negative charge ortho to a carbonyl group.

The other possible mechanism leading to triazolo-1,4-semiquinones is 1,3-dipolar addition of  $\text{HN}_3$ . Although this type of addition of  $\text{HN}_3$  is not known to occur with quinones, it is behaviour well established for organic azides ( $\text{RN}_3$ )<sup>91</sup> and for  $\text{HN}_3$  with alkynes<sup>49,92</sup> and may, in quinones, be

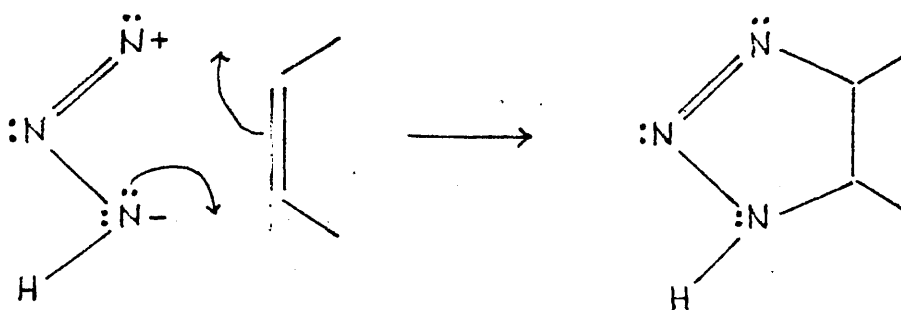


Scheme 9

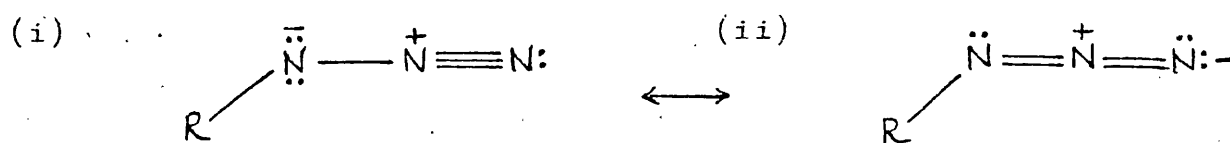
favoured by the juxtaposition of electron-withdrawing groups.<sup>47</sup>

A dipolar addition of  $\text{HN}_3$ , with the iminic proton still attached, must proceed through a "bent" form of the azide in which the two outer nitrogens bear opposite charges<sup>52</sup>

(cf. page 24 ).



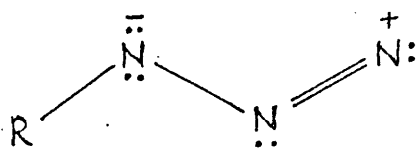
This is feasible because the bending energy is no more than 20 kcal/mole and may be as little as 5-6 kcal/mole.<sup>93</sup> The two main contributors to the ground state of covalent azides<sup>94</sup> are (i) and (ii)



but if energy required to convert an electron pair associated with a  $\pi$  bond to a lone pair of electrons is not very great,<sup>93, 52</sup> then the dipolar form (iii) may, on activation, become important.



(iii)

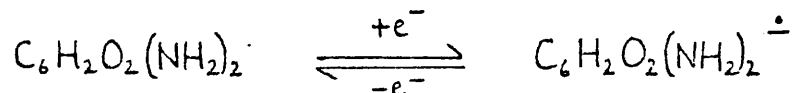


The shape of the group depends on the hybridisation of the middle nitrogen and a change to near- $sp^2$  would result in a decrease in the -N- bond angle. This does not necessarily mean that there is a single resonance form. The bent form may only figure marginally in the ground state but is still capable of influencing the course of reaction and making the all-important facilitating transition state more likely.<sup>52</sup>

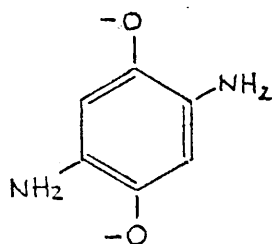
If both types of addition do occur, they both take place in the same reaction solution and probably at the same time, although there is a delay in the build-up of sufficient concentration of radical resulting from Path 3 (Scheme 9). If this delay did not occur, we would probably not see the triazolo- radicals. When bis-triazolo-1,4-semiquinone is generated from the corresponding quinone (Path 4), the signal persists for hours rather than minutes and never decays in favour of a signal of the diamino species. It may be, therefore, that the decay of XVI or XVIII (Scheme 9) is accelerated by the presence of other reaction products.

The function of sodium dithionite in generating the radicals is, of course, a reducing one.<sup>1,11</sup> Substituted amino-semiquinones require a very high reduction potential to be generated from the parent quinones<sup>14</sup> (in the vicinity of  $-1.0 \text{ V}^{95}$ ) so that the following equilibrium, in an

electrolytic reduction,



must lie well over to the left. It is therefore interesting that we observe the hitherto unreported 2,5-diamino-1,4-semiquinone (Paths 3 and 5, Scheme 9) with apparent ease and in high concentration and probably indicates that the radical requires the dianion



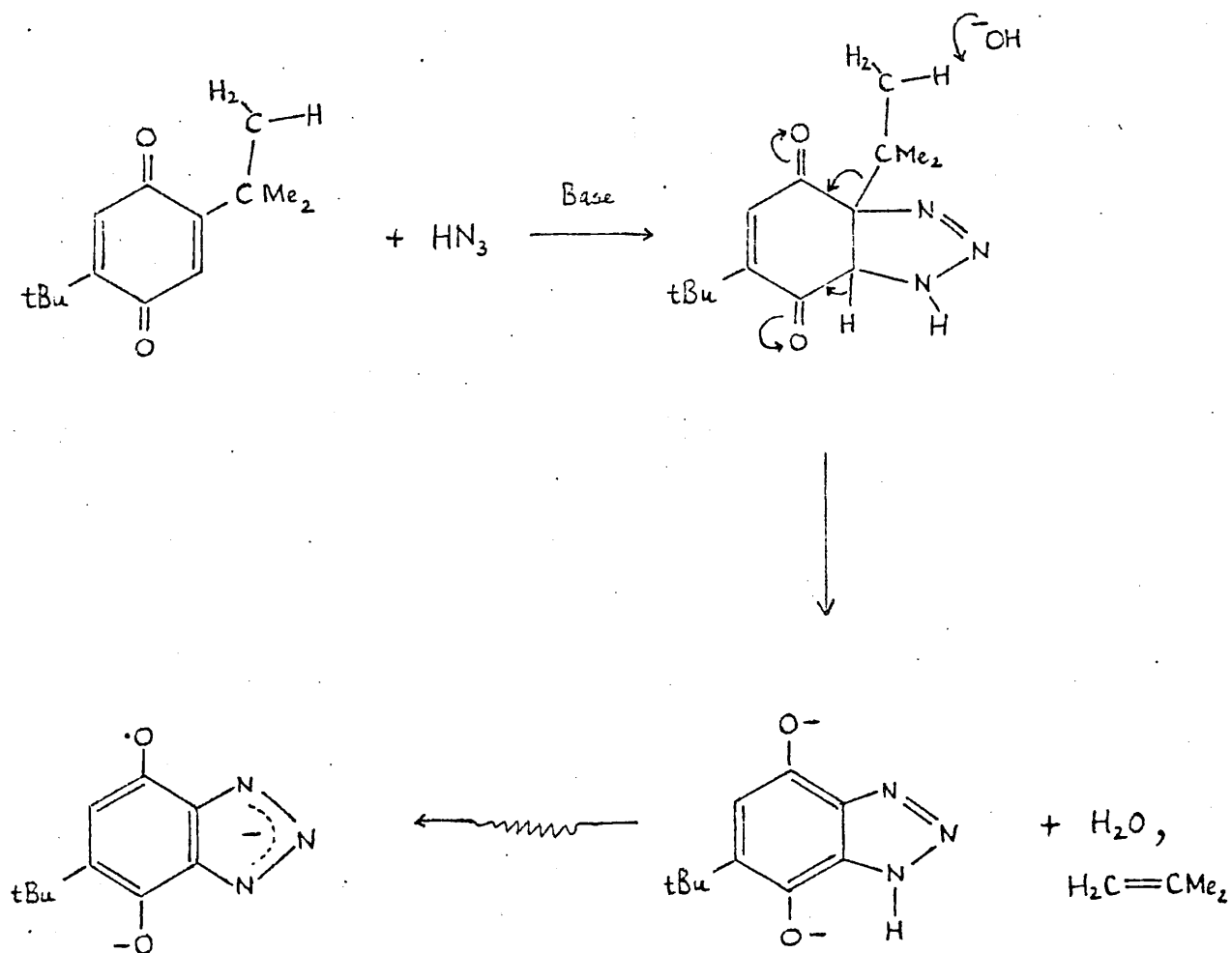
as its precursor.

Failure to produce the radical directly from the diaminoquinone may be partly due to competitive reactions involving the sensitive  $\alpha$ -amino-carbonyl moieties.

We did not detect an azidosemiquinone from the starting material 1,4-benzoquinone, but the spectrum of 2-azido-3,6-di-t-butylsemiquinone (page 74,) showed only one small nitrogen coupling. This suggests that the azido group is twisted out of the plane of conjugation so that the effects, on the unpaired electron, of only the nearest nitrogen are felt. It is interesting that 2-t-butyl-triazolosemiquinone is observed

after reaction between the di-t-butyl-substituted quinone and sodium azide. The basic conditions required to generate the radical (see Ch. 2-1), may account for the dealkylation, allowing a base-catalysed elimination of a t-butyl group as iso-butene (see Scheme 10) after addition of  $\text{HN}_3$ .

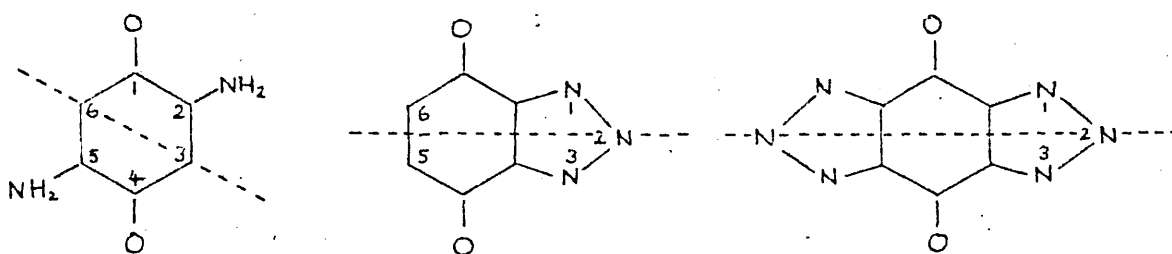
Scheme 10



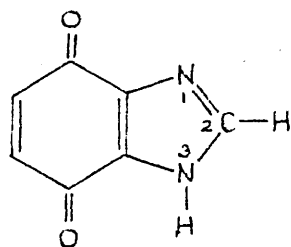
## 2. Symmetry Considerations

Interpretation of the coupling constants in e.s.r. spectra does not, in principle, permit unambiguous assignments and here, theoretically computed spin densities are useful.

McLachlan negative spin densities are predicted for the 3 and 6 ring positions in the diamino-semiquinone<sup>40</sup> (cf. Ref. 97) and for the 2 position in the triazolosemiquinones<sup>40</sup> and must correspond to the position of nodal planes when the odd electron is in an antisymmetric orbital.<sup>25</sup>



The two smaller coupling constants in the triazolo-1,4-semiquinone (XVI) spectrum are both due to nitrogen. Thus, we do not encounter the problem which arises in the case of imidazo-1,4-semiquinone (XVII), whose small proton coupling cannot be assigned by inspection alone and may be due either to the imidazolic hydrogen  $\begin{array}{l} \diagup \\ \text{C-H} \\ \diagdown \end{array}$  or to an iminic hydrogen  $\begin{array}{l} \diagdown \\ \text{N-H} \\ \diagup \end{array}$ , both of which are present in the parent quinone:<sup>32,78</sup>



The spin density at carbon 2 is also negative<sup>40</sup> and must give origin to a small coupling constant.<sup>25</sup> If a nodal plane bisects this atom then the sign of the wave-function at  $N_1$  should be opposite to the sign at  $N_3$  and the molecular orbital in which the odd electron resides, antisymmetric with respect to positions 1 and 3 and positions 5 and 6. Using the interleaving theorem,<sup>98</sup> this result is predicted for the 7<sup>th</sup> molecular orbital (the odd-electron orbital in the triazolo- and imidazolo- semiquinones). Fig. 25 illustrates the systematic development of the orbitals of triazolo-1,4-semiquinone from simpler molecular fragments.

It is encouraging that the Hückel parameters for nitrogen<sup>40</sup> ( $h_N=1.3$ ,  $k_{CN}=k_{NN}=1.0$ ) reproduce the experimental couplings, especially in the triazolo- and imidazolo-1,4-semiquinone, XVI and XVII, whereas previous calculations report a 20% difference between experiment and theory.<sup>32</sup>

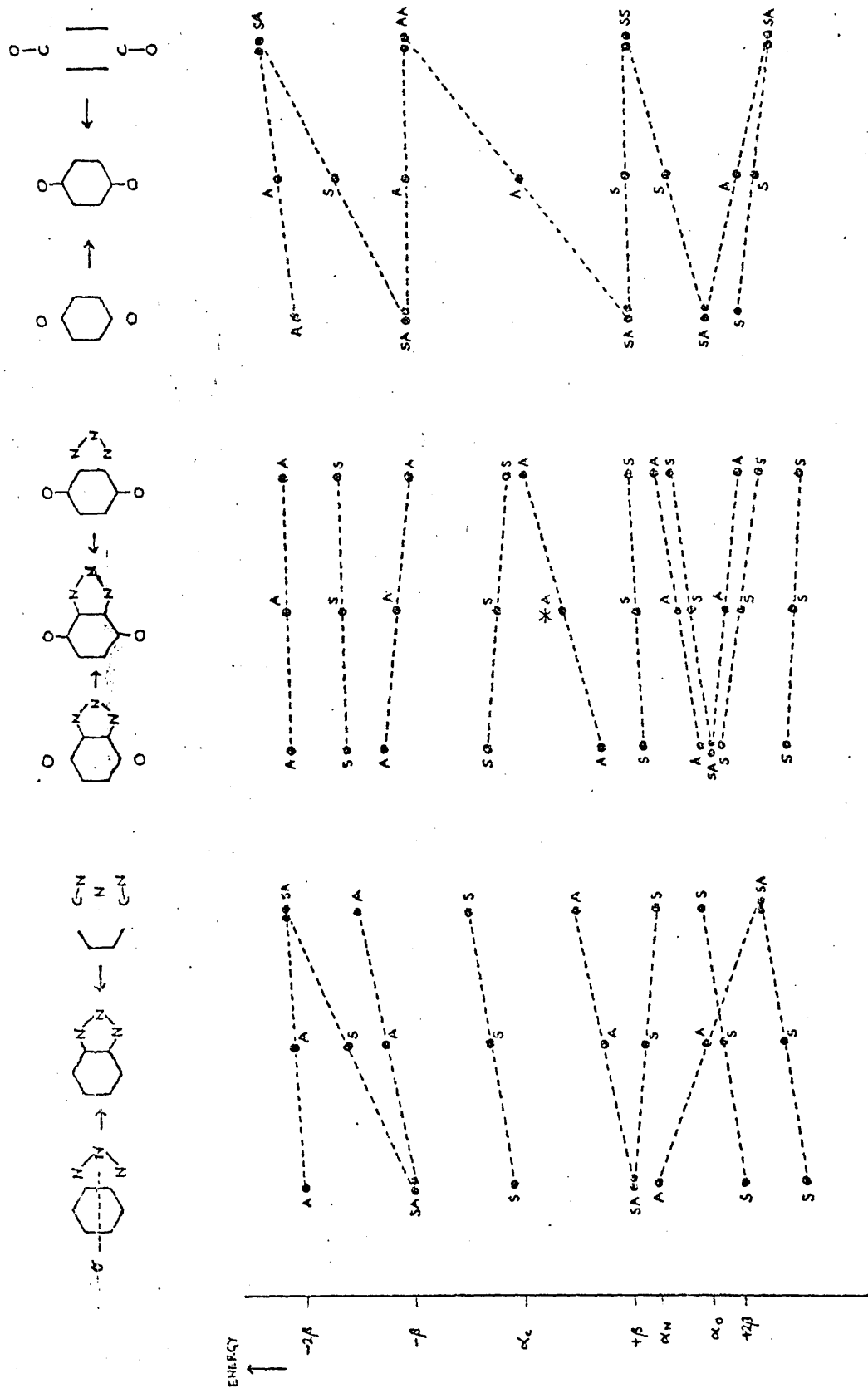


Figure 25

Schematic Development of the Orbitals of 2,3-Triazolo-1,4-semiquinone using the Interleaving Theorem, 98  $\sigma$  symmetry plane, \*odd electron orbital.

### 3. Amino-group Spin Densities

The amino-group in aminophenoxy radicals and aminosemiquinones ought to be strictly comparable. On theoretical grounds, aminoproton hyperfine coupling should be an indication of the spin density at the nitrogen atom.<sup>39</sup> Eq. 15 (page 19) holds for aminobenzene radical cations<sup>34,84</sup> and aminophenoxy radicals<sup>86</sup> (see Table 11, page 83) and aminoproton coupling is given by Eq. 16 (page 80) where  $Q_{NH}^H$  is -30 Gauss. The relationship between amino-group hyperfine couplings in 2,5-diamino-1,4-semiquinone where  $a_N = 2.5$  Gauss and  $a_{NH}^H = 0.9$  Gauss, is evidently different. From the theoretical spin density on the nitrogen atom ( $\rho_N = 0.096$ ), the empirical value for  $Q_{NH}^H$  is found to be about -10 Gauss. This discrepancy may be due to a difference in the charge densities of the two systems<sup>99</sup> or may indicate that the assumption of a planar equilibrium configuration for the semiquinone amino-group is unjustified.<sup>100</sup>

The implications of the pairing theorem for alternate hydrocarbons<sup>101</sup> are that the value of  $Q$  should decrease in the case of a negatively charged radical ion.<sup>99,102</sup> The following equation<sup>102</sup> may be written for aminoproton couplings,

$$a_{NH}^H(0) = Q_{NH}^H(0) \rho_N^\pi \pm K_{NH}^H \rho_N^{\pi 2}$$

where  $Q_{NH}^H(0)$  is an appropriate neutral parameter and  $K_{NH}^H$  is

a correction constant for excess negative charge density.

Using the value for  $Q_{\text{NH}}^{\text{H}}$  of -30 Gauss for  $Q_{\text{NH}}^{\text{H}}(\text{C})$ , leads to a value of +32 Gauss for  $K_{\text{NH}}^{\text{H}}$ , which is rather a large correction, when the literature reports changes of the order of  $\pm 15\%$ .<sup>103</sup>

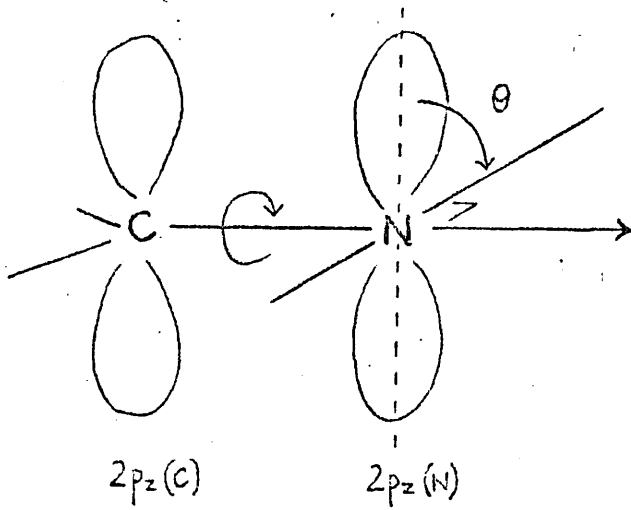
The low proton splitting may also be interpreted in terms of out-of-plane movement of the C-N-H bond. There are two mechanisms<sup>100,104</sup> (see Fig. 26) which may determine the extent of the proton's interaction with the unpaired electron and the sign of its coupling constant. Spin polarisation (see Fig. 23, page 80) generates negative spin density at the proton, proportional to  $\rho_{\text{N}}$ ;<sup>39</sup> however when the proton is pushed out of the nodal plane of the aromatic  $\pi$  system, some direct overlap between the proton and this system would result in a positive spin density at the proton<sup>100,104,105</sup> whose magnitude is determined by the angle  $\theta$ , (see Fig. 25).

The effects of rotation about the C-NH<sub>2</sub> bond would be temperature dependent and such a dependence for aminoproton coupling has been observed.<sup>106</sup> The much reduced coupling at high temperature has been interpreted in terms of a contribution by positive spin density.<sup>107</sup>

Unrestricted rotation about the C-NH<sub>2</sub> bond would cause a time-averaged angle ( $\theta$ ) of  $45^\circ$  to affect the extent of these mechanisms (see Fig. 26). If both spin polarising and hyperconjugative mechanisms contribute to the proton hyperfine coupling at all angles except  $\theta = 0^\circ, 90^\circ$ , an equation can be written, using previous nomenclature,<sup>105,107</sup>



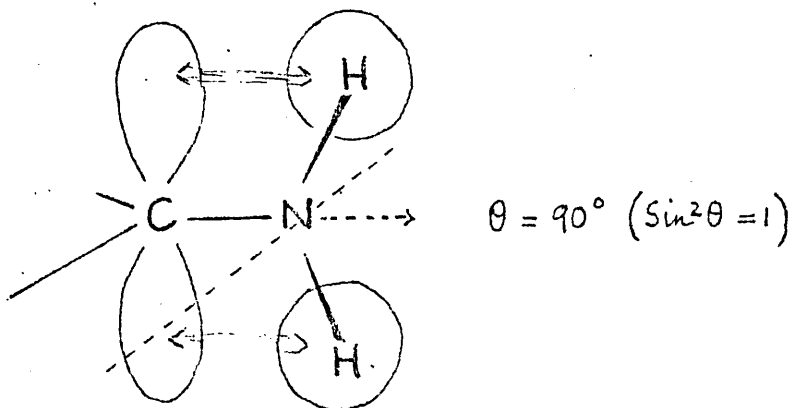
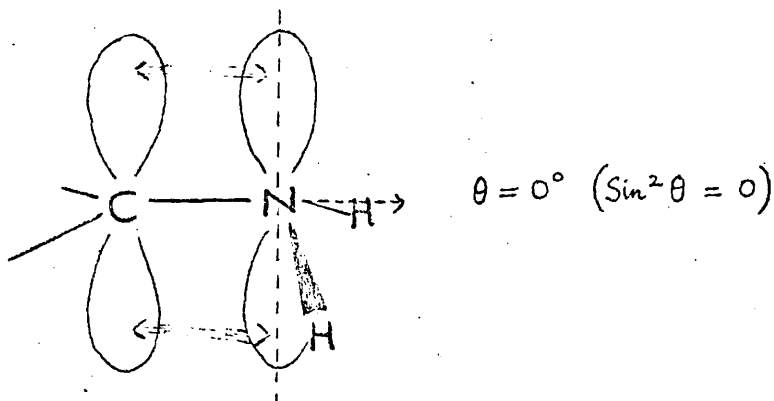
Rotation about C-N bond



$\theta$  = angle of twist of  $2p_z(N)$   
 out of plane of  $2p_z(C)$  orbital  
 As  $\theta$  increases, overlap  
 decreases as  $\cos^2\theta$ .

N-H bonds and  $2p_z(C)$  become  
 coplanar as function of  
 $\sin^2\theta$ .

2 extreme conformations of  $C-NH_2$



$$a_{NH}^H = Q_H^\pi \rho_N + Q_H^\sigma \rho_C \quad \dots \text{Eq. 19}$$

where the parameter  $Q_H^\pi$  would decrease as a function of  $\cos^2 \theta$  and the parameter  $Q_H^\sigma$  would increase as a function of  $\sin^2 \theta$ . This would also imply that  $\rho_N$  is a decreasing function of  $\cos^2 \theta$ , as the nitrogen  $2p_z$  orbital is twisted away from the region of maximum  $\pi$ -overlap but this may be compensated for by an appreciable contribution to  $\rho_N$  by a wagging vibration.<sup>107</sup> Resultant proton coupling would therefore be:

$$a_{NH}^H(\theta) = Q_H^\pi \rho_N (\cos^2 \theta) + Q_H^\sigma \rho_C (\sin^2 \theta) \quad \dots \text{Eq. 20}$$

$\rho_N$  and its adjacent  $\rho_C$  are computed to be 0.096 and 0.172, respectively. If we assume a value for  $\theta$  of  $45^\circ$  and use the phenoxyl  $Q_{NH}^H$  value (-30 Gauss) for  $Q_H^\pi$ , Eq. 20 becomes:

$$0.9 = (-30)(0.096)(0.5) + Q_H^\sigma (0.172)(0.5)$$

whence

$$Q_H^\sigma = +23 \text{ Gauss}$$

so that supplying values in Eq. 19, aminoproton coupling is given by the relation

$$a_{NH}^H = -30 \rho_N + 23 \rho_{C \text{ adjacent}}$$

Further experimental work on suitable amino compounds would be required to investigate the scope of a relationship such as that proposed in Eq. 20.

#### 4. Linewidth variation in the spectrum of triazolo-1,4-semiquinone

Variation in the linewidths of different hyperfine lines has been observed in the room temperature spectra of the triazolo-radicals, in which high field lines are of lower amplitude, and broader, than those at low field. Similar linewidth variations have been observed<sup>108,39,110</sup> at low temperatures ( $-50^{\circ}\text{C}$  or below), but at higher temperatures the effects appear to subside and all hyperfine components have essentially the same width.<sup>108,39</sup> Since theoretical expressions for the linewidths have been offered in the literature,<sup>39,100,110</sup> we have made a preliminary investigation of the spectrum of triazolo-1,4-semiquinone (Fig. 13) to see

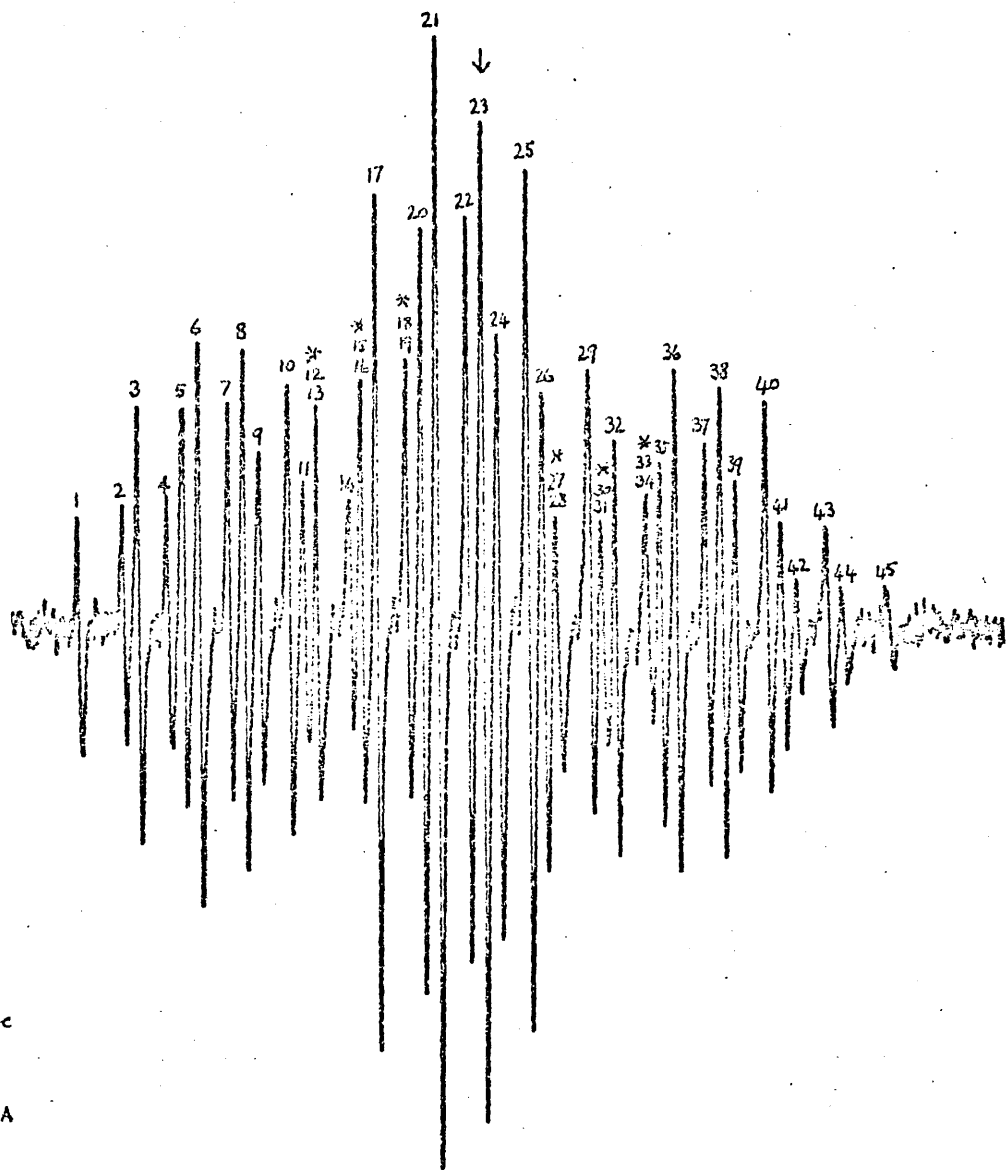
if such an expression can be made to fit experimental measurements made upon this spectrum.

Fig. 27 shows the spectral lines numbered 1 to 45, from the low field end, with the degeneracy of each line,  $D_i$ . It can be seen that 12 lines are overlapped. Each line is specified by "spectral index" numbers,  $\tilde{M}_i$  (see Table 17) which are equal in magnitude to the quantum numbers  $M_i$ , associated with each coupling constant,  $a_i$ ,<sup>39,109</sup> but are here defined as being positive on the low field side of the spectrum. The experimental parameter<sup>108</sup> is a measurement of the peak-to-peak amplitude,  $A_i$ , of the line  $i$ , since for line shapes that are mainly Lorentzian the amplitudes are inversely proportional to the square of the width.<sup>108</sup> The experimental relative width,  $W_i$ , for the  $i^{\text{th}}$  line is defined in terms of a reference line,  $r$ , of degeneracy  $D_r$  (which in this case is line 23, the central line) by the relation<sup>108</sup>

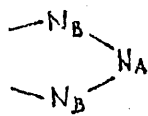
$$W_i = \left[ (D_i/A_i)(A_r/D_r) \right]^{\frac{1}{2}} \quad \dots\text{Eq. 21}$$

According to the general theory of linewidths,<sup>109</sup> an expression for triazolo-1,4-semiquinone may be written,

$$W_i = 1 + B_{N_A} \tilde{M}_{N_A} + C_{N_A} \tilde{M}_{N_A}^2 + B_{N_B} \tilde{M}_{N_B} + C_{N_B} \tilde{M}_{N_B}^2 + D_{N_A N_B} \tilde{M}_{N_A} \tilde{M}_{N_B} \\ + B_{H_A} \tilde{M}_{H_A} + C_{H_A} \tilde{M}_{H_A}^2 + D_{N_A H_A} \tilde{M}_{N_A} \tilde{M}_{H_A} + D_{N_B H_B} \tilde{M}_{N_B} \tilde{M}_{H_B} \quad \dots\text{Eq. 22}$$

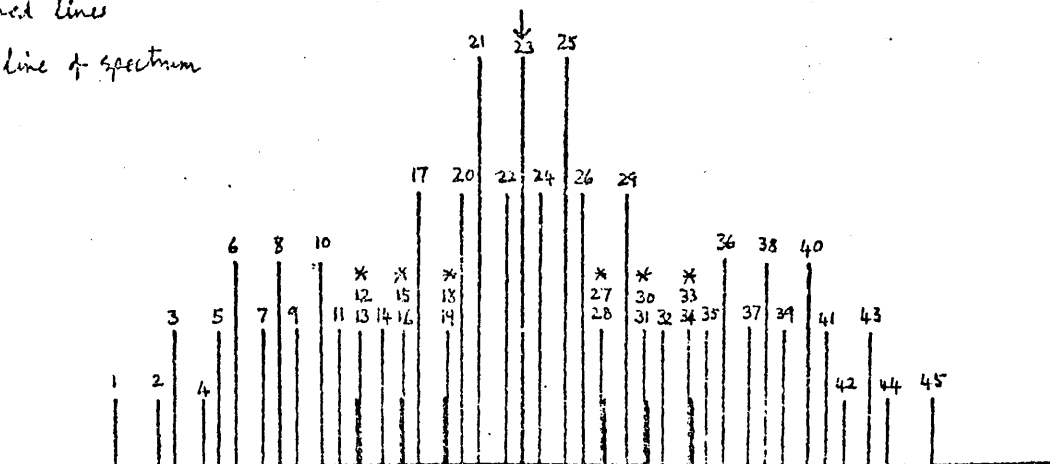


Nomenclature



\* overlapped lines

↓ centre line of spectrum



Degeneracy,  $D_i$

1 12 123 232 321 2 2 1 4 1 4 6 4 6 4 6 4 2 4 2 2 2 3 2 3 2 3 2 1 2 1 1

Fig. 27 Labelling of spectral lines in triazolo-1,4-semiquinone for line-width analysis.

with which the data for all but overlapped lines (see Fig. 27) may be analysed.<sup>108,39</sup> The values of the B, C and D parameters are obtained by fitting the expression (Eq. 22) to the experimental values,  $W_i$ , giving the following relation:<sup>\*</sup>

$$\begin{aligned}
 W_{\text{theo.}} = & 1 - 0.0612 \tilde{M}_{N_A} - 0.0178 \tilde{M}_{N_A}^2 - 0.1186 \tilde{M}_{N_B} \\
 & + 0.0207 \tilde{M}_{N_B}^2 + 0.0339 \tilde{M}_{N_A} \tilde{M}_{N_B} - 0.0249 \tilde{M}_H \\
 & + 0.0178 \tilde{M}_H^2 + 0.0047 \tilde{M}_{N_A} \tilde{M}_H - 0.0177 \tilde{M}_{N_B} \tilde{M}_H
 \end{aligned}$$

The values for  $W_{\text{theo.}}$  are close to the experimental data (see Table 17) and the parameters (see Table 18) are consistent in magnitude with similar data for other compounds.<sup>108,39,109,110</sup>

Prediction of the anisotropic data for the radical leads to the sign of the isotropic hyperfine splittings, via the parameters B and D.<sup>39,103,110</sup> Previous evidence<sup>109</sup> suggests that in the case of triazolo-1,4-semiquinone, the sign of the  $B_N$  parameters are negative if the spin density on the appropriate nitrogen is positive (if the magnetogyric ratio,  $\gamma_N$  is positive<sup>109,111</sup>). For the principal nitrogen lines ( $M_H = 0$ ),

$$W_i = 1 \pm B + C \quad (\text{where } B < 0)$$

---

\*  $W_{\text{theo.}}$  = theoretical relative width for each line,  $W_i$ .

Table 17

Line-width analysis data for triazolo-1,4-semiquinone at room temperature

Line Number <sup>a</sup>	Spectral Index Numbers <sup>b</sup>			Degeneracy D <sub>i</sub>	Experimental Results			
	$\tilde{M}_{NA}$	$\tilde{M}_{NB}$	$\tilde{M}_H$		Measured Amplitude <sup>c</sup> , A <sub>i</sub>	Relative Width <sup>d</sup> , W <sub>i</sub>	Calculated Relative Width <sup>e</sup> , W <sub>theo.</sub>	Deviation x10 <sup>3</sup>
1	1	2	1	1	3.55	0.8336	0.7932	-40
2	0	2	1	1	3.58	0.8301	0.8031	-27
3	1	1	1	2	6.46	0.8739	0.8335	-40
4	-1	2	1	1	3.72	0.8143	0.7739	-40
5	0	1	1	2	5.90	0.9144	0.8773	-37
6	1	0	1	3	8.31	0.9437	0.9187	-25
7	-1	1	1	2	5.90	0.9144	0.8821	-32
8	0	0	1	3	7.70	0.9803	0.9929	13
9	1	-1	1	2	4.92	1.0014	1.0418	40
10	-1	0	1	3	6.65	1.0549	1.0316	-23
11	0	-1	1	2	3.85	1.1320	1.1499	18
14	-1	-1	1	2	3.41	1.2028	1.2225	19
17	1	1	0	4	12.66	0.8828	0.8571	-26
20	0	1	0	4	11.31	0.9340	0.9021	-32
21	1	0	0	6	16.77	0.9394	0.9210	-18
22	-1	1	0	4	11.01	0.9467	0.9116	-35
24	1	-1	0	4	8.95	1.0500	1.0264	-24
25	-1	0	0	6	12.71	1.0791	1.0434	-36
26	0	-1	0	4	7.09	1.1797	1.1393	-40
29	-1	-1	0	4	6.58	1.2245	1.2166	-8
32	1	1	-1	2	6.15	0.8956	0.9127	17
35	0	1	-1	2	5.40	0.9558	0.9625	6
36	1	0	-1	3	7.41	0.9993	0.9589	-40
37	-1	1	-1	2	5.10	0.9835	0.9767	-7
38	0	0	-1	3	6.96	1.0311	1.0426	11
39	1	-1	-1	2	4.31	1.0699	1.0465	-23
40	-1	0	-1	3	5.80	1.1295	1.0908	-38
41	0	-1	-1	2	3.40	1.2046	1.1642	-40
42	1	-2	-1	1	1.72	1.1975	1.1755	-22
43	-1	-1	-1	2	2.98	1.2867	1.2462	-40
44	0	-2	-1	1	1.49	1.2867	1.3271	40
45	-1	-2	-1	1	1.26	1.3992	1.4431	44

a The numbering system is that of Fig. 27. Lines overlapped are excluded from the analysis.

b These are the same as the quantum numbers for the nitrogens and protons and correspond in sign ( $\tilde{M}_i = M_i$ ) if the splitting constant  $a_i$  is positive but are opposite in sign if  $a_i$  is negative.<sup>110</sup>

c Measured peak-to-peak amplitude of the experimental line, i.

d Ratio of the reduced amplitude ( $A_i/D_i$ ) of line i to reduced amplitude of central line ( $A_{23}/D_{23}$ ) calculated from Eq. 21.

e Calculated from Eq. 22.

Table 18

Calculated values for the  
line-width equation parameters (see Eq.22)

$B_{N_A}$	-0.0612
$C_{N_A}$	-0.0178
$B_{N_B}$	-0.1186
$C_{N_B}$	0.0207
$D_{N_A N_B}$	0.0339
$B_H$	-0.0249
$C_H$	0.0178
$D_{N_A H}$	0.0047
$D_{N_B H}$	-0.0177



and the lower sign (i.e.  $M_N$  negative) gives the larger  $W_i$ . Experimentally, the high field principal nitrogen lines are broader. For a positive magnetogyric ratio, a positive coupling constant means that low field lines have  $M_I > 0$ <sup>111</sup> so that the broadened lines indicate  $a_N > 0$ . The parameter  $B$  actually gives the sign of  $(a\rho)$ , as opposed to simply  $(a)$ ,<sup>109</sup> and the same linewidth trend is indicated for both  $N_A$  and  $N_B$ .

The signs of the  $D$  parameters are more difficult to interpret. It is unclear whether the sign of  $D_{ij}$  leads directly to the relative signs of the splittings of the nuclei in the cross terms<sup>39,108,109</sup> or whether to the relative signs within the product  $(a_i\rho_i)(a_j\rho_j)$  (cf. Ref. 109). The positive sign of  $D_{N_A N_B}$  appears to be in contradiction with the negative McLachlan spin density at  $N_A$  and the antisymmetry of the odd electron orbital for triazolo-1,4-semiquinone (see p. 102). In any case, our other  $D$  values are inconsistent in sign; we should also expect that if  $a_N$  and  $a_H$  are of opposite sign,<sup>109</sup> (and Refs. within) a positive value for  $D_{N_A N_B}$  would imply a negative value for  $D_{N_A H}$ .

REFERENCES

1. P. Ashworth and W. T. Dixon, J.C.S. Perkin II, 1972, 1130, 1974, 739; Chem. Comm., 1971, 1150 and references within.
2. B. Venkataraman, B. G. Segal and G. K. Fraenkel, J. Chem. Phys., 1959, 30, 1006.
3. C. Trapp, C. A. Tyson and G. Giacommetti, J. Amer. Chem. Soc., 1968, 90, 1394 and references within.
4. J. R. Bolton and A. Carrington, Proc. Chem. Soc., 1961, 385.
5. G. Vincow and G. K. Fraenkel, J. Chem. Phys., 1961, 34, 1333.
6. K. A. Lott, E. L. Short and D. N. Waters, J. Chem. Soc., (B), 1969, 1232 and references within.
7. P. D. Sullivan and J. R. Bolton, J. Amer. Chem. Soc., 1968, 90, 5366.
8. E. Lieber, J. S. Curtice and C. N. R. Rao, Chem. Ind. (London), 1966, 586.
9. J. H. Boyer and F. C. Canter, Chem. Rev., 1954, 54, 1.
10. "The Chemistry of the Azido Group", ed. S. Patai, John Wiley and Sons (Interscience) 1971.
11. Y. Matsunaga and C. A. McDowell, Canad. J. Chem., 1960, 38, 1167.
12. G. A. Russell, R. Konaka et al., J. Amer. Chem. Soc., 1968, 90, 4646.
13. A. T. Bullock and C. B. Howard, Trans. Faraday Soc., 1970, 66, 1861 and references within.
14. J. L. Huntington, Diss. Abstr. Int., 1970-71, 31, I, 90B.

15. Chemical Society Specialist Periodical Reports, E.S.R., Vol. II, Chapter 10 by A. J. Dobbs.
16. N. M. Atherton "Electron Spin Resonance", Ellis Horwood (John Wiley), 1973, Ch.1, p.4; J. E. Wertz and J. R. Bolton "Electron Spin Resonance", McGraw-Hill Book Company, 1972, Ch.1, p.12.
17. G. K. Fraenkel and B. Segal, Ann. Rev. Phys. Chem., 1959, 10, 435.
18. H. M. McConnell, J. Chem. Phys., 1956, 24, 632;  
H. M. McConnell and H. H. Dearman, *ibid.*, 1958, 28, 51;  
H. M. McConnell and D. B. Chesnut, *ibid.*, p.107.
19. H. M. McConnell, C. Heller, T. Cole and R. W. Fessenden, J. Amer. Chem. Soc., 1960, 82, 766.
20. H. M. McConnell and C. H. Holm, J. Chem. Phys., 1957, 27, 314.
21. C. A. Coulson "Valence", Oxford University Press, London, 1961, 2nd. Ed., Ch.3.
22. C. A. Coulson, R. Mallion and B. O'Leary, "Hückel Theory for Organic Chemists", London Academic Press, 1978;  
N. V. Riggs "Quantum Chemistry", McMillan, London, 1969, Ch.4.
23. A. D. McLachlan, Mol. Phys., 1960, 3, 233.
24. G. Vincow, J. Chem. Phys., 1963, 38, 917.
25. W. T. Dixon, M. Moghimi and D. Murphy, J.C.S. Faraday II, 1974, 70, 1713.
26. J. N. Murrell, S. F. A. Kettle and J. M. Tedder, "Valence Theory", London, Wiley, 1965, Ch.9, p.127.
27. C. L. Honeybourne, Tetrahedron Lett., 1971, 52, 4927;  
J.C.S. Faraday II, 1975, 71, 1343.

28. R. L. Ward, J. Amer. Chem. Soc., 1962, 84, 332.
29. N. M. Atherton, F. Gerson and J. N. Murrell, Mol. Phys., 1962, 5, 509.
30. E. W. Stone and A. H. Maki, J. Chem. Phys., 1963, 39, 1635.
31. J. C. M. Henning and C. de Waard, Phys. Letters, 1962, 3, 139.
32. M. K. V. Nair, K. S. Santhanam and B. Venkataraman, J. Magn. Resonance, 1973, 9, 229; Mol. Phys., 1970, 19, 585.
33. B. L. Barton and G. K. Fraenkel, J. Chem. Phys., 1964, 41, 1455.
34. M. T. Melchior and A. H. Maki, J. Chem. Phys., 1961, 34, 471.
35. M. Karplus and G. K. Fraenkel, J. Chem. Phys., 1961, 35, 1312.
36. J. C. M. Henning, J. Chem. Phys., 1966, 44, 2139.
37. N. M. Atherton, J. N. Ockwell and R. Dietz, J. Chem. Soc. (A), 1967, 771.
38. A. Carrington, Chem. Soc. Ann. Reports, 1964, 61, 27.
39. B. L. Barton and G. K. Fraenkel, J. Chem. Phys., 1964, 41, 695.
40. This work.
41. W. T. Dixon, P. M. Kok and D. Murphy, J.C.S. Faraday II, 1977, 73, 709.
42. E. Oliveri-Mandala, Gazz. Chim. Ital., 1915, 45, II, 120; E. Oliveri-Mandala and E. Calderaro, ibid., 1915, 45, I, 307.

43. L. F. Fieser and J. L. Hartwell, *J. Amer. Chem. Soc.*, 1935, 57, 1482.
44. H. W. Moore and H. R. Sheldon, *J. Org. Chem.*, 1968, 33, 4019.
45. H. W. Moore, H. R. Sheldon and D. F. Shellhamer, *J. Org. Chem.*, 1969, 34, 1999.
46. J. H. Boyer, *J. Amer. Chem. Soc.*, 1951, 73, 5248.
47. R. Escales, *Chem.-Ztg.*, 1905, 29, 31.
48. K. Fries, P. Ochwat and W. Pense, *Ber.*, 1923, 56, 1291;  
K. Fries and P. Ochwat, *ibid.*, 1923, 56, 1299;  
A. Korczynski and S. Namyslowzki, *Bull. Soc. Chim. France*, 1924, 35, 1186; H. W. Moore and H. R. Sheldon, *Tetrahedron Letters*, 1968, 5431.
49. A. Michael, *J. prakt. Chem.*, 1893, 48, 94;  
O. Dimroth and G. Fester, *Ber.*, 1910, 43, 2219.
50. L. I. Smith, *Chem. Rev.*, 1938, 23, 193.
51. R. Huisgen, *Proc. Chem. Soc.*, 1961, 357.
52. R. Huisgen, *Angew. Chem. (Int. Ed.)*, 1963, 2, 633.
53. W. I. Awad, A. R. A. Raong and A. Boulos, *J. Chem. U.A.R.*, 1966, 9, 267.
54. L. Wolf and G. K. Grau, *Annalen*, 1912, 394, 68.
55. L. F. Fieser and E. L. Martin, *J. Amer. Chem. Soc.*, 1935, 57, 1844.
56. F. M. Dean, P. G. Jones and P. Sidisunthorn, *J. Chem. Soc.*, 1962, 5186.
57. F. R. Benson and W. L. Savell, *Chem. Rev.*, 1950, 46, 1.
58. R. C. Elderfield "Heterocyclic Compounds", Vol. 7, Ch.5, p.408-426.

59. Anonymous, Chem. Eng. News, 1956, 34, 2450.
60. H. B. Mark and C. L. Atkin, Analytical Chem., 1964, 36, 514.
61. P. Neta and R. W. Fessenden, J. Chem. Phys., 1974, 78, 523.
62. M. R. Das and G. K. Fraenkel, J. Chem. Phys., 1963, 42, 1350 and references within; P. B. Ayscough "Electron Spin Resonance in Chemistry", Methuen, 1967, p.301.
63. W. T. Dixon, P. M. Kok and D. Murphy, Tetrahedron Letters, 1976, 8, 623.
64. E. Winkelmann, Tetrahedron, 1969, 25, 2427; W. H. Gilligan and M. J. Kamlet, Tet. Lett., 1978, 19, 1675.
65. F. Sorm, Chem. Obzov., 1939, 14, 37; Chem. Abst., 1939, 33, 7286.
66. A. I. Vogel, "A Textbook of Practical Organic Chemistry", Longmans Green, London, 3rd. Ed., 1956.
67. E. B. Vliet, Org. Syntheses, Coll. Vol. II, p.85.
68. L. F. Fieser, Organic Syntheses, 1937, 17, 68.
69. "Dictionary of Organic Compounds", Eyre and Spottiswoode, London, 1965, Vol.2.
70. "Dictionary of Organic Compounds", Eyre and Spottiswoode, London, 1965, Vol.4, p.2137.
71. J. Cason, C. F. Allen and S. Goodwin, J. Org. Chem., 1948, 13, 403; J. Cason, R. E. Harman, S. Goodwin and C. F. Allen, *ibid.*, 1950, 15, 860.
72. J. B. Conant and L. F. Fieser, J. Amer. Chem. Soc., 1923, 45, 2194.

73. J. M. Bruce and A. Chaudhry, J.C.S. Perkin I, 1972, 372.
74. H. W. Moore and W. Weyler, J. Amer. Chem. Soc., 1971, 93, 2812.
75. M. O. Forster and H. E. Fierz, J. Chem. Soc., 1907, 1350.
76. W. T. Dixon and D. Murphy, J.C.S. Perkin II, 1975, 850; W. T. Dixon, D. M. Holton and D. Murphy, J.C.S. Faraday II, 1978, 74, 521.
77. J. B. Wright, Chem. Rev., 1951, 48, 397.
78. G. F. Pedulli, A. Spisni et al., J. Mag. Res., 1973, 12, 331.
79. P. Ashworth and W. T. Dixon, J.C.S. Perkin II, 1972, 2264.
80. H. W. Moore, D. L. Maurer, D. S. Pearce and M. S. Lee, J. Org. Chem., 1972, 37, 1984.
81. D. Murphy, unpublished work.
82. T. E. Gough, Canad. J. Chem., 1969, 47, 331.
83. M. C. R. Symons, Adv. Phys. Org. Chem., 1963, 1, p.283.
84. F. A. Neugebauer, S. Bamberger and W. R. Groh, Tetrahedron Lett., 1973, 25, 2247.
85. A. D. McLachlan, Mol. Phys., 1958, 1, 233.
86. W. T. Dixon and D. Murphy, J.C.S. Faraday II, 1976, 72, 1221.
87. C. A. Coulson "Valence", Oxford University Press, London, 1961, p.362.
88. E. Lieber, E. Oftedahl and C. N. R. Rao, J. Org. Chem., 1963, 28, 194 and references within.
89. T. Itai and S. Kamiya, Chem. Pharm. Bull. (Tokyo), 1963, 11, 348.



90. G. R. Harvey and K. W. Ratts, *J. Org. Chem.*, 1966, 31, 3907.
91. P. A. S. Smith "Open-Chain Nitrogen Compounds", Benjamin N.Y. 1966, Vol.2, p.211-256.
92. L. W. Hartzel and F. R. Benson, *J. Amer. Chem. Soc.*, 1954, 76, 667.
93. J. D. Roberts, *Chem. Ber.*, 1961, 94, 273.
94. L. Pauling "The Nature of the Chemical Bond", Cornell University Press, N.Y. 1945, 3rd. Printing, p.200.
95. R. L. Hauser, *J. Org. Chem.*, 1938, 33, 3968.
96. R. O. C. Norman "Principles of Organic Synthesis" Methuen (Science Paperback), 1970, p.583.
97. H. L. Strauss and G. K. Fraenkel, *J. Chem. Phys.*, 1961, 35, 1738.
98. W. T. Dixon, *J.C.S. Faraday II*, 1977, 73, 1475; *ibid.*, 1978, 74, 511.
99. J. P. Colpa and J. R. Bolton, *Mol. Phys.*, 1963, 6, 273; J. R. Bolton, *J. Chem. Phys.*, 1965, 43, 309 and references within.
100. R. Poupko, A. Loewenstein and B. L. Silver, *J. Amer. Chem. Soc.*, 1971, 93, 580 and references within.
101. J. R. Bolton and G. K. Fraenkel, *J. Chem. Phys.*, 1964, 40, 3307.
102. J. R. Bolton, *J. Phys. Chem.*, 1967, 71, 3702.
103. J. R. Bolton, *J. Phys. Chem.*, 1967, 71, 3099; J. E. Wertz and J. R. Bolton, "Electron Spin Resonance" McGraw-Hill Book Co., 1972, p.123.

104. T. E. Gough and G. A. Taylor, *Can. J. Chem.*, 1969, 47, 3717.
105. P. Ashworth and W. T. Dixon, *J.C.S. Perkin II*, 1973, 1533.
106. K. Scheffler and H. B. Stegman, *Tetrahedron Lett.*, 1964, 3035.
107. A. J. Stone and A. Carrington, *Trans. Faraday Soc.*, 1965, 61, 2593.
108. J. H. Freed and G. K. Fraenkel, *J. Chem. Phys.*, 1963, 39, 326; *ibid.*, 1964, 1815.
109. A. Hudson and G. R. Luckhurst, *Chem. Rev.*, 1969, 191.
110. E. de Boer and E. L. Mackor, *J. Chem. Phys.*, 1963, 38, 1450.
111. N. M. Atherton "Electron Spin Resonance" Ellis Horwood (John Wiley) 1973, p.339.

LIST OF TABLES

	Page
1. Molecular orbital parameters	20
2. E.s.r. coupling constants of aminosemiquinones from the literature	29
3. Commercial materials	33
4. Syntheses of starting materials	34
5. E.s.r. coupling constants for aminosemiquinones	51
6. E.s.r. coupling constants for triazolosemiquinones	70
7. "Experimental" spin densities and couplings for the anilino radical cation	77
8. Variation of ring proton spin densities with $h_N$ value in the aniline radical cation	78
9. Correlation of experimental couplings and theoretical spin densities in the aniline radical cation	79
10. Correlation of experimental aminoproton coupling with calculated nitrogen spin density in aminobenzene radical cations and aminophenoxyis	82
11. Calculated coupling constants for aminobenzene radical cations and aminophenoxyis	83
12. Calculated coupling constants for heterocyclic semiquinones	87
13. Ratio of experimental nitrogen and aminoproton couplings in amino-substituted radicals	89

14. Correlation of experimental aminoproton coupling with theoretical nitrogen spin density 90
15. Calculated coupling constant in aminosemiquinones 91
16. Comparison between calculated and experimental hydroxyl proton splitting 92
17. Line-width analysis data for triazolo-1,4-semiquinone at room temperature 111
18. Calculated values of the line-width equation parameters 112

LIST OF FIGURES

	Page
1. An e.s.r. transition for $M_S = \pm\frac{1}{2}$	4
2(a) Four possible spin states for a system with $M_S = \pm\frac{1}{2}$ , $M_I = \pm\frac{1}{2}$ showing effective field, $H_{eff}$ , felt by the electron in the vicinity of the nucleus	7
2(b) The energy levels and allowed transitions between them shown as arrows for the above system, as a function of the applied field, H.	7
3. Degeneracy ratios of a set of n equivalent nitrogens	8
4. Hückel orbital energies for benzene and p-benzoquinone with the reference energy taken as $\alpha$	14
5. Showing the occupancy of the unperturbed (Hückel) and perturbed (modified) molecular orbitals (Aufbau)	16
6. Spectrum of 2,5-diamino-1,4-semiquinone (XI)	37
7. Wing of spectrum of (XI) at expanded field scan	40
8. Reconstruction of wing of spectrum of (XI) showing two different coupling assignments	41
9. Simulation of spectrum of (XI)	43
10. Spectrum of 2-amino-5-methyl-1,4-semiquinone (XII)	44
11. Spectrum of 2-amino-1,4-naphthosemiquinone (XIII)	47

12.	Spectrum of 2-amino-5-oxy-1,4-semiquinone (XIV)	48
13.	Spectrum of triazolo-1,4-semiquinone (XVI)	53
14.	Stick diagram of spectrum of (XVI)	57
15.	Spectrum of bis-triazolo-1,4-semiquinone (XVIII)	59
16.	Wings of spectrum of (XVIII) and stick diagram	60
17.	Spectrum of 2-methyl-triazolo-1,4-semiquinone (XX)	63
18.	Spectrum of 2-t-butyl-triazolo-1,4-semiquinone (XXI)	65
19.	Spectrum of (XXI) at expanded field scan	67
20.	Spectrum of triazolo-1,4-naphthosemiquinone (XXII)	69
21.	Spectrum assigned to tetraazido-1,4-semiquinone (XXIII)	72
22.	Spectrum assigned to 2-azido-3,6-t-butyl-1,4-semiquinone (XXIV)	74
23.	Spin-polarisation in the amino-fragment	80
24.	Methyl group parameters	88
25.	Schematic development of the orbitals of 2,3-triazolo-1,4-semiquinone using the interleaving theorem	102
26.	Conformations of the amino-fragment	105
27.	Labelling of the spectral lines of triazolo-1,4-semiquinone for line-width analysis	109

## Electron Spin Resonance Spectra of Amino- and Triazolo-semiquinones

BY THE LATE WILLIAM T. DIXON, PATRICIA M. HOYLE AND DAVID MURPHY\*

Department of Chemistry, Bedford College, Regent's Park, London NW1 4NS

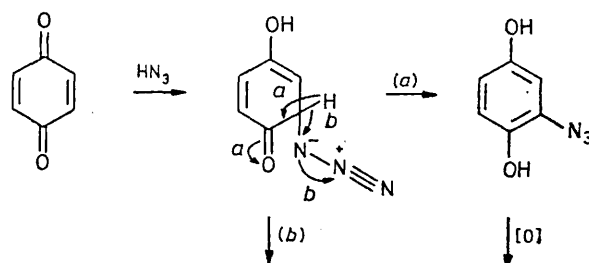
Received 15th March, 1978

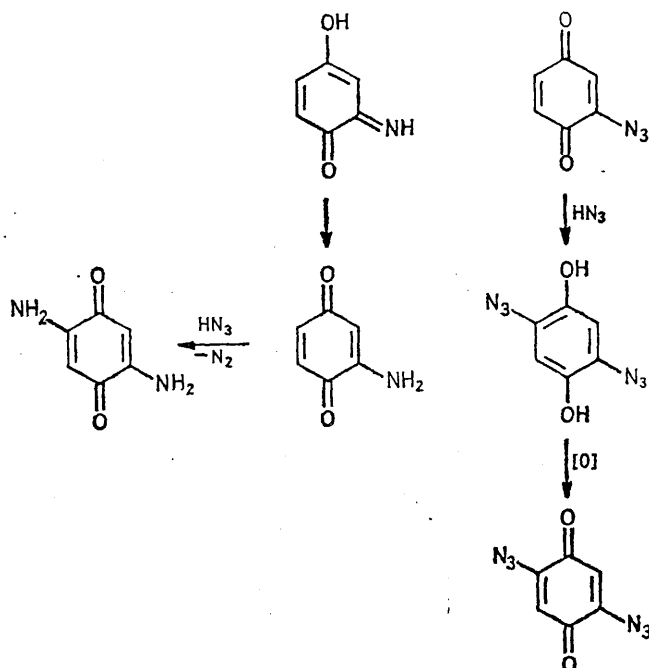
E.s.r. spectra of hitherto unobserved amino- and triazolo-semiquinones have been obtained by auto-oxidation of the products of the reaction between *p*-benzoquinone and hydrogen azide. The calculated spin distributions, using the McLachlan S.C.F. method, of aminophenoxy, amino-semiquinones and triazolossemiquinone radicals, agree well with the experimental values. The observed amino proton splittings fall into two categories; those of the radicals from amino benzene radical cations and from aminophenoxy are given by the relationship  $a_{\text{NH}} = \rho_{\text{N}} \times -3.0 \text{ mT}$ , while those of the aminosemiquinones are given by  $a_{\text{H}} = \rho_{\text{N}} \times -1.0 \text{ mT}$ . An analogous relationship ( $a_{\text{OH}} = \rho_{\text{O}} \times -1.0 \text{ mT}$ ) accounts for some hydroxyl proton splittings.

In spite of the versatile part played by the azido-group in aromatic chemistry, no e.s.r. spectrum has been reported for any organic azido-radical. We have, therefore, attempted to obtain a number of azidoquinones, which on mild reduction we would expect to give azidosemiquinones. In addition, since the azido-group can be regarded as a conveniently blocked amino-group from which  $\text{—NH}_2$  is released on mild reduction, we anticipated that this work might lead to some hitherto elusive unsubstituted aminobenzosemiquinones.

### ADDITION OF HYDROGEN AZIDE TO QUINONES

Reaction of  $\text{HN}_3$  with quinones follows the general pattern of additions to  $\alpha, \beta$ -unsaturated carbonyl compounds; the initial addition<sup>1, 2</sup> is usually followed by enolisation, oxidation, and further addition.<sup>3-5</sup> In some cases aminosemiquinones are formed directly, presumably because an internal oxidation-reduction reaction is preferred to the enolisation step.<sup>6</sup> The reactions are summarised in Scheme 1.





SCHEME 1

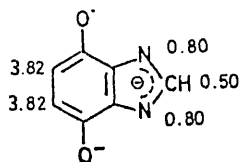
## EXPERIMENTAL

In a typical experiment, *p*-benzoquinone (0.1 g) in water or *N,N*-dimethylformamide (DMF), (5 cm<sup>3</sup>), was treated with saturated aqueous sodium azide (1-2 cm<sup>3</sup>). The solution was investigated in the usual way<sup>7</sup> for observing e.s.r. spectra using a static system, following auto-oxidation<sup>7, 8</sup> or one electron reduction.<sup>8</sup> *p*-Benzoquinone, 1,4-naphthoquinone, 2-methyl-*p*-benzoquinone and DMF were commercial materials purified by the usual methods. 2,3; 5,6-*bis*-Triazolo-*p*-benzoquinone,<sup>9</sup> 2,3-triazolo-1,4-naphthoquinone<sup>9</sup> and 1,4-diacetoxy-2,5-diazidobenzene<sup>3</sup> were prepared as in the literature. All materials used had physical constants which agreed well with those of the literature.

## RESULTS

## TRIAZOLOSEMIQUINONES

Intense e.s.r. spectra were generated from the products obtained by allowing solutions of *p*-benzoquinone in water, and in aqueous DMF, to react with excess sodium azide. The spectra were those of 2,3; 5,6-*bis*-triazolo-*p*-benzosemiquinone(I), splittings  $a_N = 1.22(4)$  and  $a_N = 0.88(2) \times 10^{-4}$  T, and 2,3-triazolo-*p*-benzosemiquinone(II), splittings  $a_H = 3.50(2)$ ,  $a_N = 0.90(2)$ , and  $a_N = 0.65(1) \times 10^{-4}$  T, respectively. Confirmation of these assignments was obtained by the generation of I from



III



an authentic sample of 2,3; 5,6-*bis*-triazolo-*p*-benzoquinone<sup>9</sup> and from the close resemblance of II to its imidazole analogue III.<sup>10</sup> Radicals I and II would arise following one-electron reduction of the products resulting from the 1,3-dipolar addition<sup>11</sup> of  $\text{HN}_3$  to *p*-benzoquinone (see Scheme 2), analogous to the well characterised addition<sup>12</sup> of  $\text{PhN}_3$  to *p*-benzoquinone. E.s.r. spectra of triazolo-

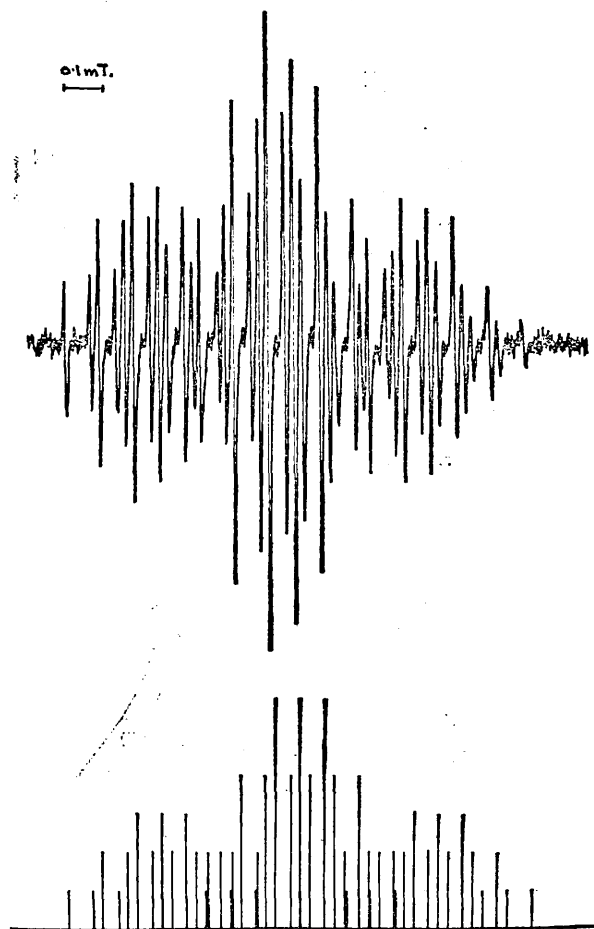


FIG. 1.—E.s.r. spectrum of radical II.


semiquinones were also obtained on addition of  $\text{HN}_3$  to 2-methyl-*p*-benzoquinone and to 1,4-naphthoquinone. 2,3-Triazolophthoquinone was also prepared<sup>9</sup> and reduced to give a spectrum identical with that of the latter semiquinone. The e.s.r. parameters of the triazolesemiquinones are summarised in table 1.

#### AMINOSEMIQUINONES

A well resolved e.s.r. spectrum of 2,5-diamino-*p*-benzosemiquinone (IV) was also obtained on treatment of *p*-benzoquinone with sodium azide in aqueous DMF, support for this assignment was obtained when the same spectrum resulted from the

oxygen<sup>15, 16</sup> parameters ( $h_N = 1.3$ ,  $k_{CN} = 1.0$ ,  $h_O = 1.6$ ,  $k_{CO} = 1.3$ ,  $h_{OH} = 2.0$ ,  $k_{COH} = 1.1$ ,  $Q_{CH} = -3.0$  mT,  $Q_N = 2.5$  mT) very satisfactory agreement was obtained (see table 3). The predictions obtained for the triazolo- and amino-semiquinones, given in tables 1 and 2, are again in good agreement with the experimental values.

TABLE 3.—CALCULATED\* VALUES OF E.S.R. PARAMETERS ( $a/10^{-4}$  T) FOR AMINOBENZENE RADICAL CATIONS AND AMINOPHENOXYLS [experimental values from ref. (17), (20), (21) and (22) in parentheses]

substituents in	$a_1$	$a_2$	$a_3$	$a_4$	$a_5$	$a_6$
						
1-NH <sub>2</sub>	$a_N = 7.70$ (7.68) $a_H = 9.24$ (9.58)	5.60 (5.82)	-1.65 (1.52)	9.03 (9.58)	-1.65 (1.52)	5.60 (5.82)
1,4-(NH <sub>2</sub> ) <sub>2</sub>	$a_N = 4.71$ (5.3) $a_H = 5.65$ (5.88)	2.02 (2.10)	2.02 (2.10)	$a_N = 4.71$ (5.3) $a_H = 5.65$ (5.88)	2.02 (2.10)	2.02 (2.10)
1-O <sup>-</sup> ,2-NH <sub>2</sub>	—	$a_N = 5.03$ (4.76) $a_H = 6.06$ (5.30)	-0.5 (0.1)	4.24 (4.25)	2.52 (2.95)	1.04 (1.01)
1-OH,2-NH <sub>2</sub>	—	$a_N = 6.21$ (6.75) $a_H = 7.94$ (8.10)	0.87 (2.6)	2.32 (1.6)	5.02 (6.6)	-1.33 (0.9)
1-O <sup>-</sup> ,3-NH <sub>2</sub>	—	-0.53	$a_N = 2.51$ $a_H = 3.01$	13.4	-3.25	11.74
1-OH,3-NH <sub>2</sub>	—	0.515 (3.05)	$a_N = 5.91$ (7.0) $a_H = 7.09$ (8.25)	9.66 (8.6)	-2.78 (2.05)	11.39 (10.45)
1-O <sup>-</sup> ,4-NH <sub>2</sub>	—	2.99 (2.75)	1.57 (1.75)	$a_N = 4.63$ (5.25) $a_H = 5.56$ (5.56)	1.57 (1.75)	2.99 (2.75)
1-OH,4-NH <sub>2</sub>	—	1.16 (0.5)	2.99 (4.0)	$a_N = 5.61$ (6.60) $a_H = 6.73$ (8.00)	2.99 (4.0)	1.16 (0.5)

\*  $a_H$  from  $a_H = \rho_N \times -3.0$  mT.

## DISCUSSION

Previous investigations<sup>23-26</sup> of nitrogen substituted semiquinones have revealed a clear pattern of stability of the radicals. Ring substitution or nitrogen substitution leads to stability and to well characterised spectra, but unsubstituted radicals are generally unstable and any observed spectra were poorly defined.<sup>23, 25, 26</sup> We have obtained four aminosemiquinones in reasonable concentration, presumably because the rapid decomposition<sup>26</sup> is matched by fast formation from the azido-intermediates. As radicals II and IV are both observed following reactions in aqueous DMF, there is probably competition between the two types of addition<sup>2, 11</sup> of hydrogen azide to *p*-benzoquinones. If this is so, then the observed e.s.r. spectrum depends upon the conditions of the subsequent autoxidation or reduction; this situation is exactly similar to that in the hydroxylation<sup>8, 27</sup> of aromatic substrates. This suggestion is acceptable because it has been estimated<sup>28</sup> that the bending energy of the azido-group is no greater than 84, and may be as little as 20-25 kJ mol<sup>-1</sup>. The absence of >NH proton splittings can be attributed to the weak acidity of the triazoles,<sup>9</sup> leading to ionisation under the experimental conditions. The unambiguous assignments of the nitrogen splittings in the triazolosemiquinones demonstrate that the unpaired

electron is in an orbital which is anti-symmetrical with respect to the plane bisecting the  $C_{(2)}-C_{(3)}$  and  $C_{(5)}-C_{(6)}$  bonds, perpendicular to the plane of the nuclei. This result is easily predictable using the interleaving theorem.<sup>29</sup> Fig. 2 illustrates the systematic development of the orbitals of radical II from those of benzene.

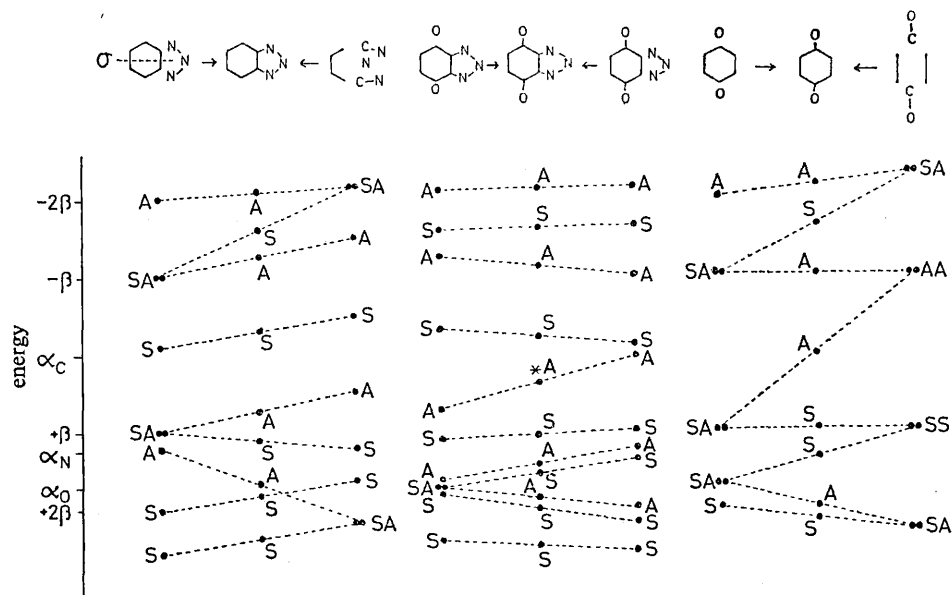


FIG. 2.—Schematic development of the orbitals of 2,3-triazolobenzosemiquinone using the interleaving theorem,<sup>29</sup>  $\sigma$ , symmetry plane, \*, odd electron orbital.

The results of the m.o. calculations showed that the set of nitrogen parameters chosen has given reliable predictions over a wide range of nitrogen substituted radicals. As in the oxygen series<sup>16</sup> agreement with experimental results is good for

TABLE 4.—COMPARISON BETWEEN CALCULATED ( $a_{OH} = \rho_O \times -1.0$  mT) AND EXPERIMENTAL HYDROXYL PROTON SPLITTINGS (experimental values in parentheses)

radical	$a_{OH}/10^{-4}$ T
2-hydroxy-1,4-benzosemiquinone <sup>30</sup>	0.38 (0.31)
3-hydroxy-1,2-benzosemiquinone <sup>30</sup>	0.34 (0.36)
2,6-dihydroxyphenoxyl <sup>31</sup>	0.62 (0.72)
4-hydroxyphenoxyl <sup>32</sup>	1.80 (1.90)
3-hydroxy-2-acetylphenoxyl <sup>15</sup>	0.98 (1.00)

both amino-groups and for heterocyclic nitrogen. It is of interest that the  $-\text{NH}_2$  proton splittings fall into two distinct groups. In the first group, typified by the amino-benzene radical cations and aminophenoxyl radicals the experimental splittings can be satisfactorily estimated by the relationship  $a_{\text{NH}} = \rho_{\text{N}} \times -3.0$  mT. In the second group, the aminobenzosemiquinones, the  $-\text{NH}_2$  proton splittings are small, and are given by the relationship  $a_{\text{NH}} = \rho_{\text{N}} \times -1.0$  mT. The earlier generalisation,<sup>25</sup>  $a_{\text{N}} \approx a_{\text{H, NH}}$  is not applicable. The explanation for the different  $Q_{\text{H, NH}}$  values required is

likely to be found in terms of the differing total charges on the species, as established<sup>33</sup> for hydrocarbon radical ions. We have found that the second value can be used to estimate corresponding —OH proton splittings. Table 4 gives the comparison between experimental and calculated ( $a_{\text{OH}} = \rho_{\text{O}} \times -1.0 \text{ mT}$ ) values for a number of observable —OH splittings.

P. M. H. thanks the University of London for a university research studentship.

- <sup>1</sup> E. Oliveri-Mandala and E. Calderas, *Gazzetta*, 1915, 45 II, 120.
- <sup>2</sup> R. Escales, *Chem.-Ztg.*, 1905, 29, 31.
- <sup>3</sup> H. W. Moore, H. R. Sheldon and D. F. Shellhamer, *J. Org. Chem.*, 1969, 34, 1999.
- <sup>4</sup> R. Adams and W. Moje, *J. Amer. Chem. Soc.*, 1952, 74, 5560.
- <sup>5</sup> R. Adams and D. C. Blomstrom, *J. Amer. Chem. Soc.*, 1953, 75, 3405.
- <sup>6</sup> L. F. Fieser and J. L. Hartwell, *J. Amer. Chem. Soc.*, 1935, 57, 1482.
- <sup>7</sup> P. Ashworth and W. T. Dixon, *J.C.S. Perkin II*, 1972, 1130.
- <sup>8</sup> P. Ashworth and W. T. Dixon, *J.C.S. Perkin II*, 1974, 739.
- <sup>9</sup> L. F. Fieser and E. L. Martin, *J. Amer. Chem. Soc.*, 1935, 57, 1844.
- <sup>10</sup> G. F. Peduli, A. Spisni, P. Vivarelli, P. Dembech and G. Seconi, *J. Magnetic Resonance*, 1973, 12, 331.
- <sup>11</sup> R. Huisgen, *Angew Chem. Int. Edn*, 1963, 2, 633.
- <sup>12</sup> L. Wolf and G. K. Grau, *Annalen*, 1912, 394, 68.
- <sup>13</sup> A. D. McLachlan, *Mol. Phys.*, 1960, 3, 233.
- <sup>14</sup> K. A. Lott, E. I. Short and D. N. Waters, *J. Chem. Soc. B*, 1969, 1232.
- <sup>15</sup> W. T. Dixon, M. Moghimi and D. Murphy, *J.C.S. Faraday II*, 1974, 70, 1713.
- <sup>16</sup> W. T. Dixon, P. M. Kok and D. Murphy, *J.C.S. Faraday II*, 1977, 73, 709.
- <sup>17</sup> F. A. Neugebauer, S. Bamberger and W. R. Groh, *Tetrahedron Letters*, 1973, 2247.
- <sup>18</sup> H. M. McConnell, *J. Chem. Phys.*, 1956, 24, 764.
- <sup>19</sup> A. Carrington and J. dos Santos Viega, *Mol. Phys.*, 1962, 5, 21.
- <sup>20</sup> P. Neta and R. W. Fessenden, *J. Phys. Chem.*, 1974, 78, 523.
- <sup>21</sup> W. T. Dixon and D. Murphy, *J.C.S. Faraday II*, 1976, 72, 1221.
- <sup>22</sup> M. T. Melchior and A. H. Maki, *J. Chem. Phys.*, 1961, 34, 471.
- <sup>23</sup> Y. Matsunaga and C. A. McDowell, *Canad. J. Chem.*, 1960, 38, 1167.
- <sup>24</sup> G. A. Russell, R. Konaka, E. T. Strom, W. C. Danen, K. Y. Chang and G. Kaupp, *J. Amer. Chem. Soc.*, 1968, 90, 4646.
- <sup>25</sup> A. T. Bullock and C. B. Howard, *Trans. Faraday Soc.*, 1970, 66, 1861.
- <sup>26</sup> J. L. Huntington, *Diss. Abstr. Int.*, 1970-71, 311, 90B.
- <sup>27</sup> W. T. Dixon, P. M. Kok and D. Murphy, *Tetrahedron Letters*, 1976, 623.
- <sup>28</sup> J. D. Roberts, *Chem. Ber.*, 1961, 94, 273.
- <sup>29</sup> W. T. Dixon, *J.C.S. Faraday II*, 1977, 73, 1475; 1978, 74, 511.
- <sup>30</sup> W. T. Dixon, D. M. Holton and D. Murphy, *J.C.S. Faraday II*, 1978, 74, 521.
- <sup>31</sup> W. T. Dixon and D. Murphy, *J. C. S. Perkin II*, 1975, 850.
- <sup>32</sup> T. E. Gough, *Canad. J. Chem.*, 1969, 47, 331.
- <sup>33</sup> J. R. Bolton, *J. Chem. Phys.*, 1965, 43, 309.

(PAPER 8/472)